Variations of developmental events, *skn-1* and *pie-1* expression, and gene regulatory networks in nematodes with different modes of reproduction

Inaugural - Dissertation

zur

Erlangung des Doktorgrades

der Mathematisch-Naturwissenschaftlichen Fakultät

der Universität zu Köln

vorgelegt von

Abraham Nsah, Ndifon

aus Kamerun

Köln, 2013

Berichterstatter:	Prof. Dr. E. Schierenberg
	Priv. Doz. Dr. M. Kroiher
Tag der letzten mündlichen Prüfung:	24. Mai 2013

Angelika, Tracy, Monique und Felix

Table of Contents

Abbreviations III

1 Introduction 1

2 Materials and Methods 13

3 Results 42

3.1 P granules distribution in nematodes 42

3.1.1 Cross reactivity of *C. elegans* P granule antibody 44

3.1.2 *Acrobeloides* species show very early P granule perinuclear distribution 46

3.1.3 Panagrolaimidae species show perinuclear localisation of P granules 48

3.2 Isolation of gene homologs 50

3.2.1 Isolation of *par-6* gene homolog with degenerated primers 50

3.3 *In situ* hybridisation on whole mount embryos with *Acrobeloides* sp. (PS 1146) *par-6* construct 55

3.4 PAR-6 Antibody production from *Acrobeloides sp.* (PS 1146) 55

3.5 Heterologous RNAi is possible in *C. elegans* but is not inducible in *Panagrolaimus sp.* (PS1159) 56

3.5.1 Inconclusive efficiency of RNAi by feeding in *Panagrolaimus sp.* (PS1159) 57

3.6 Isolation of gene fragments from other nematodes 58

3.7 Evaluation of interacting gene networks and gene analysis 60

3.7.1 In genomes of different nematode species, a SKN-1 homolog is absent 60

3.7.2 Not all available genomes of nematode species contain a PIE-1 homolog 64

3.7.3 Bioinformatic analysis of SKN-1 homologs from selected nematode species 67

3.7.4 Bioinformatic analysis of PIE-1 homologs from selected nematode species 70

3.7.5 PAR-2 is present only in the genus *Caenorhabditis* 71

3.8 Striking differences in the early embryonic expression pattern of *skn-1, mex-1,* and *pie-1* mRNAs among related nematodes 73

3.8.1 The distribution of *skn-1* mRNA is similar in all *Acrobeloides* species 75

3.8.2 *skn-1* mRNA localisation differs between *Panagrolaimus sp.* (PS1159) and the closely related *Propanagrolaimus sp.* (JU765) 77

3.9 MAP kinase activity and MSP genes in parthenogenetic nematodes 86

3.9.1 MAP kinase genes are conserved in parthenogenetic nematodes 86

3.9.2 Major sperm protein is not detectable in parthenogenetic nematodes 91

3.9.3 Intact MSP genes are present in parthenogenetic nematodes 95

4 Discussion 98

4.1 Perinuclear localisation of P granules and regulation of early zygotic transcripts .. 98

4.2 Differences in mRNA expression and protein sequence challenge a conserved role of SKN-1 100

4.3 Variations in ZF1 and ZF2 motifs indicate differences in regulation of PIE-1 in nematodes 102

4.4 Evolutionary modification of PIE-1 function and somatic degradation 104

4.5 Modification of gene regulatory networks 105

4.6 MAP kinase activity and MSP genes in parthenogenetic nematodes 106

5 Outlook 108

6 Abstract 109

7 Zusammenfassung 111

8 References 113

9 Declaration 124

10 Acknowledgements 125

Abbreviations

Amp	Ampicillin
A.n.	*Acrobeloides nanus*
A. maximus	*Acrobeloides maximus*
PS1146	*Acrobeloides sp.* (PS1146)
BCIP	5-bromo-4-chloroindolyl phosphate
B.m.	*Brugia malayi*
bp	Base pairs
BSA	bovine serum albumin
°C	degrees Centigrade
cDNA	complementary DNA
C.e.	*Caenorhabditis elegans*
C.b.	*Caenorhabditis briggsae*
C.br.	*Caenorhabditis brenneri*
CGC	Caenorhabditis Genetics Centre
D.c.	*Diploscapter coronatus*
D.m.	*Drosophila melanogaster*
DEPC	diethyl pyrocarbonate
DMF	dimethyl formamide
dNTP	Deoxyribonucleotide triphosphate
dsRNA	Double stranded ribonucleic acid
DNA	Deoxyribonucleotide acid
E. coli	*Escherichia coli*
EDTA	Ethylendiaminetetraacetatic acid
EtOH	Ethanol
GSP	gene specific primer
g	gram
IPTG	isopropyl-β-D-thiogalactoside
L	Litre
LB	Luria-Bertani Medium
h	Hour(s)
H_20dest	distilled Water
KOH	potassium hydroxide
M	mole cm^{-3} (molar)
m	metre
MAPK	mitogen-activated protein kinase
MeOH	Methanol
mex-1	*muscle excess gene*
min	Minute(s)
ml	millilitre
mRNA	messenger ribonucleic acid
NaCl	Sodium chloride
NBT	nitrobluetetrazolium
ng	Nanogramm
nm	nanometre
OD	Optical density
PCR	polymerase chain reaction

PDZ	PSD95 (post synaptic density protein)
pie-1	pharynx and intestine in excess
PS1159	*Panagrolaimus sp.* (PS1159)
par	partitioning defective gene
PAR	partitioning defective protein
PB1	PKC-3 binding 1
pH	power of Hydrogen
PBS	phosphate buffered saline
PBST	phosphate buffered saline Tween20
PKC	protein kinase C
PVA	Polyvinyl alcohol
RNA	Ribonucleic acid
RNAi	RNA mediate interference
rpm	rotations per minute
RT-PCR	reverse transcription-polymerase chain reaction
RT	room temperature
sec	Second(s)
SDS PAGE	Sodium dodecyl sulphate polyacrylamide gel
skn-1	skn excess gene
STF	Streck Tissue Fixative
TBE	Tris Boric acid EDTA
UV	Ultraviolet
UTR	untranslated region
v/v	volume per final volume
w/v	weight per volume

1 Introduction

Overview of nematodes

The 19th-century German embryologist Karl Ernst von Baer first noted that there was a striking similarity between animal species during periods of their embryonic development (von Baer, 1828). The phylum nematoda is very old, its origin dating back to the Precambrian more than 500 million years ago (Ayala et al., 1998; Rodriguez-Trelles et al., 2002; Douzery et al., 2004; Poinar, 2011). Most nematodes are free-living organisms, inhabiting almost every possible habitat, but there are also parasitic species (Cobb, 1914; Hamilton et al., 1990). Usually nematode eggs can develop outside the mother from the first cleavage onward, and they are transparent, although to a variable degree (Hugot et al., 2001; Schulze and Schierenberg, 2009) and the freshly hatched juveniles appear to have essentially invariant species-specific cell numbers (Sulston et al., 1983; Schulze et. al., 2012). The phylum nematoda is very large and a variety of selected representatives appear to be excellent candidates for a comparative study of early embryogenesis (Lambshead, 1993; Schierenberg 2005). Many strains can be cultured in the laboratory on simple agar plates and the free-living hermaphroditic nematode *Caenorhabditis elegans,* has become one of the best studied model systems.

C. elegans embryogenesis: the reference system

Since the 1970s, the small (about 1 mm long), soil nematode *C. elegans* has been extensively studied (Sulston and Horvitz, 1977; Kimble and Hirsh, 1979; Sulston et al., 1980, 1983), and widely considered a model system both through its amenability to genetic approaches as well as its quasi-fixed developmental lineage (Brenner, 1974). *C. elegans* was chosen as a model organism because it has a small number of cells, a small genome, a rapid life cycle, a hermaphroditic mode of reproduction and a simple body plan with a transparent cuticle through which one can observe cell development and differentiation (Sulston and Horvitz, 1977; Kimble and Hirsh, 1979; Sternberg and Horvitz, 1981). Gene expression can be manipulated via mutations and RNA interference (Fire et al., 1998; Tabara et al., 1998; Timmons and Fire, 1998). Development from first cleavage to hatching is very rapid, approximately

14 hours after fertilisation (at 25 °C) the embryo hatches as a first stage larva (L1) composed of 558 cells (Kimble and Hirsh, 1979). The eggs (about 55 x 35 µm in size) are remarkably transparent and body parts easily visible under the microscope (Byerly et al 1976; Deppe et al., 1978). *C. elegans* hermaphrodites have a didelphic (two armed) gonad, with the two proximal ends of each respective arm meeting at the vulva (Kimble and Hirsh, 1979; Sulston and Horvitz, 1983).

The analysis of *C. elegans* provided a wealth of developmental data with many percularities compared to other models such as mouse and *Drosophila* (Fitch and Thomas, 1997; Sommer, 2000; Stathopoulos and Levine, 2005). It has been the first metazoan whose genome was completely sequenced (The *C. elegans* Genome Consortium 1998), the complete wiring diagram of the nervous system has been described (White et al., 1986), ground-breaking methods like gene silencing with RNAi (Fire et al., 1998) and visualisation of gene expression in vivo with the GFP technique (Chalfie et al., 1994) have been originally established in this system and finally the developmental fate of all 558 cells present at hatching have been determined (Sulston et al., 1983).

Nematodes have a similar overall body structure. However, many aspects e.g. mode of reproduction, ecology, or particular morphology of structures like pharynx or vulva vary hugely. But what appears most profound is the divergence exhibited across nematodes concerning the pattern of development (Skiba and Schierenberg, 1992; Malakhov, 1994; De Ley and Blaxter, 2002; Schulze et al., 2012). The wealth of early developmental variations appears paradoxical in a way, as these do not have any obvious impact on structure or performance of the resulting worms, since nematodes do not show the wide range of morphological diversity found in other phyla such as Arthropods or Molluscs (Fitch and Thomas, 1997; Aguinaldo et al., 1997).

C. elegans early embryonic development

Upon fertilisation, immediately after fusion of the two pronuclei, the zygote divides into two unequal cells, a larger, anterior somatic cell AB and a smaller, posterior germline cell P1. The AB cell divides with a transverse spindle orientation into ABa and ABp (Figure 1-1). Both AB blastomeres are initially equipotent but nevertheless execute different developmental programs due to inductive signals that they (and at

least some of their descendants) receive from neighbouring cells (Goldstein, 1992). P1 cleaves with a longitudinal spindle orientation unequally into a somatic cell EMS and a new germline cell P2. Further unequal divisions of P2 and its daughter P3 generate the somatic founder cells C and D, respectively (for review, see Gönczy and Rose, 2005). Soon after the division of P3, leading to the 24-cell stage, the two daughters of the gut precursor E initiate gastrulation by moving into the interior of the embryo (Sulston et al., 1983; Figure 1-1).

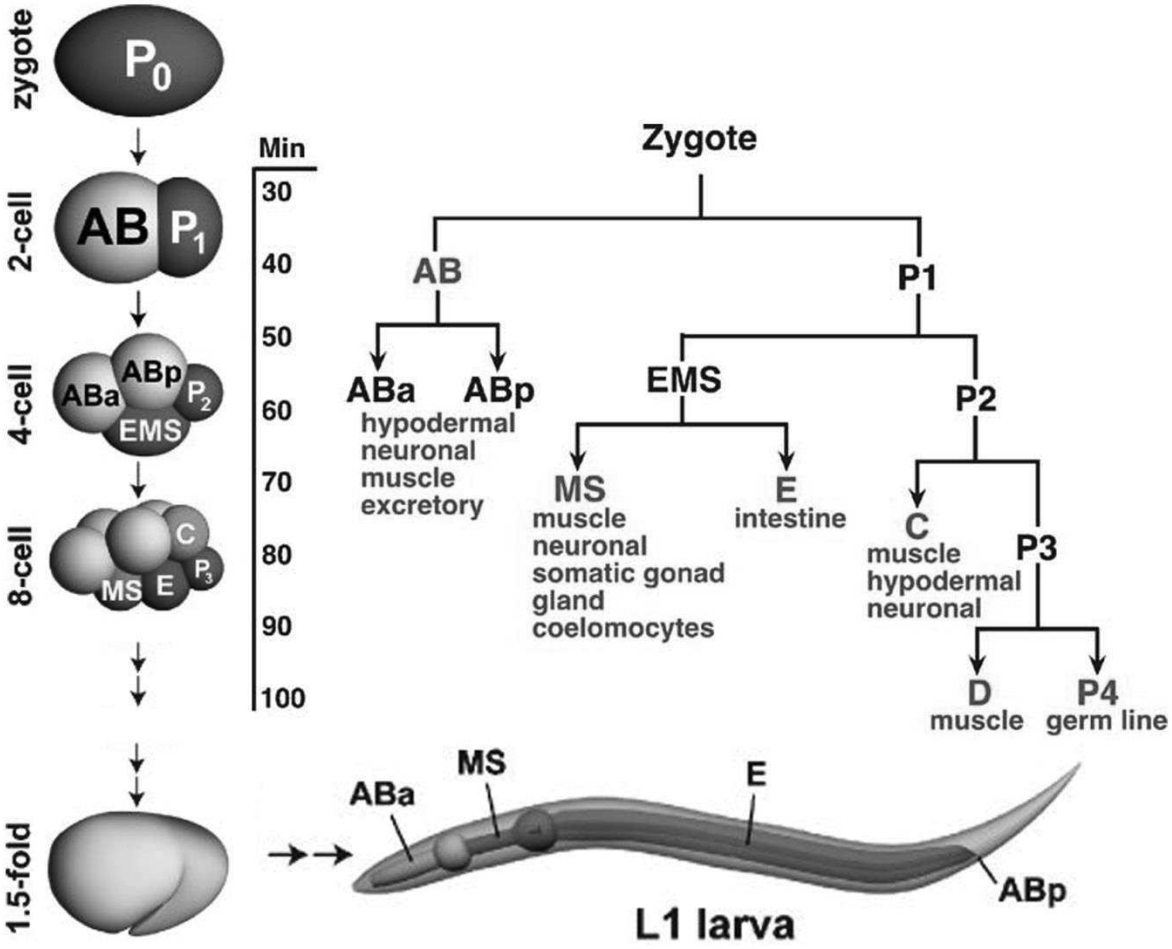

Figure 1-1: The early *C. elegans* lineage showing the origin of major tissue types. Founder cells (red) and their derivatives (blue) are indicated along with the approximate timing of unequal cleavages divisions after fertilization (at 25 °C). The lineal origins of the digestive tract are shown on a simplified representation of the first-stage juvenile, or L1 larva. For simplicity, additional tissues generated by a minority of AB, MS and C descendants are not indicated (Adapted from Sulston et al., 1983 and Maduro, 2006).

Nematodes studied in this project

The phylum nematoda was traditionally subdivided into two branches, Secernentea and Adenophorea (Chitwood and Chitwood, 1950) based on comparative studies of morphological features (Traunspurger, 2002). Based mainly on molecular sequence data, a modern nematode phylogeny was suggested by Blaxter et al., (1998), extended and modified by De Ley and Blaxter (2002), with five clades in three subclasses. Recently, from a larger set of species 339 nearly full-length small-subunit rDNA sequences were analyzed and revealed a backbone of twelve consecutive dichotomies that subdivide the phylum nematoda into twelve clades (Holterman et al., 2006; Figure 1-2).

Several attempts have been made to trace the evolution of embryonic diversity in nematodes by looking at processes like early axis specification (Goldstein et al., 1998), cleavage pattern, arrangement of blastomeres (Dolinski et al., 2001; Houthoofd et al., 2003), germline behavior and gastrulation (Schierenberg and Lahl 2004; Schierenberg, 2005b). In the initially apolar *C. elegans* egg, the first symmetry-breaking event establishing an anterior-posterior (a-p) axis is initiated by the entry of the sperm at fertilization (Goldstein and Hird, 1996). An asymmetric division of the zygote P_0 produces the anterior somatic founder cell AB and its posterior sister, the germline cell P1 (Figure 1-1). In parthenogenetic species such as *Acrobeloides nanus,* already the first steps in embryogenesis differ from *C. elegans* (Wiegner and Schierenberg, 1998), and the sperm is not used for the establishment of the early a-p axis (Goldstein et al, 1998). Therefore, in parthenogenetically reproducing nematodes the mechanism of polarity establishment and cell specification must be modified compared to *C. elegans* and several obstacles must be overcome in the germ cells due to the absence of sperm (Kallenbach, 1985; Kuntzinger and Bornens, 2000; Riparbelli and Callaini, 2003).

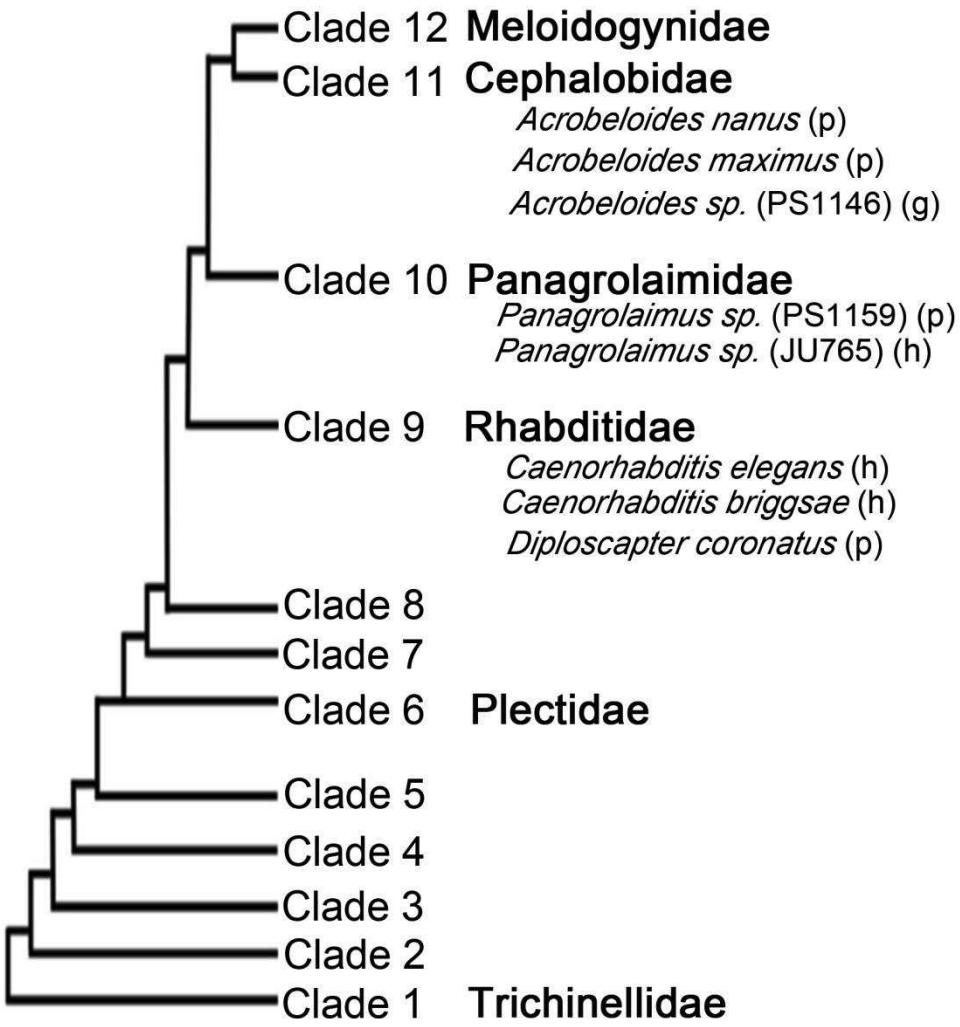

Figure 1-2: Simplified phylogenetic tree of nematodes based primarily on rDNA sequence data, classified into 12 clades, adapted from Holterman et al., 2006. g = gonochoristic, h = hermaphroditic and p = parthenogenetic.

Parthenogenesis is frequently observed in certain free-living nematode taxa. Several such species are being cultured and studied in our laboratory (Skiba and Schierenberg 1992; Lahl et al., 2003, 2006), including the *Diploscapter*, *Acrobeloides and Panagrolaimus* species. This offers us the opportunity to analyze in detail developmental peculiarities that accompany the parthenogenetic type of reproduction.

The greatest advantage of using nematodes to study how development evolves is the potential to employ what is known about *C. elegans* development as a basis for identifying to what extent evolution of certain features has occurred, and for identifying candidate genes that may have been mutated to account for the observed modifications of development.

Table 1: Sequence of early cleavages in different nematodes from selected clades. For better visibility germline cells are shown in red.

C. elegans **(clade 9)**		***A. nanus*** **(clade 11)**		**JU765 (clade 10)**		**DF5050 (clade 10)**		**PS1159 (clade 10)**	
P_0	2*	P_0	2	P_0	2	P_0	2	P_0	2
$^{1}AB^{2}$	3	P_1	3	P_1	3	P_1	3	P_1	3
P_1	4	P_2	4	$^{1}AB^{2}$	4	$^{1}AB^{2}$	4	$^{1}AB^{2}$	4
$^{2}AB^{4}$	6	$^{1}AB^{2}$	5	P_2	5	P_2	5	P_2	5
EMS	7	P_3	6	$^{2}AB^{4}$	7	$^{2}AB^{4}$	7	$^{2}AB^{4}$	7
P_2	8	$^{2}AB^{4}$	8	EMS	8	P_3	8	P_3	8
$^{4}AB^{8}$	12	EMS	9	$^{4}AB^{8}$	12	EMS	9	EMS	9
MS	13	$^{4}AB^{8}$	13	P_3	13	$^{4}AB^{8}$	13	$^{4}AB^{8}$	13
E	14	$^{1}MS^{2}$	14	MS	14	MS	14	MS	14
C	15	$^{1}E^{2}$	15	E	15	E	15	E	15
$^{8}AB^{16}$	23	$^{1}C^{2}$	16	C	16	$^{8}AB^{16}$	23	C	16
P_3	24	$^{8}AB^{16}$	24	$^{8}AB^{16}$	24	C	24	P_4	17
$^{2}MS^{4}$	26	$^{2}MS^{4}$	26	$^{2}MS^{4}$	26	$^{2}MS^{4}$	26	$^{8}AB^{16}$	25
$^{2}C^{4}$	28	$^{2}C^{4}$	28	$^{16}AB^{32}$	42	P_4	27	$^{2}MS^{4}$	27
$^{16}AB^{32}$	44	$^{16}AB^{32}$	44	$^{2}C^{4}$	44	$^{16}AB^{32}$	43	$^{16}AB^{32}$	43
$^{2}E^{4}$	46	$^{2}E^{4}$	46	$^{4}MS^{8}$	48	$^{2}C^{4}$	45	$^{2}C^{4}$	45
$^{4}MS^{8}$	50	$^{4}MS^{8}$	50	$^{2}E^{4}$	50	$^{4}MS^{8}$	49	$^{4}MS^{8}$	49

*, total cell numbers after cleavage in this lineage. For strain names, see Table 12.

Different modes of reproduction in nematodes

An extensive variation in the reproductive mode has been found among nematodes (Laugsch and Schierenberg, 2004; Denver et al., 2011). It is generally accepted that the gonochoristic mode (requiring males and females) is original and other variants like hermaphroditism (females produce sperm and oocytes) and parthenogenesis

(only females and eggs develop without fertilisation by sperm; Lahl et al., 2006) are derived forms (Cho et al., 2004; Kiontke et al., 2004, 2007). Most nematodes follow either the ancestral gonochoristic mode of reproduction or a hermaphroditic mode of reproduction. The former one is thought to give at least long-term advantages because of the continuous recombination of alleles, resulting for instance in the loss of lethal mutations (Maynard-Smith, 1978; Kondrashov, 1993) or a better resistance to parasites (Hamilton et al., 1990).

C. elegans is an internally self-fertilizing hermaphrodite where oocytes arrest during meiosis and need to be induced by a sperm-derived signal to resume their meiotic program (Miller et al., 2001; Hajnal and Berset 2002) in order to become haploid and ready for fertilisation. The sperm then delivers the centriole necessary to generate embryonic cleavage spindles. In *C. elegans* it is also the sperm that induces formation of the primary embryonic axis, i.e. the area of its entrance into the egg defines the posterior pole (Goldstein and Hird 1996, Cowan and Hyman 2004).

Parthenogenesis has been considered as a way to generate new species (Ramirez-Perez et al., 2004; Woolley et al., 2004). Here embryogenesis must be initiated in the absence of sperm and parthenogenetic nematodes must establish certain modifications during oogenesis and/or early embryogenesis. Thus, nematodes appear particularly well suited to study the molecular basis of different modes of reproduction.

P granules

In animals ranging from nematodes to mammals, germ cells or germ cell precursors possess distinctive cytoplasmic organelles made up of RNAs and proteins (Strome and Wood, 1982; reviewed by Vononina, 2011). In *C. elegans*, they are called P granules and are associated with germ line identity, fertility and maintenance (Strome and Wood, 1982; reviewed by Seydoux and Braun, 2006). P granules localise asymmetrically to germ cell precursors in *C. elegans* early embryos and their abnormal segregation may lead to the loss of germline fate (Strome, 2005).

In *C. elegans* an early asymmetric distribution of these P granules can be detected with specific antibodies (Strome and Wood 1983; Skiba and Schierenberg, 1992). Once the germ lineage is established, P granules associate with nuclei and remain perinuclear throughout development (Strome, 2005). Electron microscopic studies

show that the P granules in germ cells accumulate near the nuclear membrane pores (Eddy, 1975; Krieg et al, 1978; Wolf et al., 1983), and thereby provide a perinuclear compartment where newly exported mRNAs are collected prior to their release to the general cytoplasm (Updike and Strome, 2010). More than 40 proteins associated with P granules either possess RNA binding domains or are thought to regulate translation, (Updike and Strome, 2010). Throughout most of the *C. elegans* life cycle, P granules are associated with clusters of nuclear pore complexes on germ cell nuclei. The perinuclear P granules have been shown to differ from cytoplasmic P granules in many respects, including structure, stability and response to metabolic changes (Updike and Strome, 2010; Sheth et al, 2010).

RNA interference

The mechanism of RNA interference (RNAi) has been widely researched since its discovery in 1998. Andrew Fire and his work group discovered the RNAi mechanism by injecting double-stranded RNA (dsRNA) into *C. elegans*, which resulted in the degradation of endogenous mRNA corresponding in the sequence to the injected dsRNA. RNAi is a conserved process which has been detected in all eukaryotic organisms (Geley and Müller, 2004). The establishment of the RNAi method serves as a useful tool to investigate gene functions and interactions that lead to the determination of cell fates (Fire et al., 1998; Montgomery et al., 1998). In *C. elegans* dsRNA is delivered to the organism by one of the following three methods: soaking (Maeda et al., 2001), injection (Fire et al., 1998) or feeding (Timmons et al., 1998). RNAi by feeding has many advantages. First, RNAi can be performed on a large number of worms since feeding is less labor-intensive. Second, feeding is less expensive than the other methods. Therefore, it allows rapid evaluation of a specific gene function by knocking-down specific target genes and analysis of its role and function (Kamath and Ahringer, 2003).

The *C. elegans* cell fate determinants SKN-1, PIE-1 and MEX-1

Early development depends on the temporal and spatial control of maternal gene products. As a first step of cell specification they are differentially segregated or degraded in *C. elegans* (Evans et al., 1994; Hunter and Kenyon, 1996; Reese et al., 2000; DeRenzo et al., 2003). The maternally produced SKN-1 is a transcription factor that functions in EMS to turn on genes required for E and MS somatic cell

fates (Figure 1-3B), but SKN-1 is present in both EMS and its germline sister P2 (Bowerman et al., 1992; Blackwell et al., 1994). In *skn-1* mutants EMS adopts a C-like fate (Maduro et al., 2001). SKN-1 binds to *end-1* regulatory sequences and the Wnt pathway might regulate *end-1* expression, which in turn is sufficient to initiate endoderm formation (Bowerman et al., 1992; Blackwell et al., 1994; Rocheleau et al., 1997).

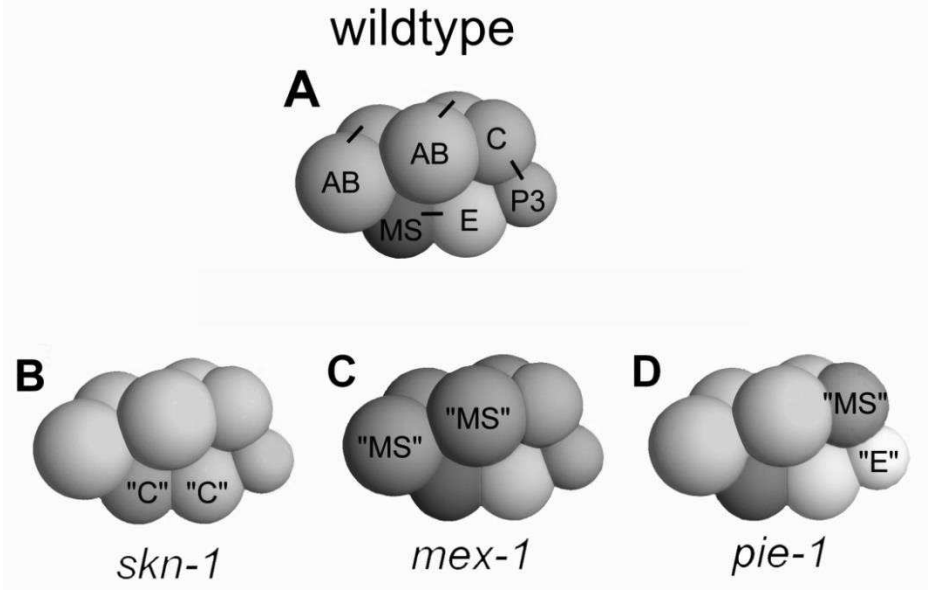

Figure 1-3: A simplified sketch demonstrating the integration of differential distribution of maternal gene products and cell-cell signaling mainly based on mutant analysis. In *skn-1* mutants EMS adopts a C-like fate. MEX-1 makes sure that SKN-1 is predominantly shunted into P1 as in the *mex-1* mutant this does not happen and AB cells behave MS-like. PIE-1 concentrates in the nucleus of P2 preventing there the activity of SKN-1, this way allowing the preservation of pluripotency in the germline. If *pie-1* is defective P2 converts into an EMS-like blastomere (adapted from Schierenberg, 2013).

PIE-1 is a CCCH zinc finger protein that is segregated preferentially to the germline blastomere at each P lineage division, and functions by inhibiting both initiation and elongation phases of transcription probably by blocking the chromatin remodeling proteins (Mello et al., 1996; Seydoux and Dunn, 1997; Zhang et al., 2009). One role of PIE-1 is to prevent expression of SKN-1 target gene expression in the posterior P2 cell (and presumably prevent expression of other somatic differentiation genes in P3 and P4 and thereby protect germline fate (Mello et al., 1992; Strome et al., 2001; Seydoux and Schedl, 2001). The germline blastomere specific localisation of PIE-1 is the result of selective enrichment towards the presumptive germline blastomere prior to division, coupled with selective degradation of any PIE-1 remaining in the

somatic blastomeres following division (Reese et al., 2000). PIE-1 levels drop shortly after the primordial germ cell P4 divides into Z2 and Z3 at the ~100-cell stage (Mello et al., 1996). Lifting of PIE-1 repression presumably sets the stage for turn-on of expression in the nascent germline of genes appropriate for germline development. In embryos lacking PIE-1 function, P2 develops like an EMS cell, generating SKN-1-dependent MS and E fates in its descendants (Figure 1-3D).

At the anterior pole of the embryo, the maternal factor MEX-1 restricts appearance of ectopic MS-like fates by preventing appearance of high levels of SKN-1 protein in the early AB lineage (Bowerman et al., 1993; Seydoux and Fire, 1995). In embryos lacking MEX-1 function, the AB grand-daughters adopt MS-like fates (Figure 1-3C). As with PIE-1, SKN-1 is required for the appearance of ectopic MS-derived tissues in MEX-1 mutant embryos, consistent with the ectopic activation of the normal MS specification pathway in the AB lineage. MEX-1 is a CCCH-type zinc finger protein similar to PIE-1, and like PIE-1, is found in the P lineage, where it functions in PIE-1 localisation (Mello et al., 1992; Guedes and Priess, 1997; Schisa et al., 2001). Hence, the role of MEX-1 in preventing AB-specific accumulation of SKN-1 is apparently indirect.

Oocyte-to-embryo transition and MAP kinase activity in nematodes

Throughout the animal kingdom, female gametes typically interrupt their development during oogenesis at various stages of meiosis. In response to external stimuli, this arrest is released, and oocyte maturation can take place. Then oocytes resume meiotic divisions, ovulate and get competent for fertilisation. An important step during oocyte maturation in all animals is mitogen-activated protein (MAP) kinase activation (reviewed by Nebreda and Ferby, 2000; Abrieu et al., 2001). MAP kinases are ubiquitous serine-threonine protein kinases expressed in all eukaryotic cells (Waskiewicz and Cooper, 1995; Widmann et al., 1999) and can be subdivided into five groups: The Erk1/2, p38, Jnk, Erk3/4, and Erk5 subfamilies (Widmann et al., 1999). They are activated by MAP kinase kinase mediated dual phosphorylation of two distinct amino acids, Threonine and Tyrosine, in a T-X-Y motif of the activation loop (Rossomando et al., 1989).

There are MAP kinase orthologs from several subfamilies present in *C. elegans*. The Erk1/2 ortholog MPK-1 (Lackner et al., 1994; Wu and Han, 1994) is the best studied

representative. MSP was first described as a major component of *C. elegans* sperm representing 15 % of its total protein content (Klass and Hirsh, 1981). In *C. elegans*, MSP comprises a large multigene family of about 50 highly conserved members including more than 20 pseudogenes. The number of MSP genes detected in other nematodes is variable, from one in *Ascaris suum* to 1-13 in other mammalian intestinal parasites, 1-4 in filarial nematodes or 5-12 in plant and insect parasitic species (Scott et al., 1989; Cottee et al., 2004). MSP sequences are highly conserved in all nematodes (Smith, 2006). All MSP genes of *C. elegans* are expressed at the same time and only during the terminal stages of spermatogenesis (Ward and Klass, 1982; Klass et al., 1982).

Reports from the *C. elegans* literature highlight that resumption of meiosis and ovulation depend on sperm and sperm-released factors, thereby avoiding cost if no sperm is available. Whether or not the molecules regulating the *C. elegans* oocyte-to-embryo transition are functionally conserved in nematodes with different reproductive modes, is not known. Using *C. elegans* as a reference, we investigated two key steps of oocyte-to-embryo transition, MAP kinase activation and MSP signaling, in parthenogenetic nematodes where sperm is absent.

Aims of this study

The study of embryonic development, as part of the ontogeny of a single species, such as *C. elegans* (clade 9) is not an indicator for the pattern of development in the nematode phylum. The enormous diversity in development and reproduction in nematodes shows that *C. elegans* cannot be regarded as the standard reference nematode system (Rudel and Sommer, 2003; Kiontke et al, 2004). How the cellular processes evolved and which molecular components underlie these variations is poorly understood.

The aim of my PhD project has been to investigate and broaden the presently limited knowledge of embryonic development in other nematodes other than *C. elegans.* In specific, the following aspects were addressed:

1. Localisation of germ line-specific P granule as a polarity marker in selected parthenogenetic, gonochoristic and hermaphroditic nematodes
2. To identify homologs of well-known *C. elegans* genes that are essential for the establishment of early embryonic polarity.

3. Spatio-temporal expression of maternally-supplied mRNAs in selected nematodes from different clades with different modes of reproduction.

4. To test the efficacy of RNA interference in *Panagrolaimus* sp (PS1159).

5. Genome analysis of the *pie-1* and *skn-1* gene interaction networks in nematode development.

5. MAP kinase activity and MSP genes in parthenogenetic nematodes.

We want to obtain a better idea to what extent the mode of reproduction goes along with evolutionary modifications of early development in nematodes by investigating how early cell determinants are distributed among closely related species. This work is therefore a contribution to understanding some molecular aspects which may account for differences in embryonic development.

2 Materials and Methods

Nematode strains and cultivation

Nematodes were cultivated under standard conditions on agar plates with the uracil-requiring strain of *E. coli* OP50 as a food source, essentially as described by Brenner (1974). To reduce contamination with other bacteria, we used minimal medium plates with low-salt content that provide a thinner bacterial lawn (Lahl et al., 2003).

Table 2: List of nematodes strains

Nematode	Mode of reproduction	Source
C. elegans (N2)	hermaphroditic	*Caenorhabditis* Genetics Centre, Minnesota, MN, USA
*Panagrolaimus sp. (*PS1159)	parthenogenetic	Marie-Anne Felix, Paris, France
Panagrolaimus superbus (DF5050)	gonochoristic	David Fitch, New York, USA
Propanagrolaimus sp. (JU765)	hermaphroditic	Marie-Anne Felix, Paris, France
Acrobeloides nanus (ES501)	parthenogenetic	Einhard Schierenberg, Cologne, Germany
Acrobeloides sp. (PS1146)	hermaphroditic	Marie-Anne Felix, Paris, France
Acrobeloides sp. (SB374)	gonochoristic	Walter Sudhaus, Berlin, Germany
Diploscapter coronatus	parthenogenetic	Paul De Lay, Riverside, CA, USA

Cultivation of nematodes

For the growth of the nematodes, agar culture media inoculated with an *E. coli* strain OP50 as source of food were used (Brenner, 1974). For RNAi *E. coli* strain HT115 was used.

E. coli (OP50) culture media

- 20 g peptone
- 5 g NaCl

- 0,01 g uracil
- Add 1000ml dH_2O (autoclave), adjust pH 4,7

LB medium by Luria-Bertani

- 10 g Bacto-tryptone
- 5 g bacto-yeast extract
- 10 g NaCl
- To 950 ml deionized H_2O

LB medium with Ampililin

- 200 ml LB medium
- 400 µl Amicillin

LB medium with Amp and Tet

- LB medium with ampicillin
- 1,5 % Tetracycline

Molecular cloning

Cloning of gene fragments for *in situ* hybridization probe synthesis

Degenerate primers for genes of interest were designed based on the available gene nucleotide sequences of other species from NCBI GenBank data base to isolate the partial cDNA fragments. The PCR amplified cDNA fragments were gel purified, cloned into pBluescript cloning vector (Promega, Madison, WI) and sequenced.

RNA extraction

Worms were grown on plates and approximately 0.5 - 0.75 g of worm were harvested. Following centrifugation they were shock frozen in liquid nitrogen. The pellets were then placed in Tri-Mix, 1 ml Tri-Mix per 25 mg worm, and homogenised for 30 min. The homogenised mixture was placed in 1.5 ml Eppendorf tubes, and 200 µl chloroform was added per 1 ml. After 5 min this was centrifuged at 14.000 g for 10 min.

The supernatant was pipetted into clean tubes, and 0.025 vol 1 M acetic acid and 0.5 vol 100% EtOH were added. This was allowed to precipitate overnight at -20 °C, followed by centrifugation for 20 min at 14,000 g. The supernatant was discarded

and the pellet was resuspended in 125 µl Gu-mix. 0.025 vol 1 M acetic acid and 0.55 vol 100% ethanol were added, and the suspension was left to precipitate overnight at –20 °C. The solution was then centrifuged and the supernatant discarded, and then washed twice in 500 µl 70 % ethanol. The RNA pellet was finally dissolved in 20 µl H_20 treated with diethyl pyrocarbonate (DEPC).

Table 3: List of buffers used for RNA extraction

Reagents	Composition
Guanidinium thiocyanate solution	4 M Guanidinium thiocyanate (GuSCN) 0.5% Sarcosyl 25 mM Sodium Citrate (pH 7.0) Solution heated to 65 °C to dissolve (GuSCN)
Guanidinium mix (Gu-Mix)	360 ml β-Mercaptoethanol 50 ml Guanidinium thiocyanate solution
TRI-Mix	500 µl Gu-Mix 500 µl Phenol (pH 4.0) 100 µl 2 M Sodium acetate (pH 4.2)

cDNA synthesis from Total-RNA

To synthesis cDNA, a reaction mixture with a total volume of 20 µl was prepared as follows. X µl (5 ng) from the extracted RNA was added to 2 µl 3' CDS primer at room temperature and the mixture was incubated at 70 °C in a water bath for 5 min and then cooled on ice. 1 µl RiboLock™ (Fermentas), 1 µl dNTP-mix (10 mM) and 4 µl 5x buffer was added and incubated for 2 min in a 43 °C water bath. 1 µl Reverse transcriptase was added, and the solution was left for a further 90 min at 43 °C to allow the reverse transcription of the RNA into cDNA, thereupon immediately put on ice to stop further transcription. Following this, the solution was increased to 100 µl with the addition of 80 µl H_20.

Polymerase chain reaction (PCR)

The polymerase chain reaction is a method for the in vitro amplification of target genes (Mullis et al., 1986). It is based on a repetitive cycle of the three steps: DNA

denaturation, hybridization of the primers to the DNA template, and elongation of the primers by polymerases. Critical to the rapid and uncomplicated success of PCR is the use of thermostable polymerases.

Because the *Taq*-Polymerase is not working correctly, the *Pwo*-Polymerase was used in addition. *Pwo*-Polymerase has got proof-reading activity, thus avoiding mistakes in the process of amplification. An advantage of the *Taq*-Polymerase is the production of an adenine overhang that is useful for TA-cloning. The following components were prepared for a PCR reaction.

Standard PCR reaction mixture:	**total volume of 50µl**
Template	2 µl
TL buffer (10x)	5 µl
$MgCl_2$ (50 mM)	2 µl
dNTPs (10 mM)	1 µl
Forward primer (10 mM)	2 µl
Reverse primer (10 mM)	2 µl
Taq/Pwo-Polymerase (0,5 U/µl)	3 µl
H_2O	33 µl

Table 4: PCR reaction conditions

94 °C	1 min	
75 °C	Pause	Initial denaturing
X cycles		Addition of polymerase
94 °C	30 sec	
X °C	30 sec	Denaturing
68 °C	X min	Annealing
Final		Elongation
68 °C	10 min	
72 °C	10 min	Elongation, proofing
20 °C	∞	

X represents a number that varied according to the required amplification (cycles), the particular annealing temperature of the primers being used, or the time needed to create the size of the template/desired product (elongation).

Table 5: PCR reaction solutions for the different PCR types used. Amounts in µl

Solutions	Degenerated	Gene specific	Colony	Sequencing
TL buffer (10x)	5	5	2.5	-
$MgCl_2$ [50 mM]	2	2	1	-
dNTPs [10 mM]	1	1	1	-
Reagent Mix*	-	-	-	2
H_20	17	33	17.5	6
Template	2	2	-	1
Forward primer [10 mM]	10	2	1	1*
Reverse primer [10 mM]	10	2	1	1*
Taq/Pwo polymerase	3	3	1	-
Total	50	50	25	10

* For sequencing PCR, the reagent mix came from the BigDye® Terminator v3.1 Sequencing kit (Applied Biosystems, Darmstadt). Either forward or reverse primers were used accordingly.

Degenerated PCR

Known PAR-6 protein homologs from different organisms were retrieved from GenBank (http://www.ncbi.nlm.nih.gov/) a multiple sequence alignment was constructed using the Clustal W programme (Thompson et al., 1994). From the conserved block of amino acids, degenerated primer pairs were designed and used for degenerate PCR. As template, the synthesised *Acrobeloides sp.* (PS1146) cDNA (section 2.3.2) was used to amplify the conserved region of the *Acrobeloides sp.* (PS1146) *par-6* gene.

To avoid non-specific binding, hot start PCR was performed unless otherwise stated. In this case, the PCR reaction was first heated up to 94 °C for complete degeneracy and afterwards cooled down to 75 °C. At 75 °C the polymerase was added. Thus the annealing of the primers begins at higher temperatures, with more specificity.

PCR with gene specific primers

Gene-specific PCR primers were generated on the basis of the well-known nucleic acid sequences of the initial fragments following PCR with degenerated primer. For each pair of primers chosen, the annealing temperatures were adjusted to a maximum difference of 2 °C.

Nested and semi-nested PCR

For nested PCR the PCR product of a preceding PCR was always used as template. Nested PCR involves two sets of forward and reverse primers that lie within the primers used for the first PCR. A modification of the nested PCR was the semi-nested PCR where a new single nested primer was used. The second primer corresponds already to one of those used in the first PCR thereby increases the purity and specificity of the product.

Colony PCR

A colony PCR was designed to quickly screen for positive plasmid inserts and correct insert size directly from transformed *E. coli* colonies using either universal T3 and T7 or M13 and Reverse primers. For the template, bacteria colonies are used. The reaction for colony PCR was first heated to 96 °C for 5 min to set free the DNA from the bacteria sample.

Rapid amplification of cDNA ends (RACE)

RACE PCRs allow the amplification of full-length cDNA when just a part of the sequence is known. Usually the known sequence is the coding sequence of a gene. Based on this, the gene ends can be defined by RACE PCR.

5´RACE takes advantage of the spliced leader sequence at the beginning of the 5´end (Blumenthal, 2005). Priming at this sequence facilitates the generation of the 5´cDNA.

The poly (A) tail at the 3´end of mRNAs is used as a priming site in the 3´RACE. The use of an Oligo-dT-adaptor primer allows the addition of a specific sequence to the 3´end. An antisense-primer that is complementary to the adaptor sequence is utilized for the amplification of the 3´cDNA. To obtain highly specific sequences, RACE PCR was carried out in a nested variant with the use of two primer pairs.

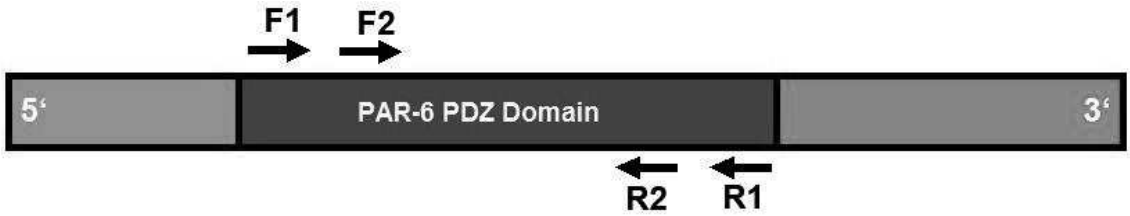

Figure 3.1: Scheme for *par-6* RACE PCR. The position and orientation of the primers used for *par-6* RACE PCR are shown with arrows. Primers marked in grey were used for 5´RACE PCR. Primers shown in black were used for 3´RACE PCR.

Agarose gel electrophoresis

This was used to visualise and verify the quality of the PCR products and restriction endonuclease digests. Unless otherwise stated, a 1 % agarose gel was used. The gel was made using 0.5 X TBE and universal agarose, containing 5 μl of [10 mg/ml] ethidium bromide. The electrophoresis was done at a constant voltage of 110 V in 1X TBE buffer. The DNA bands were visualised using UV light and the gel was photographed in a UV (312 nm) light chamber with mounted camera (Olympus C2040 Zoom; Olympus, Hamburg) above. Digital processing was done using the ArgusX1 V2 software and the images were printed using a Mitsubishi P91D Thermoprinter.

Table 6: Solutions and buffers for agarose gel electrophoresis

• Ethidium bromide	1 g Ethidium bromide in 100 ml H_20
• TBE buffer (5X)	54 g Tris, 27.5 g Boric acid, 20 ml 0.5 M EDTA, in 1 L H_20
• TE buffer (0.5X)	0.045 M TrisBorate (pH 7.5); 0.001 mM EDTA
• Loading dye	30 % Glycerol, 0.3 % Bromophenol blue, 0.3 % xylene cyanol

Lambda genomic DNA (48kb) cut with PstI was used as a molecular weight marker to estimate the desired bands. Tracking of the runs were ensured by diluting the samples in 5 µl of loading dye.

DNA purification from Agarose gel

DNA purification from the 1 % agarose gel was done according to the QIAEX II Agarose Gel Extraction protocol (Qiagen GmbH, Hilden).

Ligation (T/A Cloning)

The pBluescript® II KS vector (Stratagene), was used for cloning. The vector was digested with the restriction enzyme *Eco*RV, followed by addition of 3' T overhangs by *Taq* polymerase (Hadjeb and Berkowitz 1996). The T/A cloning strategy used, is based on the fact that *Taq* polymerase predominantly adds an extra adenine overhang to PCR products during the final elongation stage of PCR.

Ligation reaction mix (10 µl)

- X µl DNA (10 ng, in Tris 10 mM pH 8.5)
- 1 µl ligase buffer (10X)
- 1 µl linearised pBluescript® KS vector (35 ng/µl)
- 0.5 µl T4 ligase
- 7.5 - X µl H_20

The ligation reaction was incubated overnight at 14 °C.

Transformation

Having ligated DNA into the vectors as described above, the vectors were used to transform competent *E. coli* XL-1 Blue cells (Inoue et al., 1990). 10 µl of the ligation solution was added to a 100 µl bacteria aliquot, and incubated on ice for 20 min. The cells were heat-shocked for 45 sec at 42 °C and left on ice for 3 min. 900 µl LB medium was then added to the cells, and incubated in an incubator shaker (New Brunswick Scientific, USA) for 1 hour at 37 °C. After an hour of incubation, 200 µl of the bacteria in solution was plated on selective LB plates containing 100 µg/ml ampicillin and incubated overnight at 37 °C.

Plasmid-DNA minipreparation

Bacteria colonies were picked and cultured at 37 °C overnight in 3 ml LB ampicillin medium. The overnight culture was centrifuged twice (2 min, 8.000 x g) discarding the supernatant each time. The bacterial pellet was resuspended in 200 µl of Merlin I solution to lyse the bacteria cells. 200 µl of Merlin II solution was added to the resuspended bacterial suspension and the tubes were inverted 10 times to clear the suspension. At next, 200 µl of Merlin III was added and left for 5 min at RT to neutralise the turbid solution. Then, the solution was centrifuged at 20,000 x g for 10

min. The supernatant without any cell debris (~ 600 µl) was transferred into identically labelled fresh tubes containing 1 ml of Merlin IV resin slurry. The suspension was further incubated for 5 min on the test tube rotator.

The resin-DNA slurry was loaded onto a fresh miniprep column assembled on a vacuum pump and the resin bed was allowed to be formed under constant suction. Due to a high salt buffer, DNA was selectively adsorbed onto the silica membrane of the column. In order to further purify the DNA, washing of the resin bed to remove protein contamination and salts proceeded twice with 1 ml each of potassium wash solution. The column matrix was left to dry via the vacuum pump for 7 min, removing any ethanol and liquid traces. The column was transferred onto a fresh tube and the plasmid DNA eluted by the addition of 50 µl 10 mM Tris pH 8.5 (warmed to 70 °C) to the column and briefly centrifugation at 10.000x g. The DNA eluted was stored at -20 °C for further use and also to prevent any degradation.

Table 7: List of buffers used for plasmid-DNA minipreparation

Merlin I	50 mM Tris HCl, (pH 7.6), 10 mM EDTA, 100 µg/ml RNAse A (DNAse free)
Merlin II	0.2 M NaOH, 1% SDS
Merlin III (500 ml)	61.35 g potassium acetate, 35.7 ml acetic acid, made up to 500 ml with sterile ddH_20
Merlin IV*	66.84 g Guanidium hydrochloride, 33.33 ml Merlin III, 15 g silica gel powder. Heat at 65 °C; bring to pH 5.5 with 10 M NaOH. Fill up to 100 ml with sterile ddH_20. Shake properly before use.
Potassium wash	1,6 ml 5 M potassium acetate, 830 µl 1 M Tris pH 7,5, 8 µl 0,5 M EDTA, 55 ml 100 % EtOH, filled up with sterile ddH_20 to a total volume of 100 ml

* Mixture stirred with gentle heating in a clean 250 ml glass beaker. The pH was adjusted to 5.5 using 10 M NaOH. Deionised H_20 was added up to 100 ml, before 15 g of silica gel powder was added and thoroughly mixed.

Restriction of plasmid DNA with restriction enzymes

The digested insert was cut out of the ligated plasmid with restriction endonuclease. 200 ng mini-prep product (DNA) was added to 2 µl 10x restriction buffer (dependant on the endonucleases used), 0.5 µl endonuclease, then adjusted to a final volume of

20 µl with H_20. This was incubated for 2 hours at 37 °C, and then checked for proper digestion by agarose gel electrophoresis.

Sequencing

DNA sequencing was done at the Cologne Center for Genomics (CCG, University of Cologne) with the ABI 3730 DNA Analyzer (Applied Biosystems) following the Sanger protocol (Sanger et al., 1977). Prior to sequencing, DNA was amplified via PCR using the Big Dye v3.1 Sequencing Kit and either forward or reverse vector specific primer.

PCR Reaction mixture:	**total volume of 10µl**
DNA from Mini-prep	100-200 ng
Sequencing buffer (5x)	2,25 µl
Primer (3 pM)	1 µl
Big Dye v3.1	0,25 µl
H_2O	x µl

Table 8: Sequencing PCR programme

Step	Temperature	Time	Cycles
Initial denaturation	96 °C	1 min	1
Denaturation Primer annealing Elongation	96 °C 45 °C 60 °C	10 sec 15 sec 4 min	30

Identification and quantification of nucleic acids

Photodocumentation

DNA fragments, separated via gel electrophoresis, were illustrated under UV light on a UV light desk. Gel photos were taken with a camera (Olympus, C2040 Zoom) and they were digitally processed with the help of the ArgusX1 V2 software. Additionally, agarose gel pictures were printed with the Mitsubishi P91D Thermo printer.

Determination of concentration by Nanodrop

The quantification of nucleic acids was carried out on the nanodrop spectrophotometer. 1 µl of nucleic acid was utilized for the OD measurement. For determining the quality of the nucleic acid, the OD_{260}/OD_{280} ratio was evaluated.

Poly-L-Lysine slides

Teflon- coated slides were utilized as embryo carriers for proper analysis. First of all, dirt and fat were cleaned off the slides with EtOH. After drying of the slides, 2 µl Poly-L-Lysine was pipetted onto a well of the slide and quickly uniformly distributed with a pipette tip. The slides were incubated for at least 20 minutes at 70 °C.

Used solution

Poly-L-Lysine:

- 200 ml H_2O
- 200 mg Gelatine
- 40 mg $CrK(SO_4)_2$ x 12 H_2O, solved at 40°C
- 1 mg/ml Poly-L-Lysine solution, solved for 12 hours

RNA interference

Using gene specific primers, partial sequences of the desired genes homolog from *Panagrolaimus* sp. (PS1159) were cloned and used to test for embryonic lethal RNAi phenotypes in mixed nematode populations. Feeding constructs for RNA-mediated interference of the *Panagrolaimus* sp. PS1159 genes was be amplified by PCR using the gene specific primer pairs and cloned into the L4440 expression vector. Cloned plasmids were transformed into HT115 feeding bacteria, an RNase III-deficient *E. coli* strain with IPTG-inducible expression of T7 polymerase. Standard NGM agar plates containing 1 mM iso-propyl-β-Dthiogalactopyranoside (IPTG), 50 ug/ml ampicillin and 12.5 ug/ml tetracycline were prepared. The plates were seeded with the HT115 feeding bacteria transformed with an L4440 plasmid vector containing the target gene fragment. The transgenic feeding bacteria serve as food source for the *Panagrolaimus* nematodes. GFP construct is used as a negative

control. The plates were grown at 20 °C overnight to allow bacteria lawn to form and begin induction and expression of dsRNA for the target genes.

Axenised eggs were prepared from gravid *Panagrolaimus* sp. PS1159 nematodes by bleaching adult worms with hypochlorite. The axenised eggs were subsequently washed several times in PBS to remove excess hypochlorite including bacterial contamination, and then spread onto the prepared NGM agar plates. Ingestion of the HT115 bacteria should generate an RNAi effect in *Panagrolaimus* sp. (PS 1159). The plates were incubated at 20°C and allowed to develop until L3/L4 stage.

In order to verify the RNAi effect, single L3 or L4 larvae are transferred onto a 12-well NGM/IPTG/Amp/Tet agar plate and monitored daily. Staged animals are allowed to grow to adulthood and lay eggs until laying ceased. The number of the eggs laid per adult worm was scored after removal of the parent worm from the plates. Hatched progeny were subsequently monitored for any developmental abnormalities and or embryonic lethal RNAi phenotypes. Counts of surviving embryos from control and RNAi treated cultures were calculated and compared.

Collection of Embryos

Embryos from the nematode of interest were washed off from the agar plates and collected in glass cups. All liquid was removed, and then 150 µl hypochlorite solution added to the embryos in order to break open the eggshell and to eliminate bacteria. The incubation time depended on the nematode species, but lasted on average two to three minutes. Subsequently, cold PBS was filled in the glass cups for the inactivation of hypochlorite. The embryos were first washed thrice with 500 µl cold PBS and then thrice with 500 µl cold water. After each washing step the embryos were centrifuged for one minute at 750 x g and the supernatant was discarded. The eggs were glued onto poly-L-Lysine coated slides and covered with a cover slide (24x32 mm). For storage, the slides were frozen in liquid nitrogen.

Hypochlorite solution:

- 12 parts sodium hypochlorite
- 5 parts KOH 5 M
- 17 parts dH_2O

Table 9: Duration of hypochlorite treatment

Species	Hypochlorite treatment (sec)
Acrobeloides nanus	90
Acrobeloides sp. (1146)	90
Diploscapter coronatus	120
Panagrolaimus sp. (PS1159)	90
Panagrolaimus sp. (JU765)	120
Panagrolaimus superbus	105

Construction of the expression vector for PAR-6 protein antibody production

From the 5' end of *Acrobeloides* sp. (PS 1146) *par-6* cDNA sequence, the gene was cloned starting at the translated amino acid position 14 into the expression vector pQE30 (Qiagen). This construct produced an N-terminal 6xHis Tag (MRGSHHHHHHGS-*par-6).* In order to obtain the desired *par-6* gene fragment, cloning was done by PCR using the gene specific primers *par-6expfor* and *par-6exprev*. The plasmid was cleaved with BamHI and *Hin*dIII before the isolated *par-6* fragment was ligated into purified pQE30 vector. The ligation mixture was transformed into the *E. coli* strain M15 cells. Ligation and transformation were carried out using T4 DNA ligase. Transformants were selected on plates containing both ampicillin and kanamycin. They were screened for correct insertion of coding fragment by restriction analysis of the pQE-30 plasmid DNA and sequencing of the cloning junctions.

Protein induction

Culturing was done overnight at 37 °C in 3 ml LB medium with Kanamycin (25 µg/ml) and Ampicillin (100 µg/ml) with shaking. The next day, 10 µl overnight culture was added to 5 ml LB medium diluted 1:20 with Ampicilin and Kanamycin and incubated at 37 °C for 1 hour. To induce protein expression, 5 µl IPTG was added and allowed to grow at 37 °C for 4 hours. The cells were grown at 37 °C on a shaker until an OD_{600} betwenn 0,8 and 1 was reached. Before protein expression, a 1ml sample as a noninduced control was taken. The cells were pelleted at 8000 x g for two minutes and stored at -20 °C until further analysis. Protein expression was started by induction with IPTG to a final concentration of 1mM. Expression was held for at least three hours. At the end of the expression period, a 1ml sample as an induced control

was taken and the cells were also pelleted. All other cells were harvested by centrifugation at 10000 x g for 25 minutes. They were stored at -20 °C until further use. For a negative control, one culture was grown without IPTG.

Solutions

LB medium with ampicillin and kanamycin:

- 1000 ml LB medium
- 2 ml ampicillin
- 500 µl kanamycin

Cell lysis

For efficient cell lysis, the reagent GuHCl was utilized for lysis under denaturing conditions. The cell pellet was resuspended in lysis buffer A at 5ml per gram pellet weight. The supernatant was discarded and the cells lysed by resuspending the pelleted cells in a 50 µl mixture of 100 µl beta mecaptoethanol in 1ml SDS. To further denature the expressed protein, the pellet was boiled for 15 min with intermittent vigorous vortexing, and then centrifuged for 5 min at full speed. To pellet the cellular debris, the lysate was centrifuged at 1377x g for 30 minutes. The supernatant, which contains the cleared lysate, was was transferred into a new tube.

Solutions

Lysis buffer A:

- Lysisbuffer X
- 6 M GuHCl
- • adjusted to pH 8

Purification of recombinant protein

For purification of the recombinant protein, the 6xHis tag of the protein is exploited. The Tag enables the binding of the protein to Ni-NTA resin. Protein binding was carried out in a batch mode, as well as washing and elution. 0,5ml Ni-NTA per 10 ml cell lysate was added and mixed for 60 minutes on a rotator. The lysate-resin mixture was centrifuged for 10 minutes at 1377x g. Then, the pellet was washed twice with 15 ml washing buffer. A centrifugation step for three minutes followed

after each washing. The wash fractions were collected and stored at -20 °C. The protein was eluted several times in 1ml elution buffer. Each time, the sample was centrifuged for three minutes. Protein fractions were stored at -20 °C.

Solutions

Wash buffer:

- 100 mM NaH_2PO_4
- 10 mM Tris
- 8 M urea
- adjusted to pH 6,3

Elution buffer:

- 100 mM NaH_2PO_4
- 10 mM Tris
- 8 M urea
- adjusted to pH 4.5

Extraction of Antibodies from Serum

At first, serum was diluted with an equal volume of PBS. While the serum was stirred gently, an equal volume of saturated ammonium sulfate (4,1 M at 25°C) was added slowly by drop wise. The solution was kept at room temperature for 60 minutes. Subsequently, the solution was centrifuged at 1377 x g for 22 minutes. The supernatant was discarded and the precipitate was resuspended in PBS and that in the same volume of the original serum. Its half volume of ammonium sulfate was added slowly under mixturing conditions followed by incubation at room temperature for 60 minutes. The solution was centrifuged again at 1377 x g for 22 minutes and the supernatant was removed. After that, the precipitated antibody was resuspended in a small volume PBS (1/5 of the original serum). The antibody solution was stored at 4 °C.

Solutions

PBS:

- 4 mM KH_2PO_4
- 16 mM Na_2HPO_4
- 115 mM NaCl
- filled up with H_2O to a total volume of 1000 ml, adjusted to pH 7.4.

Composition of SDS PAGE resolving and stacking gels

Resolving gel

Solution components	Component vol (ml) per gel mould vol 5 ml
H_20	1.6
30 % Acrylamide mix	2.0
1.5 M Tris (pH 8.8)	1.3
10 % SDS	0.05
10 % ammonium persulfate	0.05
TEMED	0.002

Stacking gel

Solution components	Component vol (ml) per gel mould vol 4 ml
H_20	2.7
30 % Acrylamide mix	0.67
1.5 M Tris (pH 6.8)	0.5
10% SDS	0.04
10% ammonium persulfate	0.04
TEMED	0.004

Staining and destain solutions

Solution	**Composition**
Staining solution	0.25 % Commassie Brillaint blue R250, 50 % Methanol, 10 % acetic acid, 40 % H_20
Destain solution	5 % methanol, 2.5 % acetic acid, 92.5 % H_20

For detection and analysis of proteins expressed from the cloned genes, the following gels were used for SDS PAGE analysis. 15 µl was loaded onto an SDS PAGE gel and electrophoresed at 70 V for 30 min and then 100 V.

Preparation of digoxigenin-labelled RNA probes

PCR to generate probe synthesis template

PCR reactions with gene specific primers were used to amplify the desired template from *Panagrolaimus* cDNA. The amplified gene sequences were cloned into the linearised pBluescript II KS vector (containing promoters for T3 or T7 bacteriophage RNA polymerases). The eluted DNA was then ligated overnight, and used to transform bacteria, followed by a minipreparation. The minipreparation product plasmid DNA was sequenced to verify for the desired gene fragment. A PCR was performed using the M13 and Reverse primers with the correct plasmid DNA as template to further confirm amplification of the PCR product. The PCR product was run on a 1 % agarose gel, and the desired band corresponding to the cloned gene of interest was eluted and used for RNA probe synthesis.

Probe synthesis

The plasmid DNA was used as templates to generate the RNA probes, with the following reaction parameters: x µl PCR product (200 ng DNA), 1 µl RNA polymerase 10x buffer, 1 µl Digoxygenin (DIG) RNA labelling mix, 1 µl T3 or T7 RNA polymerase, 0.5 µl RiboLock™ RNAse inhibitor and add up to yield a total reaction mixture of 10 µl with H_20 (DEPC). After 2 hours incubation at 37 °C, 10 µl H_20 (DEPC), 2 µl EDTA [200 mM], 2.5 µl LiCl [4 M] and votexed before 80 µl ethanol (99.8 %, ice-cold) were added to the reaction, and again left at -20 °C overnight to precipitate. The next day, the solution was centrifuged at 4 °C for 20 minutes at 10.000 x g and the supernatant was discarded. The RNA pellet was washed twice in 200 µl 70 % EtOH (DEPC) and again dissolved in 25 µl H_20 (DEPC). 25 µl [12 M] LiCl was added to the RNA solution and vortexed. Further precipitation took place at -20 °C overnight. The same centrifugation and washing steps were repeated as in the previous day, and any residual EtOH was completely removed and the RNA pellet was shortly allowed to dry at room temperature. For longer storage, the RNA pellet was eventually stored in 70 % EtOH at -20 °C in order to prevent RNA degradation. Else while, the RNA pellet was resuspended in 25 µl H_2O DEPC, diluted 1:5 in hybridization mix and then used for *in situ* hybridization. To confirm

transcription and synthesis of RNA, 2 µl of the transcription reactions was verified on a 1 % agarose gel and measured with the nanodrop.

Preparation of embryos for *in situ* hybridisation

Worms were cultured on nutrient agar plates covered with a lawn of Escherichia coli, strain (OP50) as food source. Mixed-stage *Panagrolaimus sp.* (PS1159) embryos were collected and digested for 2 minutes in sodium hypochloride solution. The digestion reaction was stopped by washing three times with diluted PBS, followed by another three times washing with water. The pre-treated embryos were transferred onto poly-L-Lysin coated slides and covered with a glass coverslip. Care was taken not to burst open the embryos, as this would result in very high background. To permeabilise the embryos, the slides were shock frozen in liquid nitrogen and the coverslip immediately popped off. The slides were rehydrated by incubating in 100 % methanol (MeOH) at -20 °C. The embryo specimens were again washed consecutively for 15 minutes with 1 ml 90 %, 70 % and 50 % methanol to get rid of excess MeOH.

Fixation and hybridisation procedures were done as described by Seydoux and Fire (Seydoux and Fire, 1994) with some modifications. 1 ml Streck Tissue Fixative (STF) was added to the embryo preparations to fix them for 90 minutes at 37 °C, then washed twice in water and finally in 2 x SSC to rehydrate the embryos and get rid of the fixative.

Pre-hybridisation and hybridisation of the embryos

To prevent background staining, embryos were prehybridised for 90 minutes at 42 °C with a prehybridisation solution in a covered humidity chamber. 100 µl of the pre-warmed sense or antisense digoxigenin-labelled RNA probes were added accordingly to the specimens and incubated overnight at 42 °C in the humidity chamber. The embryos were subsequently washed twice with 2X SSC (2 times), once with 60% formamide buffer and again twice with 2X SSC for 10 min. To remove excess unbound probe, further washing was done in TN solution. The slides were then blocked with 5 % milk blocker solution and incubated at room temperature for 30 minutes.

The anti-DIG antibody diluted 1:2.000 with milk blocker solution was added to the embryos, and the probes incubated at 37 °C for 2 hours in the humidity chamber to avoid evaporation during incubation. The slides were again washed twice in TN and then TNM, for 10 minutes each. For detection, embryos were subjected to 100 µl of staining solution and carefully arranged onto the moist chamber. The top of the chamber was sealed and the colour reaction was left to develop at room temperature in the dark. The staining reaction was stopped by washing probes twice, in 500 µl stop solution for 15 minutes each. The anti-DIG-antibody conjugates to alkaline phosphatase and was visualized with the colometric alkaline phosphatase substrate NBT/BCIP (Nitro-blue terazolium)/5-Bromo-4chloro-3-indolyphosphate). The NBT/BCIP mix is advantageous due to the good localisation properties, high sensitivity and stability of precipitates. The embryo specimens were mounted in 50 % glycerol, sealed with nail polish.

Creation of linearized *in situ* probes

In situ probes were generated from a plasmid containing the desired gene. Therefore, the plasmid was linearized by restriction digest in the following scheme:

Reaction mixture: **total volume of 40 µl**

Plasmid	2 µg
Enzyme (10 U/µl)	0,5 µl
Buffer 10x	4 µl
H_2O	x µl

To create a probe of an appropriate length of 300-800 bp consisting of the gene of interest, an enzyme was chosen whose restriction site is located at the opposite side of the insert than the RNA polymerase promoter. To prevent fragmentation, the choice of an enzyme with its restriction site within the insert was avoided. Restriction digest was incubated overnight at 37 °C.

The next day, the mixture was filled up with H_2O to a total volume of 100 µl and the linearized plasmid DNA was isolated by phenol-chloroform extraction as follows; 100 µl of a Phenol/Chloroform/Isoamylalcohol mixture was given to the sample. After mixing, the sample was centrifuged for five minutes at 10000 x g. The upper phase was transferred in a new tube and 100 µl Cloroform was added. The sample was

vortexed and centrifuged and the upper phase was saved in a new tube. Then, 1/10 volume 3 M sodium acetate and 2,5 x volume 100 % EtOH were added. For DNA precipitation, the mixture was incubated at -20 °C for two hours. Afterwards, the sample was centrifuged for 20 min at 15000 x g at 4 °C. The supernatant was removed and 300µl 70 % EtOH was added to the sample. After a centrifugation step of five minutes at 15000 x g, the supernatant was discarded again. Plasmid DNA was shortly allowed to dry and then taken up in 10 µl H_2O DEPC.
The linearized and extracted DNA was now ready to use for RNA synthesis by RNA polymerases and so the following reaction was prepared:

Reaction mixture:	**total volume of 20 µl**
DNA	0,5 – 1 µg
Transcriptionbuffer 10x	2 µl
RNase Inhibitor (40 U/µl)	1 µl
RNA polymerase T3 or T7	2 µl
DIG labeling mix (10x)	2 µl
H_2O DEPC	xµl

For the purpose of later identification of the RNA, it was labeled with digoxigenin (DIG). The detection occurs with an Anti-DIG-antibody coupled to an enzyme that triggers a color reaction. RNA synthesis took place at 37 °C for two hours, followed by precipitation.
Therefore, 2 µl 0,2 M EDTA was added to the sample and it was vortexes. Furthermore 2,5 µl 4 M LiCl was filled into the tube and the content was vortexed again. After addition of 75 µl 100% EtOH, precipitation was carried out at -20 °C overnight. The following day, the sample was centrifuged at 10000 x g for 20 min at 4°C. The supernatant was removed and RNA was washed with 200 µl 70 % EtOH. A centrifugation step of five minutes at 10000 x g, at room temperature was performed. EtOH was discarded and replaced by 25 µl H_2O DEPC and 25 µl 12 M LiCl. Further precipitation took place at -20 °C overnight. The same steps of centrifugation and washing were repeated as the day before, but EtOH was completely removed and RNA was shortly allowed to dry at room temperature. Thereupon, RNA was

resuspended in 25 µl H_2O DEPC. The probe was stored at -20 °C until it was used for *in situ* hybridization. For longer storage, in order to prevent RNA degradation, the probe was diluted 1:5 in hybridization mix.

In situ hybridization

The *in situ* hybridization method is used for the detection of mRNA in cells or tissues. Crucial to the success of this method is the binding of the produced antisense RNA probe to the endogenous mRNA in the cell, and the later visualization of the hybridized RNA. Visualization was accomplished by an enzyme reaction.

In situ hybridization was performed on embryos, which were prepared as described in 2.4.2. At first, cover slides were removed rapidly with a scalpel without unfreezing of the embryos. With removal of the cover slides, it was aimed that the eggshell was further opened, making the embryos suitable for the *in situ* procedure. Fixation of the embryos started with incubation in cold 100 % MeOH for 30 minutes at -20 °C. Then, the slides were incubated in 90 %, 70 % and 50 % MeOH for 10 minutes each. After that, 50 µl of the 37 °C heated fixation solution (STF) was pipetted on the embryos and incubated for at least 30 minutes in a humidity chamber at 37 °C. The slides were washed in H_2O DEPC for 10 minutes, followed by a washing step in 2x SSC. To block unspecific binding sites, the embryos were incubated with 50µl prewarmed hybridization mix for 90 minutes at 42 °C in a humidity chamber. 50 µl *in situ* probe was given to each slide. Hybridization of the *in situ* probe with endogenous mRNA was done at 42 °C overnight. The next day, the slides were washed for 20 minutes at 42 °C at first with 2x SSC and then with formamide washing solution for 30 minutes. Two washing steps for 10 minutes with 2x SSC at room temperature followed. Next, the embryos were washed with TN solution. Thereafter, the slides were incubated with 50µl blocking solution (5 % milk in TN solution) for 30 minutes at room temperature. The slides were again washed in TN solution. Then, 50 µl anti-DIG antibody (1:2000 in blocking solution) was applied to each slide and incubated for 60 minutes at 37 °C in the humidity chamber. The anti-DIG-antibody, which is coupled with alkaline phosphatase, binds to the DIG labeled *in situ* RNA probe. Afterwards the slides were washed twice in TN solution and twice in TNM solution, for 10 minutes each. For visualization of the mRNA staining pattern, 50µl of

a developing solution was given on the slides. The developing solution contains the substrate for the alkaline phosphatase, which is located at the anti-DIG antibody. The alkaline phosphatase converts its substrate into a purple color that indicates the location of the mRNA. The developing solution was incubated until the purple color was observed. The reaction was stopped by washing the slides in stop solution. Additionally, 20 µl DAPI solution was given to the embryos for 30 minutes. In a final step, the slides were washed in stop solution and covered with a cover slide, after addition of 30 µl 50 % Glycerol/stop solution mixture to the embryos. Finally, the slides were sealed air-tightly with nail polish and stored at four degree until analysis by microscope.

Solutions used

20x SSC:

- 3 M NaCl
- 0,3 M sodium citrate

Formamide washing solution:

- 60 % Formamide
- 0,2x SSC

TN solution:

- 100 mM Tris pH 7,5
- 150 mM NaCl

Developing solution:

- 100 µl 1M Tris pH 9,5
- 30 µl 5M NaCl
- 25 µl 2M $MgCl_2$
- 500 µl 10% PVA
- 35 µl BCIP
  (50 mg/ml in 100% DMF)
- 4,5 µl NBT
  (50 mg/ml in 70 % DMF)
- 2 µl 0,5M Levamisol
- 304 µl H_2O

Hybridization mix:

- 50 % Form amide
- 10 % Dextransulfate
- 5x SSC
- 1 mg/ml DNA from herring sperm
- 0,1 mg/ml Heparin
- 0,1% Tween 20

TNM solution:

- 100 mM Tris pH 9,5
- 150 mM NaCl
- 50 mM $MgCl_2$

Stop solution:

- 1x PBS
- 50 mM EDTA

Western Blot

Proteins in a tissue sample can be detected by the western blot method. For this purpose, proteins must be separated via SDS-PAGE, transferred to a membrane, where they can be treated with antibodies for identification. For preparation of a lysate, embryos from the nematode of interest were collected in a reaction tube. The embryos were incubated three times alternately in liquid nitrogen and in a water bath at 37 °C. Recombinant protein and lysates were mixed with appropriate 2x SDS loading buffer and heated for 10 minutes at 95 °C. SDS-PAGE ran at standard conditions. A semi-dry transfer variant was executed for protein transfer. The blotting sandwich was constructed as follows: Three Whatman papers soaked in anode buffer II were placed on the anode plate. Thereon, three papers soaked in anode buffer I were placed. The used membrane Immobilon-P transfer membrane, Type PVDF (Millipore, Massachusetts, USA) was activated for five minutes by incubation in methanol and it then transferred onto the papers. After equilibration in cathode buffer, the gel was put on the membrane. Finally, three Whatman papers soaked in cathode buffer were placed on the gel. Protein transfer was performed for 90 minutes at 60 mA. For inspection of the transfer, protein bands were detected on the membrane by staining with Ponceau S for 5 minutes. The membrane was blocked for 60 minutes in 5 % milk powder/TBST and then washed for five minutes in TBST. The primary antibody, diluted in 5 % milk powder/TBST was applied to the membrane and further incubated at 4°C overnight under shaking conditions. Next, the membrane was washed thrice in TBST, each for 15 minutes. The incubation of the membrane in secondary antibody coupled to the alkaline phosphatase for two hours was done at room temperature. After antibody incubation, the membrane was washed for 15 minutes in TBST. The developing solution was given on the membrane and incubation took place in the dark until a colored reaction was observed. The enzymatic reaction was stopped by washing with TBST.

Solutions for Western blotting

Anode buffer I:

- 25 mM Tris
- 20 % MeOH
- adjusted to pH 10,4

Anode buffer II:

- 300 mM Tris
- 20 % MeOH
- adjusted to pH 10,4

Cathode buffer:

- 25 mM Tris
- 40 mM 6-aminohexanoic acid
- 20 % MeOH
- adjusted to pH 9,4

Ponceau S (10x):

- 2 g Ponceau S
- 30 g Trichloracetic acid
- 30 g Sulfosalicylic acid

TBST:

- 20 mM Tris
- 500 mM NaCl
- 0,05 % (v/v) Tween 20
- adjusted to pH 7,5

Developing solution:

- 50 mM Tris
- 5 mM $MgCl_2$
- 6,6 µl/ml BCIP
- 6,6 µl/ml NBT

Immunostaining

For visualisation of MAP kinase and MSP, we prepared and immunostained nematode gonads as described (Miller et al., 2001). Briefly,approximately 50 nematodes were dissected in 1× Egg Salts containing 0.01 % Levamisole (Sigma). After fixation in 3 % Formaldehyde (Science Services) for 1 h, specimens were washed (PBST) and incubated either with a monoclonal antibody against MAP kinase (1:1.500) that only recognises the activated, diphosphorylated form of the Erk1/2 activation loop (Sigma # M9692) or with a monoclonal antibody (1:400) raised against the C-terminus of *C. elegans* MSP (Kosinski et al., 2005). Secondary antibody was an Alexa Fluor R488 coupled goat anti-mouse antibody at a 1:1.000 dilution (Invitrogen). Microscopy was carried out with a Zeiss Axioskop fluorescence microscope. Pictures were taken with an AxioCam MRc camera (Zeiss) and arranged with the Keynote software (Apple). For detection of MSP in nematode lysates, 40 mg animals (mixed stage population) of the respective species were washed in H_2O, freeze-cracked twice in liquid nitrogen/ ice, and boiled for 10 min in SDS loading buffer. After electrophoresis on a 12 % SDS gel, proteins were electroblotted onto PVDF membranes under semidry conditions and subjected to Western detection. Primary antibody was the monoclonal anti-MSP antibody directed against the C-terminus of MSP (Kosinski et al., 2005) at 1:400 or, as a control, a 1:3.000 dilution of a mouse monoclonal anti-*α*-tubulin antibody (Sigma # T9026). Secondary antibody was a HRP-coupled goat anti-mouse antibody at

1:2.500 (Santa Cruz Biotechnology, Inc.). Antibodies were diluted in TBST/2 % milk powder. Autoradiographic films (Fuji) were developed according to standard protocols, digitally scanned and processed.

Antibody staining was performed on embryos, which were prepared as it is described above. First of all, cover slides were removed without unfreezing of the eggs. For fixation, the embryos were primarily incubated for 15 minutes in methanol at -20 °C and then for 15 minutes in acetone at -20 °C. The slides dried for 30 minutes at room temperature, then incubated in PBST for 15 minutes. For blocking of unspecific binding sites, 100 µl PBST-5 % FCS was applied to the embryos for 30 minutes. After a short washing step in PBST, the primary antibody diluted in PBST-2,5 % BSA and 50 µl of the antibody solution was applied onto the embryos. Incubation was performed in a humidity chamber at 4 °C overnight. The next day, the slides were washed thrice for 20 minutes each in PBS. 50 µl of secondary antibody, diluted in PBS, was given to the embryos and it incubated for two hours at room temperature in a humidity chamber. Then, the slides again were washed thrice for 20 minutes each in PBS. In the end, 30 µl DABCO was applied to the slides and then covered with a cover slide. To store the slides for a longer time, they were sealed with nail-polish.

Table 10: Antibodies and fluorescent dyes used for staining

Antibody/Dye	Organism	Dilution	Source
primary antibody: anti-P-granules L416	Mouse	1:70	Strome and Wood, 1983
secondary antibody: anti-rabbit-Alexa Fluor 488	Goat	1:2000	Sigma (Munich, Germany)
DAPI	-	1 µl/ml	-

Solutions

PBST:

- 4 mM KH_2PO_4
- 16 mM Na_2HPO_4
- 115 mM NaCl
- 0,1 % (v/v) Tween-20
- filled up with H_2O to a total volume of 1000 ml, adjusted to pH 7,4

PBST-BSA:

- 1x PBS
- 2 % BSA
- 0,5 % Tween-20
- 1x NaN_3

DABCO:

- 25 mg DABCO, solved in 1 ml 1x PBS
- 9 ml Glycerine

Light microscopy

The aim of microscopy is the magnification of an image, which is normally too small for the resolution of the human eye. Light, that is reflected from the object or that is passed through the object, is directed through a lens system (objective and ocular). One type of light microscopy is the differential interference contrast microscopy was used for high-contrast imaging of samples. In this case, differences in the optical density of the specimen are converted into contrast variations thereby providing an artificial spatial impression of the image.

Fluorescence microscopy

The method makes use of the fact, that a fluorochrome can be stimulated with light of a specific wavelength, resulting in an emission of light of another wavelength. This fluoresced light is imaged through the microscope objective. In this study, fluorochrome coupled antibodies were used for the detection and localisation of proteins.

Chemicals and Reaction Kits

The chemicals and consumables used during this thesis were purchased from the following companies:

- AppliChem (Darmstadt, Germany)
- Bio-Rad (Munich, Germany)

- Fermentas GmbH (St. Leon-Rot, Germany)
- Fluka (Buchs, Switzerland)
- Merck (Darmstadt, Germany)
- Roth (Karlsruhe, Germany)
- Sigma (Munich, Germany)
- VWR (Darmstadt, Germany)

Furthermore, all reaction kits used are summarized below. The kits were used according to the manufacturer and their supplied manuels.

Reaction Kits used

Reaction Kit	Company
Big Dye v3.1 Sequencing	Applied Biosystems
Invisorb Spin Plasmid Mini Two	Invitek (Berlin, Germany)
QIAEX II Gel Extraction	Qiagen (Hilden, Germany)

Laboratory Equipment

Table 11: List of equipment used

Equipment	Type	Manufacturer
Binocular	Stemi 2000	Zeiss (Germany)
Blotting chamber	-	Peqlab (Erlangen, Germany)
Centrifuge	5425	Eppendorf (Hamburg, Germany)
	5810R	Eppendorf (Hamburg, Germany)
	Heraeus Fresco 21	Thermo scientific (Germany)
	Heraeus Pico 21	Thermo scientific (Germany)
	Avanti J-E	Beckman Coulter (Krefeld,
	Z300	Germany)
	Galaxy Ministar	Hermle (Wehingen, Germany)
		VWR International (USA)
Drying chamber	Heraeus function line	Heraeus (Hanau, Germany)
Freeze dryer	-	Chaist
Incubator	BD 53	Binder (Tuttlingen, Germany)
Incubator shaker	Innova 40	New Brunswick Scientific (New

		Jersey, USA)
Magnetic stirrer	VMS-C7	VWR (USA)
Microscope	Axio Imager Z.2	Zeiss (Germany)
Microscope camera	Axiocam MRm Axiocam ICc1	Zeiss (Germany)
Microscope Objectives	10x/0,45 Plan-Apochromat 20x/0,8 Plan-Apochromat 60x/1,4 oil Plan Apochromat	Zeiss (Germany)
Microscope oil	Immersol 518N	Zeiss (Germany)
PCR machine	Personal Thermocycler Professional Thermocycler Peqstar 2xgradient	Biometra (Göttingen, Germany) Biometra (Göttingen, Germany) Peqlab (Erlangen, Germany)
pH meter	Seven Easy pH	Mettler Toledo (Schwerzenbach, Switzerland)
Pipette	P2, P20, P200, P1000	Gilson (Middleton, USA)
Pipettus	Accu-Jet	Brand (Germany)
Power supply	Peq power 300 EPS 200	Peqlab (Erlangen, Germany) Pharmacia Biotech (Germany)
Scale	AC211S TE3102S	Sartorius (Germany)
SDS gel chamber	45-1010-i	Peqlab (Erlangen, Germany)
Spectrophotometer	Nanodrop 1000 Nanospec Plus	Peqlab (Erlangen, Germany) Amersham Biosciences (Germany)
Thermomixer	Thermomixer compact 5350	Eppendorf (Hamburg, Germany)
Tube rotator	Tube rotator H560-VWR-230EU	Snijders scientific (Netherlands) VWR International (USA)
UV light desk	UV light table 312nm	Bachofer (Reutlingen, Germany)
Vacuum pump	MZ2C/1.7	Vacuubrand (Wertheim, Germany)
Vortex	Genie 2	Scientific Industries (USA)
Water bath	Sub Aqua 2	Grant (Cambridge, England)

Computer software and databases

Sequence analysis was done with the aid of Geneious (www.geneious.com). For identification of sequence similarities, the Basic Local Alignment Search Tool (Blast)

was used (Altschul et al., 1990). All images were processed with AxioVision Rel. 4.8 (Zeiss) and Adobe Photoshop Elements 8 (Adobe).

The following databases were used in this thesis:

- NCBI (http://www.ncbi.nlm.nih.gov/)
- PubMed (http://www.ncbi.nlm.nih.gov/pubmed/)
- Wormbase (www.wormbase.org)
- GeneMANIA (www.genemania.org/)
- Augustus (http://bioinf.uni-greifswald.de/augustus/)

Genes identified from the *C. elegans* gene networks were searched for in available nematode genomes from various clades for homologous partners. Genome sequence data from the *Panagrolaimus sp.* (PS1159) and the *Propanagrolaimus sp.* (JU765), as well as *R. culicivorax* were kindly provided by Phillipp Schiffer (Schierenberg lab, University of Cologne). *A. nanus* was chosen as the representative of the genus *Acrobeloides* since its genome was readily accessible thanks to Itai Yanai's lab (Technion Haifa, Israel), and *D. coronatus* from Yuji Kohara (NIG, Mishima, Japan). The *Caenorhabditis* genomic data and genomes from the other nematodes are largely accessible from the *C. elegans* Sequencing Consortium (1998) and at the National Center for Biotechnology Information (NCBI) respectively.

3 Results

3.1 P granules distribution in nematodes

The nematode *C. elegans* has been a very fruitful model system for the study of germline granules ("P granules",). P granules contain a heterogeneous mixture of RNAs and proteins which can be visualized with antibodies (Strome and Wood, 1983). In the present study *C. elegans* P granule staining was used as a starting point to establish a suitable staining method for other species, and also to serve as a reference for comparison. To visualise P granule presence, localisation and staining patterns in other closely related species of the Rhabditidae, Panagrolaimidae and Cephalobidae (see Figure 1-2), antibodies generated against *C. elegans* P granules were used, which have been reported to show cross-reactivity with P granules in several nematode species (Goldstein et al., 1998).

P granule staining in *C. elegans* as reference system

It has been shown in *C. elegans*, that P granules are detectable in the uncleaved zygote as prelocalised particles at the posterior pole of the embryo when stained with monoclonal antibodies (Pitt et al., 2000). After the first cleavage during early embryogenesis, granules are dispersed throughout the cytoplasm of the P1 cell only (Figure 3-1a). This distribution is maintained up to P3 (Figure 3-1d). In subsequent divisions, they are progressively segregated into the P2, P3, and P4 blastomeres (Figure 3-1b-d). From P3 onwards in *C. elegans* (Figure 3-1d), the granules appear more condensed and localised primarily around the outside of the nuclear envelope of the P4 germ cell when it is born (Figure 3-1e). The uniform cytoplasmic distribution of P granules is therefore only a brief period that takes place during early embryogenesis. When P4 divides around the 100-cell stage into Z2 and Z3 (Laugsch and Schierenberg, 2004), the P granules are segegrated in a perinuclear fashion into Z2 and Z3, both of which are stained (Figure 3-1g, f), and do not divide during the remainder of embryogenesis until midway through the first larval stage (Figure 3-1g).

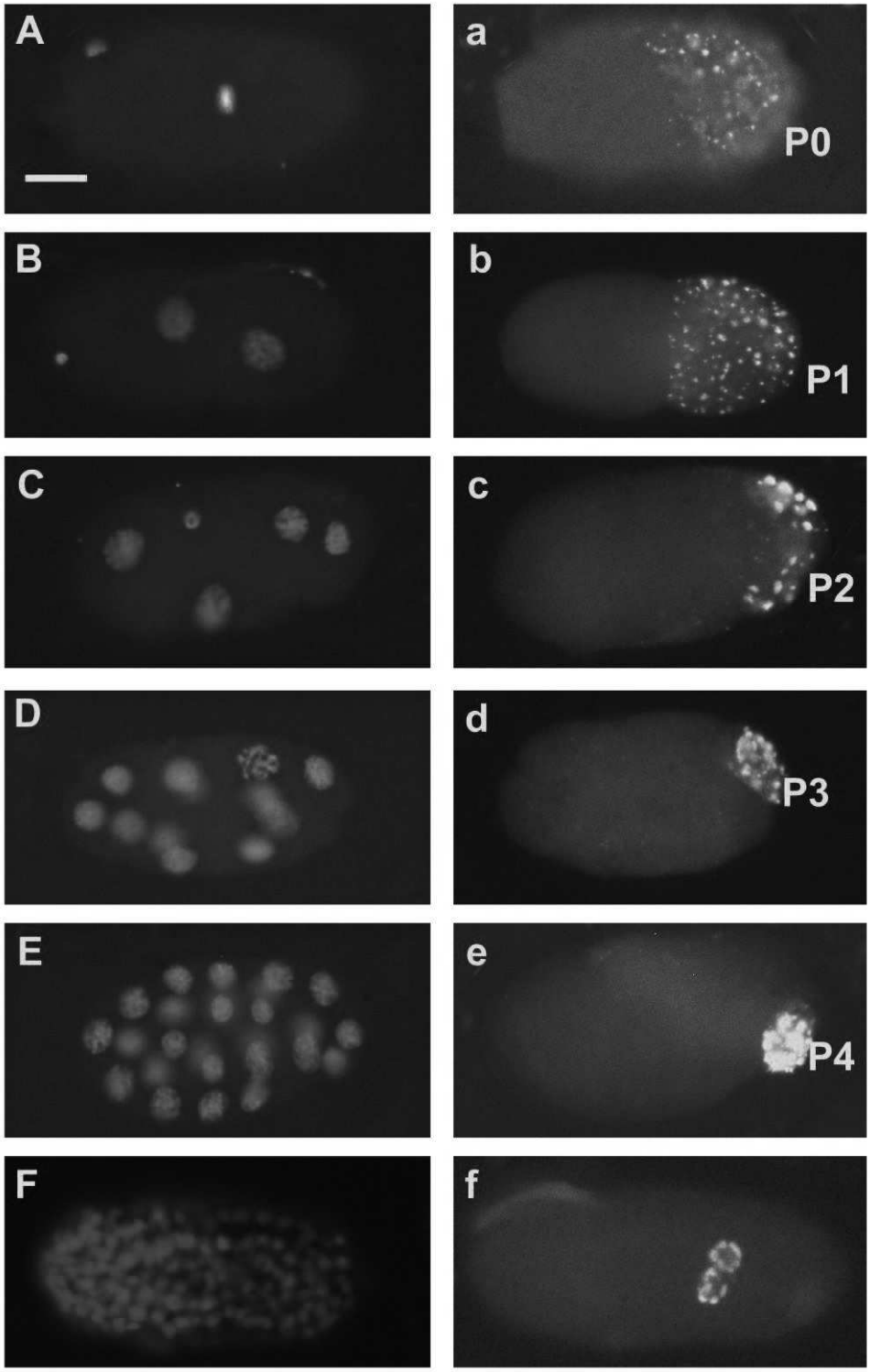

Figure 3-1: Localisation of P granules in *C. elegans*. The left panel (A-F) shows DAPI stained nuclei, and the right panel (a-f) shows P granule. a) 1-cell stage embryo P0, P granules are evenly distributed only in the cytoplasm of the posterior part of the fertilised embryo. b) 2-cell stage, the P granules are evenly dispersed in the cytoplasm of P1. c) 4-cell stage, P granules are evenly distributed in the cytoplasm of P2 only. d) Approximately 12-cell stage, with evenly distributed P granules only in the cytoplasm of P3. e) Approximately 24-cell stage, P granules mainly in P4, associated with nuclear membrane. f) Embryo with several hundred cells showing pernuclear staining of P granules in adjacent Z2 and Z3 cells. Epifluorescence, with embryos are orientated with the anterior side to the left. Scale bar = 10 µm.

3.1.1 Cross reactivity of *C. elegans* P granule antibody

Cross reactivity of *C. elegans* P granule antibody but significant differences in timing of perinuclear localisation of P granules in nematode species

C. remanei and *C. briggsae* are the closest relatives of *C. elegans*; while *C. remanei* is dioecious, *C. briggsae* is also hermaphroditic as is *C. elegans* (Cho et al., 2004; Kiontke et al., 2004). However, hermaphroditism in both sister species apparently evolved independently (Hill et. al., 2006). It was therefore imperative to verify if the *C. elegans* P granules antibody would cross react in these closely related species and also if the P granules staining patterns within these species could be correlated to the type of the reproductive mechanism in these nematodes.

In *C. briggsae,* the P granules are evenly distributed in the posterior cytoplasm in the germline cell P1 (Figure 3-2a) as in *C. elegans*. They are later exclusively segregated to the P2 cell, but in contrast to *C. elegans*, P granules in *C. briggsae* are mainly associated with the nuclear membrane and only a few are freely dispersed in the cytoplasm (Figure 3-2b). Perinuclear localisation of P granules becomes prominent in the P3 and P4 cells, as well as in both P4 daughters Z2 and Z3 (Figure 3-2c-d). This apparent association of P granules with the nuclear membrane is similar to the staining pattern observed in *C. elegans* (see above).

Examining the distribution of P granules in the dioecious *C. remanei,* it was observed that their distribution is cell cycle dependent (Figure 3-2 f-j). During interphase, the P granules were evenly distributed in the cytoplasm in P1 (Figure 3-2f). However, with the onset of mitosis, most of the P granules were observed to be associated with the nuclear membrane, and only a few remained freely distributed in the cytoplasm (Figure 3-2g). During interphase P granules were evenly distributed in the cytoplasm prior to cell division in the P3 cell (Figure 3-2h). However, with the beginning of prophase, P granules were again localised around the nuclei of all successive germline cells (Figure 3-2i-j).

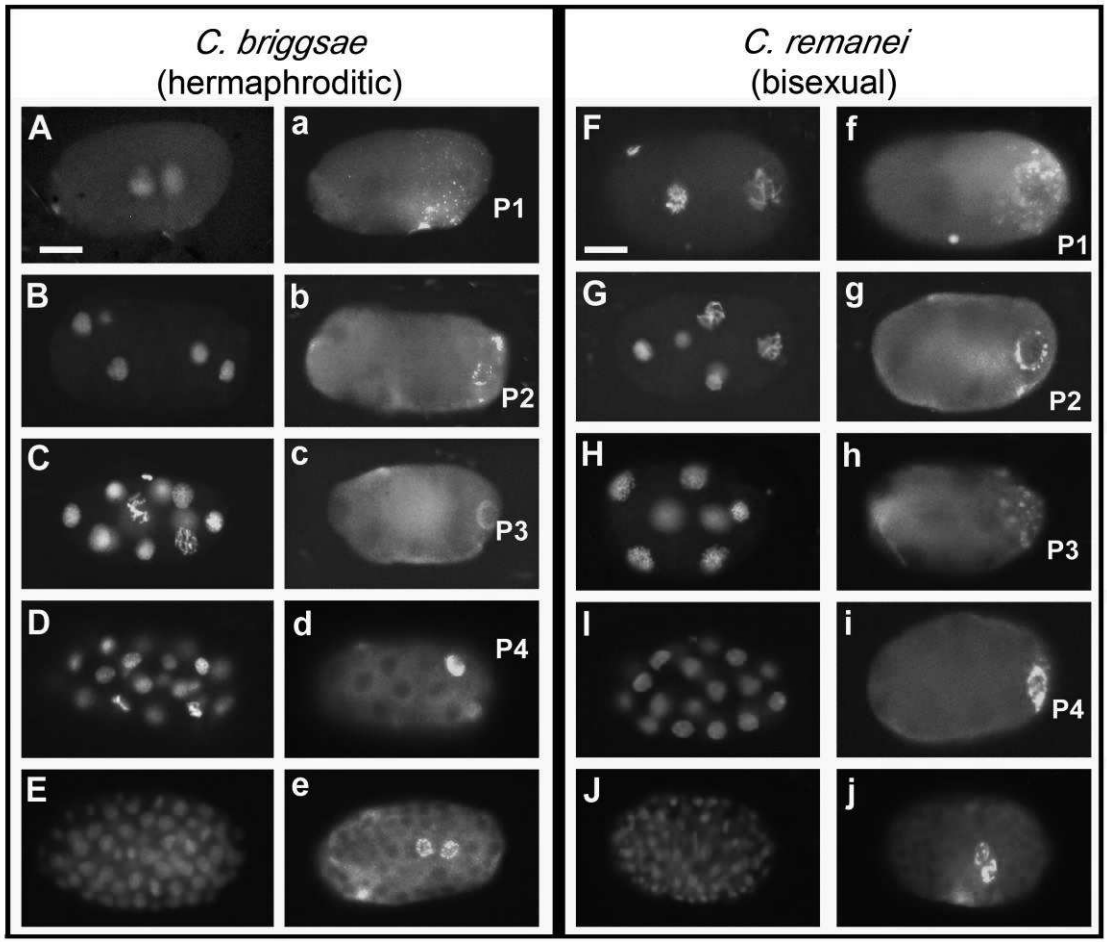

Figure 3-2: P granules distribution in the hermaphroditic *C. briggsae* and the dioecious *C. remanei*. Nuclei are DAPI stained in blue, and the respective right panels show P granule staining images. In both *C. briggsae* and *C. remanei*, as early as in the 2-cell stage P granules are localised evenly in the cytoplasm of the P1 cell and then become associated mostly with the nuclear envelope in P2, P3 and P4. Note the early perinuclear cell-cycle dependent localisation of P granules in *C. remanei*. In the late embryogenesis stages, perinuclear localisation of P granules in Z2 and Z3 was seen in both species. Embryos are orientated with the anterior side to the left. Epifluorescence. Scale bar = 10 µm. (Fotos, U. Greczmiel).

Our results demonstrate that the *C. elegans* P granules antibody also detects P granules in other *Caenorhabditis* species but the staining patterns differ significantly. In *C. briggsae* P granules are more focused around the nucleus to segregate to the next germ cell (Figure 3-2a-e) while in *C. remanei* they appear to be distributed in a cell cycle dependent manner prior or shortly after mitosis (Figure 3-2 f-j). Unlike in *C. elegans* where a late perinuclear localisation of P granules starting in the P3 cell was observed (Figure 3-2d), in *C. briggsae* and *C. remanei* the P granules show an earlier perinuclear distribution in the P2 cell (Figure 3-2b-g). Furthermore, in *C. elegans*, as a result of P granules aggregating following each germ line division, the amount of P granules seem to increase in size in the resulting

primordial germ cell P4 (Figure 3-2e), while in *C. briggsae* and *C. remanei*, the size of these germ granules at P4 appear to have change little (Figure 3-2d-i). This may be due to the fact that the amount of residual P granules that is degraded in the somatic cells is greater in *C. briggsae* and *C. remanei,* than it is in *C. elegans*.

3.1.2 *Acrobeloides* species show very early P granule perinuclear distribution

In order to further investigate the role of sperm in polarity and P granule distribution, we tested two *Acrobeloides* sister species; the hermaphroditic *Acrobeloides sp.* (PS1146) and the parthenogenic *A. nanus* where the sperm is absent and is not needed as a trigger for the establishment of early polarity (Goldstein et al., 1998). In *A. nanus*, as early as in the 1-cell stage embryo, perinuclear staining of P granules was observed. After the first division of the zygote, P granules were stained in and around the nucleus in the germline P1 (Figure 3-3a). The P2 cell is born at the 3-cell stage and the P granules are again more or less associated with the nucleus of the germ line cell P2 (Figure 3-3c). Weak residual staining was visible in the sister AB cell in 3-cell stage embryo (Figure 3-3c). At about the 10-cell stage (for early germline division, see Table 1), the P4 cell is exclusively stained and all the P granules are now localised to the periphery of the P4 nucleus (Figure 3-3d). Surprisingly, P4 does not divide further during embryogenesis in *A. nanus* (Figure 3-3e) but persists throughout embryogenesis in contrast to its hermaphroditic sister species *Acrobeloides sp.* (PS1146), where P4 divides once more (Figure 3-3i).

On the otherhand, in the 2-cell stage *Acrobeloides sp.* (PS1146) embryo, apart from staining in the P1 cell, weak staining was also seen in the somatic AB cell (Figure 3-3f). Such residual staining in the somatic blastomeres seen in both *Acrobeloides* species was absent in *C. elegans*. Beginning with the birth of the germ line blastomere P1, most P granules were found associated with the nucleus (Figure 3-3 g-i). Subsequently, the number of P granules associated with the nucleus seems to diminish and this can be accounted for by the residual P granules that remain in the sister somatic. However, by the time the primordial germ cell P4 is born, all the P granules were found around the germ cell nucleus in both species. Apparently in somatic cells, P granules dissolve in part through protein degradation and autophagy (DeRenzo et al., 2003; Zhang et al., 2009). Deducing from the DAPI stainings, P granules seem to be predominantly associated with the outer surface of the nuclear envelope at all stages in *Acrobeloides* species.

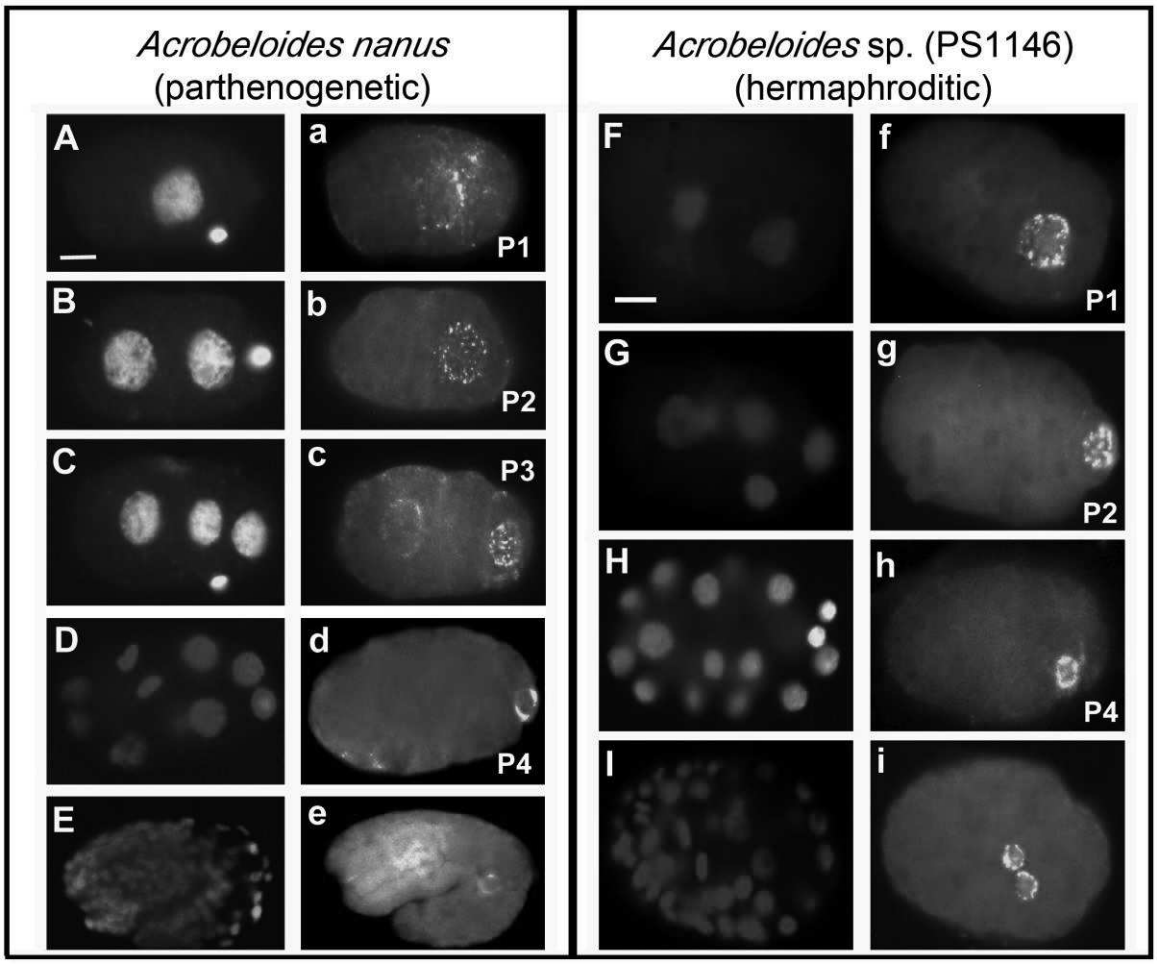

Figure 3-3: Localisation of P granules in the parthenogenetic *Acrobeloides nanus* and in the hermaphroditic *Acrobeloides sp.* (PS1146) embryos. The respective left panels in blue for each species shows images with DAPI stained nuclei, and the right panels show L416 antibody staining images of P granules. In both Acrobeloides species, there is strong early perinuclear staining as early as in the germline cell P1 and weak staining in the somatic AB cell. In *A. nanus*, P4 does not divide further in contrast to its sister species *Acrobeloides sp.* (PS1146), where P4 divides once more in the early embryo. In *Acrobeloides sp.* (PS1146) at about 200 cells, P4 daughters Z2 and Z3 are stained. Anterior is left. Epifluorescence. Scale bar = 10 µm.

Our results confirm the cross reactivity of the *C. elegans* P granules antibody that was used, since this same antibody gave clear P granule staining in both *Acrobeloides* and *C. elegans*. As a control, some embryos were stained only with the secondary antibody without previous incubation of embryos with the primary antibody. These controls did not show any P granule staining (data not shown), thus demonstrating that the structures marked with the monoclonal antibody against *C. elegans* germline are also found exclusively in the germline of *A. nanus* and *Acrobeloides sp.* (PS1146).

3.1.3 Panagrolaimidae species show perinuclear localisation of P granules

The genus Panagrolaimidae consists of many species that reproduce sexually and a few species that are parthenogenetic. From this group, the parthenogenetic species, *Panagrolaimus sp.* (PS1159) and the bisexual species, *Panagrolaimus superbus* (DF5050) were examined. The question was addressed whether both *Panagrolaimus* species stained with the *C. elegans* P granules antibody show a similar perinuclear distribution pattern as in the *Acrobeloides* species, which is independent of the type of reproduction or show a distribution such as in *C. elegans*.

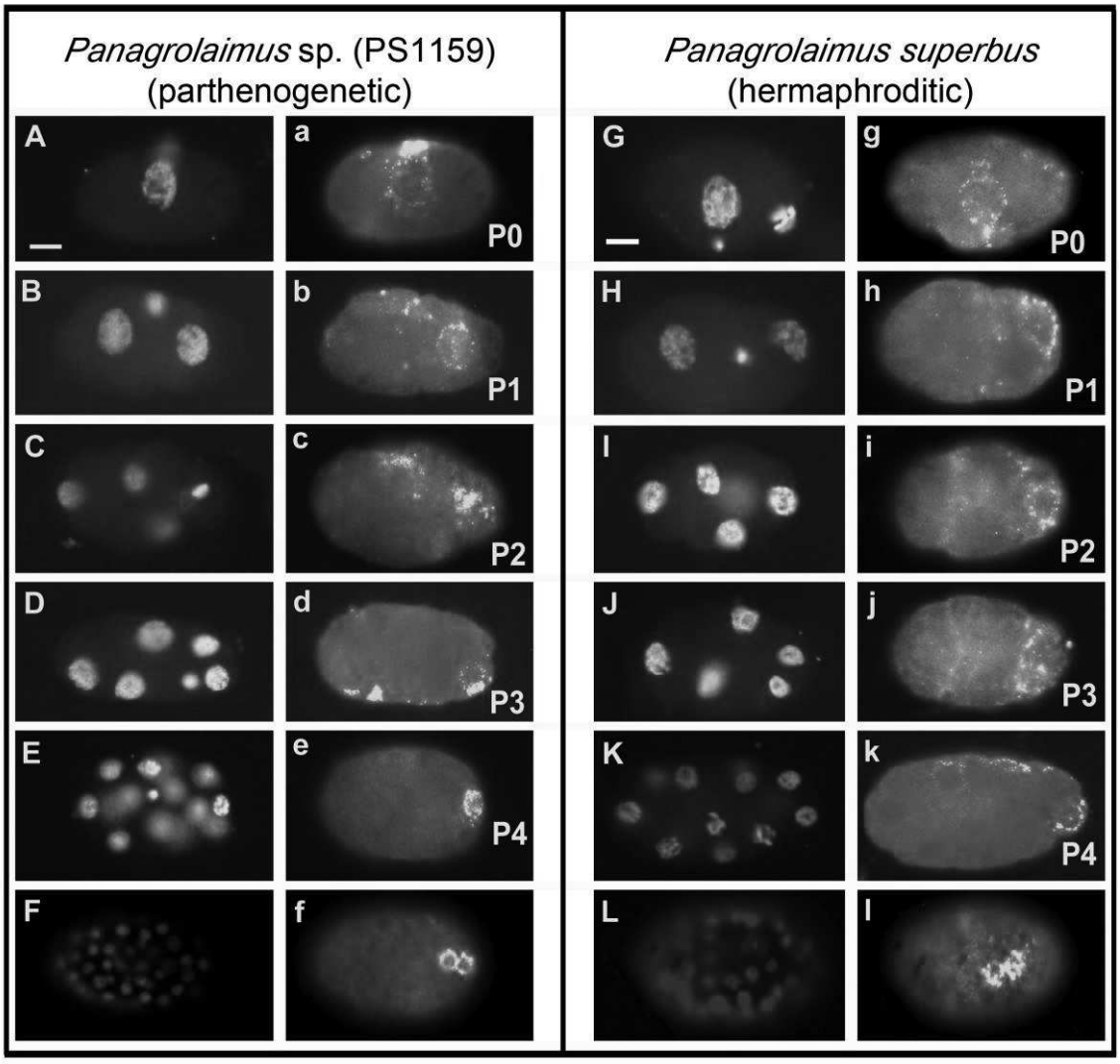

Figure 3-4: Localisation of P granules in the parthenogenetic *Panagrolaimus sp.* (PS1159) and in the hermaphroditic *Panagrolaimus superbus* embryos. The respective left panels in blue for each species shows images with DAPI stained nuclei, and the right panels show L416 antibody staining images of P granules. In both *Panagrolaimus* species, there is remarkable perinuclear staining as early as in the zygote P0, followed by successive segregation of P granules to the germline cells throughout embryonic development. Embryos are orientated with the anterior side to the left. Epifluorescence. Scale bar = 10 µm. (Fotos, U. Greczmiel).

My finding show that the distribution of P granules in both *Panagrolaimus* species (DF5050 and PS1159) is also perinuclear (Figure 3-4) and similar to that observed in the *Acrobeloides* species (Figure 3-3); with a few granules scattered all over the cytoplasm, as in *C. elegans*. This suggests that in nematode clades where parthenogenetic species are found, an early perinuclear localisation of P granules is common, regardless of the mode of reproduction.

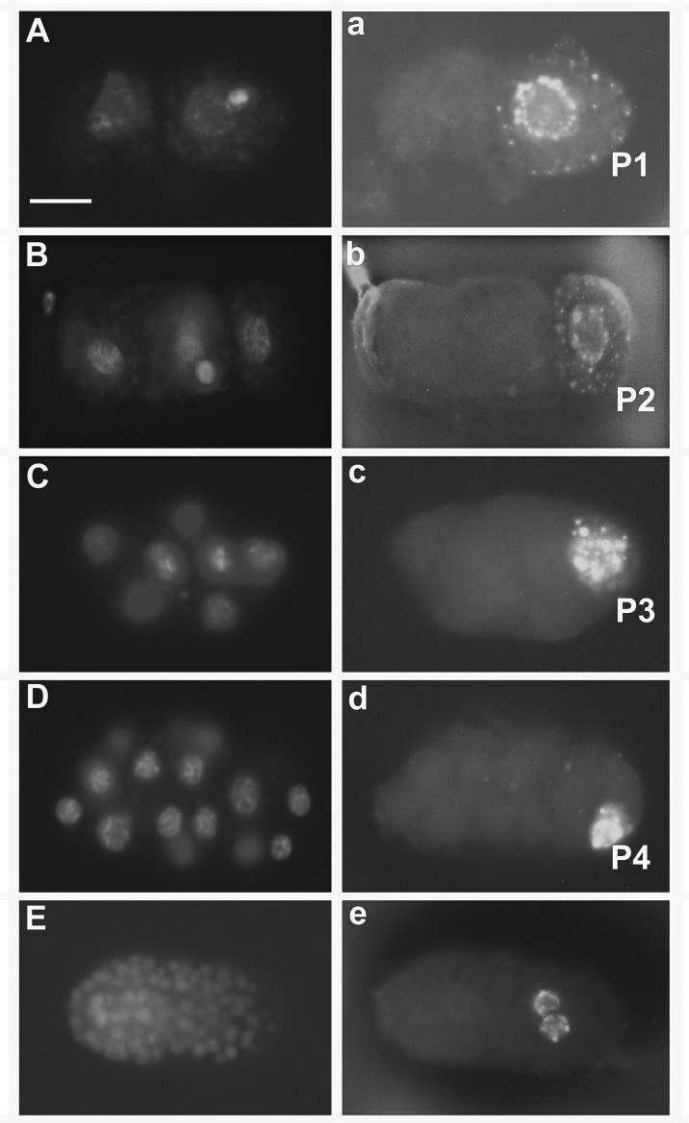

Figure 3-5: Localisation of P granules in *Propanagrolaimus sp.* (JU765). The left panel (A-E) shows images with DAPI stained nuclei, and the right panel (a-e) show P granule staining images. a) 2-cell stage embryo with P granules are predominantly distributed around the nucleus and a few in the cytoplasm of the germline cell. No staining is seen in the somatic AB cell. b) 3-cell stage with perinuclear staining in the P2 cell with some P granules again evenly dispersed in the cytoplasm of P2. c) About 7-cell stage with P granules aggregates evenly distributed in the cytoplasm of P3 only. d) P4 with P granules mainly in P4, associated with nuclear membrane. e) Embryo at with several hundred cells with pernuclear staining of P granules in adjacent Z2 and Z3 cells. Embryos are orientated with the anterior side to the left. Epifluorescence. Scale bar = 10 µm. (Fotos: A. El-jellouli).

In summary, the data presented here demonstrate that the *C. elegans* P granule antibody against the *C. elegans* germline structures cross reacts with other *Caenorhabditis*, *Acrobeloides* and *Panagrolaimus* species. It was also found that differences between species examined with respect to the distribution of the P granules, are just present in early germline before the emergence of the primordial germ cell P4. In P4 daughters Z2 and Z3, a perinuclear localisation of P granules was observed in all species, except for *A. nanus* where P4 remains undivided throughout development. Representatives of the genus *Caenorhabditis* are the only species that show P granules freely dispersed in the cytoplasm of early germline cells.

3.2 Isolation of gene homologs

3.2.1 Isolation of *par-6* gene homolog with degenerated primers

The *C. elegans par-6* gene encodes a PDZ-domain-containing protein that is conserved in Drosophila and mammals (Hung and Kemphues, 1999). During development, maternally provided PAR-6 is restricted to the anterior cortex and is required there for establishing anterior-posterior polarity in the early *C. elegans* embryo (Nance and Priess, 2002; Nance et al., 2003). To identify the *Acrobeloides sp.* (PS1146) *par-6* homolog, a PCR-based approach was used. A multiple sequence alignment of known PAR-6 PDZ homologs of different organisms (Figure 3-6) obtained from GenBank was constructed using the Vector NTI software. Degenerate primer pairs designed from the conserved PAR-6 PDZ domain block of amino acids were used to amplify the conserved kinase region of the *Acrobeloides sp.* (PS1146) *par-6*.

```
A.n   (152) KPPRRNYNISNPEDFRQVSAIIDVDVVPETHRRVRLCKHGTDRPLGFYIR
B.m   (166) RTPKRTYNISNPEDFRQVSAIIDVDIVPEAHRRVRLCKHGSDRPLGFYIR
C.e.  (125) -PPKRSYSISNPEDFRQVSAIIDVDIVPEAHRRVRLCKHGQERPLGFYIR

A.n   (202) DGTAVRLTPQGAMKVAGIFISRLVEGGLAESTGLLAVNDEVLEVNGIDVQ
B.m   (216) DGTSVRVTPQGVMKIQGIFISRLVEGGLAESTGLLAVNDEVLEVNGIEVQ
C.e.  (174) DGTSVRVTERGVVKVSGIFISRLVDGGLAESTGLLGVNDEVLEVNGIEVL

A.n   (252) GKTLDQVTDMMVANAQNLIITTKPANQRNTLQRG
B.m   (266) GKTLDQVTDMMVANAQNLIITVKPANQRNTLQRG
C.e.  (224) GKTLDQVTDMMVANAHNLIITVKPANQRNTLSRG
```

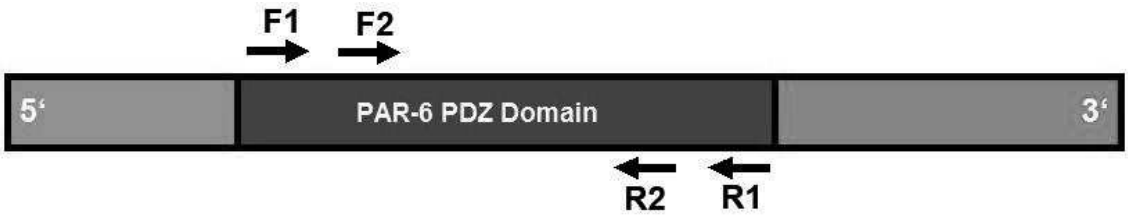

Figure 3-6: Multiple sequence comparison of the *par-6* PDZ domain sequences. Top: Conserved residues are coloured coded according to degree of conservation. Colour code for amino acids: Yellow/Red = identical, Green = block of similar, Blue = conservative, Black = non-similar. Underlined are the primer positions. The alignment was generated using the Vector NTI software (Invitrogen). Bottom: Sketch showing the positions and orientations of the degenerate par-6 primers. The arrows show the direction of the forward (F) and reverse (R) primer pairs. A.n = *A. nanus*, B.m = *B. malayi* and C.e = *C. elegans*

Nested PCR with degenerated primer pairs resulted in *Acrobeloides sp.* (PS1146) *par-6* PCR fragments of about 450 base pairs that were sequenced. BLAST searches for similarity to known sequences revealed high homologies to the PAR-6 PDZ homolog of *C. elegans* and other organisms, confirming that the sequenced fragment actual is the *par-6* gene in *Acrobeloides sp.* (PS1146).

BLAST search results show that the sequenced *Acrobeloides sp.* (PS1146) cDNA contained a PAR-6 sequence that is similar to that in other nematodes with highest homology to *B. malayi par-6.*

5’ RACE PCR with splice leader 1 (SL1) primer and gene specific primer

The 5’ end of the *par-6* gene was determined using semi-nested PCR with SL1 primer as forward primer in conjunction with a set of reverse gene specific primers designed from the previously sequenced PDZ containing domain (Figure 3-7).

Figure 3-7: Sketch showing the positions and orientations of the gene specific par-6 primers.

An amplified PCR product of about 800 bp were isolated and sequenced. BLAST search for similarity to known sequences revealed high similarities to known *par-6* fragments in related nematodes including *C. elegans*. The isolated sequence was joined with the initial PDZ domain fragment and aligned with known *par-6* homolog using the Vector NTI programme.

BLAST searches indicate that the sequenced *Acrobeloides sp.* (PS1146) cDNA fragment contained a PAR-6 sequence with highest homology to *C. elegans par-6* and the least homology to *Drosophila melanogaster*.

3' RACE PCR to identify the 3' end of *par-6* fragments

In order to isolate the remaining *Acrobeloides sp.* (PS1146) *par-6,* gene specific primers were constructed from the previously isolated degenerated *par-6* fragment. The UPM primer binds to a specific sequence at the poly-A tail in the 3' end where cDNA synthesis can be initiated. The 3' end of the *par-6* gene was determined using nested gene specific forward primers which were in conjunction with a Nested Universal Primer A Long (NUL) in a primary amplification with the outer gene specific primer.

Figure 3-8: Sketch showing the positions and orientations of the UPM, NUL and gene specific *par-6* primers.

In order to complete the entire *par-6* cDNA sequence, additional sequencing PCRs, generated further sequences using sequencing primers from the previously isolated 3' fragments. The final *Acrobeloides sp.* (PS1146) *par-6* cDNA sequence was obtained by joining the correctly sequenced fragments. The constructed *Acrobeloides sp.* (PS1146) *par-6* sequence (Figure 3-8) was 917 nucleotides long.

An open reading frame of 750 bases was found downstream of the start methionine that encodes a protein of 250 amino acids containing a partially identified PAR-6 PDZ domain homolog (Figure 3-9).

```
  1   TGGTTTAATT ACCCAAGTTT GAGAATATAA GTAGCTAATC TCTCGGACAA ACACTACTCA
 61   ATTGGACTTT ATCGATCGAT TCGTTTTTTT GTTGCAAAAT TTATTCATTC ACATAACTAA
                                                    M   S   W   N
121   ATTTTTGCTC TTTGGCCATT TTTATCATTC AGAAAACATT ATTATATATG TCTTGGAATG
      D   E   R   S   A   D   S   R   P   S   S   S   S   P   S   F   T   V   N   R
181   ACGAACGCTC GGCAGATAGT CGACCATCAT CTAGTTCACC TTCATTCACG GTGAACCGCA
      T   S   V   H   Y   V   Q   K   P   L   Q   I   P   P   F   L   P   V   K   S
241   CGTCTGTTCA TTATGTACAA AAACCTCTTC AAATTCCTCC ATTCTTACCA GTCAAATCAA
      K   F   D   S   E   F   R   R   F   S   L   P   L   N   P   D   K   L   M   T
301   AATTCGACTC GGAATTTCGA AGATTTTCTC TACCTCTAAA TCCGGACAAA TTGATGACAT
      Y   N   E   F   R   S   F   I   E   A   L   H   S   L   H   N   I   P   F   T
361   ATAATGAGTT CCGTAGCTTT ATCGAAGCGT TGCACTCGTT ACATAATATT CCGTTTACTT
      L   C   Y   N   S   T   A   G   D   L   L   P   I   T   N   D   G   D   F   R
421   TGTGTTATAA CAGTACGGCC GGAGATCTCC TGCCGATTAC GAACGACGGG GACTTCCGAA
      K   S   F   E   S   A   H   P   Y   I   K   L   L   I   Q   R   K   G   E   S
481   AATCCTTCGA ATCCGCCCAT CCATACATAA AACTATTAAT ACAACGAAAA GGTGAATCAT
      W   E   E   K   Y   G   Y   G   T   D   T   L   D   Q   K   K   K   G   L   S
541   GGGAAGAAAA ATATGGCTAC GGCACTGATA CATTAGACCA AAAAAAGAAA GGGCTTTCTA
      M   L   I   P   T   V   T   K   P   P   R   R   N   Y   N   I   S   N   P   E
601   TGCTAATCCC GACTGTGACC AAACCACCTC GAAGAAATTA TAATATTTCC AATCCTGAAG
      D   F   R   Q   V   S   A   I   I   D   V   D   V   V   P   E   T   H   R   R
661   ATTTTCGACA AGTCTCTGCG ATTATCGATG TGGATGTGGT TCCAGAAACG CATCGACGTG
      V   R   L   C   K   H   G   T   D   R   P   L   G   F   Y   I   R   D   G   T
721   TTCGTTTGTG TAAACATGGG ACTGATCGGC CACTCGGTTT TTATATTCGA GATGGAACCG
      A   V   R   L   T   P   Q   G   A   M   K   V   A   G   I   F   I   S   P   L
781   CGGTGAGACT AACCCCACAA GGAGCGATGA AAGTCGCTGG AATTTTTATA AGTCCATTAG
      V   E   G   G   L   A   E   S   T   G   L   L   A   V   N   D   E   V   L   E
841   TCGAAGGTGG TTTAGCCGAA TCTACTGGAT TGTTGGCGGT TAACGATGAG GTTTTGGAAG
      V   N   G   I   E   V
901   TCAACGGTAT AGAGGTA
```

Figure 3-9: Acrobeloides *sp.* (PS1146) *par-6* cDNA sequence. The 5' SL1 primer is shown in italics and underlined. The deduced amino acid sequence coding *Acrobeloides sp.* (PS1146) PAR-6 is in bold and its partial PAR-6 PDZ domain is underlined (Hung et al., 1998). Note that the 3' end sequence is not shown.

Analysis of the *Acrobeloides sp.* (PS1146) PAR-6

The protein alignment of *Acrobeloides sp.* (PS1146) PAR-6 with *A. nanus* PAR-6 over the first 250 amino acids showed that the amino acids are well conserved (92 %) in PAR-6 PDZ (Figure 3-10). On the other hand, *Acrobeloides sp.* (PS1146) PAR-6 is 61 % identical to *C. elegans* over the same region. The conservation of the PAR-6 protein is highest among these homologs over a 175 amino acid region containing the PDZ domain; *Acrobeloides sp.* (PS1146) and *A. nanus* cDNAs share 92 % overall similiarity and 74 % homology with *C. elegans* PAR-6.

Figure 3-10: Alignment of the predicted protein sequence of *Acrobeloides sp.* (PS1146) PAR-6 PDZ domain with its putative homolog in closely related worms, fly and human. The most conserved residues among these homolog are indicated by the blue shaded background. Identical residues are shown in yellow; closely-related residues are shown in blue. Weakly similar residues are shown in green The *Acrobeloides sp.* (PS1146) PAR-6 CRIB domain is in bold and underlined in blue. The PAR-6 PDZ domain is underlined in black. The alignment was generated using the Vector NTI software. Colour code for amino acids: Yellow = identical, Green = block of similar, Blue = conservative, White = non-similar. PS: *Acrobeloides sp.* (PS1146), A.n: *Acrobeloides* nanus, B.m: *Brugia malayi*, C.e: *Caenorhabditis briggsae*, C.e: *C. elegans*, D.c: *Diploscapter coronatus*, D.m: *Drosophila melanogaster*, H.s: *Homo sapiens*.

The *C. elegans* PDZ domain of PAR-6 contains 96 amino acids (Hung et al., 1998). The *Acrobeloides sp.* (PS1146) PAR-6 protein contains a conserved core region of about 156 residues (70 % identity between PAR-6 from *C. elegans* and *Acrobeloides sp.* (PS1146) PAR-6). This region comprises the 70 amino acids of the conserved PDZ domain. On the basis of the relatedness of *Acrobeloides sp.* (PS1146) to *A. nanus* and to *C. elegans* PAR-6, it can be speculated that the partially identified *Acrobeloides sp.* (PS1146) PAR-6 still lacks an upstream sequence of about 26 residues. Multiple sequence alignment analyses to known sequences also revealed that *Acrobeloides sp.* (PS1146) PAR-6 shares 53 % and 56 % amino acid identity with the human and *Drosophila* PAR-6 proteins, respectively, and 72 % overall identity with *C. elegans* PAR-6. Among these homologs, a 120 amino acid region containing the PDZ domain is highly conserved. The results confirmed successful isolation of the *Acrobeloides sp.* (PS1146) *par-6* gene using degenerated PCR primers and that this gene is conserved.

3.3 *In situ* hybridisation on whole mount embryos with *Acrobeloides* sp. (PS 1146) *par-6* construct

We performed *in situ* hybridisation with the *Acrobeloides sp.* (PS 1146) *par-6* probe on embryos at different developmental stages to detect a *par-6* mRNA loaclisation pattern. A PCR fragment used for *in situ* probe synthesis was generated outside the conserved PDZ domain to avoid cross reactivity of the assay to the *Acrobeloides* sp. (PS 1146) *par-6* gene and as such avoids non-specific binding of the probe to other PDZ domains in different genes. No significant difference in the staining pattern was seen with *par-6* transcripts in *Acrobeloides* sp. (PS 1146) embryos with both sense and antisense probes (data not shown).

3.4 PAR-6 Antibody production from *Acrobeloides sp.* (PS 1146)

To facilitate the study of the structure and function of *Acrobeloides sp.* (PS1146) *par-6*, we intended to produce *par-6* protein in an *E. coli* expression system and generate antibodies against the PAR-6 protein. The 5' putative coding sequence of *par-6* was cloned into an expression plasmid vector pQE30. The resultant recombinant plasmid pQE30-PAR-6 was introduced into *E. coli* strain M15. As shown on SDS-PAGE gel (Figure 3-11), no protein expression was obtained after 4 hours incubation, suggesting low PAR-6 expression in *E. coli* M15 or toxicity by the induced protein.

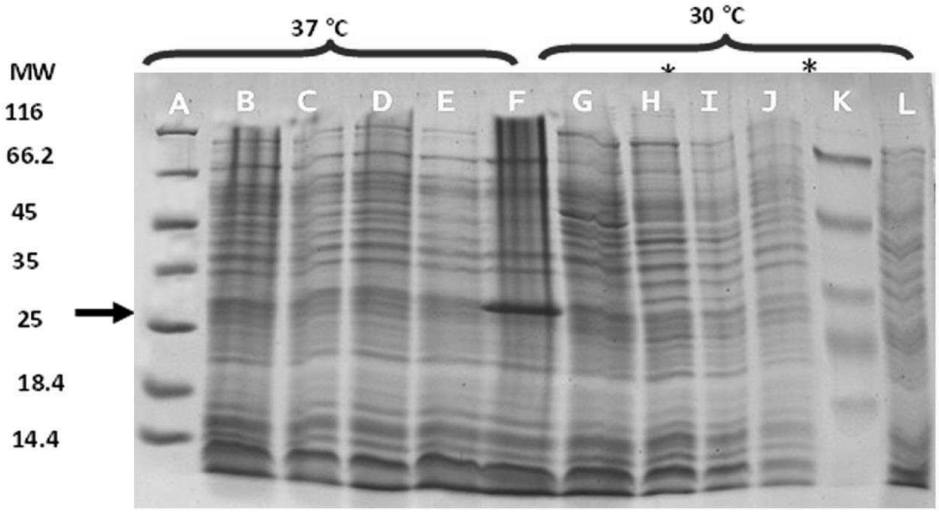

Figure 3-11: PAGE for the detection and analysis of the PAR-6 protein expression of *Acrobeloides sp.* (PS 1146).No detectable protein induction at different temperatures (37 °C and

30 °C) can be seen. MW =: Protein size molecular weight marker. Lane F: Positive control. Lanes B-F: Baterial cultured at 37 °C and Lanes G-L: Bacteria cultured at 30 °C. Lanes H and I: PQE-30 expression vector. * represent samples without IPTG induction, used as negative controls. Arrow indicates the expected size of PAR-6 protein (25.5 KDa). Prolonged culturing periods and culturing the bacteria at a reduced temperature, did not substantially increase the amount of the induced PAR-6 protein, therefore suggesting that culturing and inducing conditions need to be optimised to enable the PAR-6 expression.

3.5 Heterologous RNAi is possible in *C. elegans* but is not inducible in *Panagrolaimus sp.* (PS1159)

A previous study claimed that *Panagrolaimus* is amenable to RNAi by feeding (Shannon et al., 2008). In order to verify the efficiency and reproducibility of the RNAi method in our laboratory, as a positive control, I used a *C. elegans lmn-1* RNAi construct fed to wild type *C. elegans* larvae, with the ultimate goal of obtaining embryonic lethal RNAi phenotypes. The *lmn-1* gene encodes the sole *C. elegans* nuclear lamin that is required for a number of nuclear processes, including chromatin organisation, cell cycle progression and chromosome segregation (Gruenbaum et al., 2003).

Approximately 99 % of the eggs laid were defective and did not hatch. Microscopic inspection revealed that most of these developed to more than 100 cells but did not enter a proper morphogenesis (see Figure 3-12). A few muscle contractions were noticed as well as large vacuolar bubble-like structures with abnormal gut granules that seem to lack a functional cuticle. It should be noted that in most cases, 100 % embryonic arrest and lethality was observed and in a few cases, less than 1 % of the embryos that probably escaped the RNAi effect hatched and developed normally. This indicates a great efficiency and reproducibility of this *lmn-1* RNAi feeding construct in *C. elegans*.

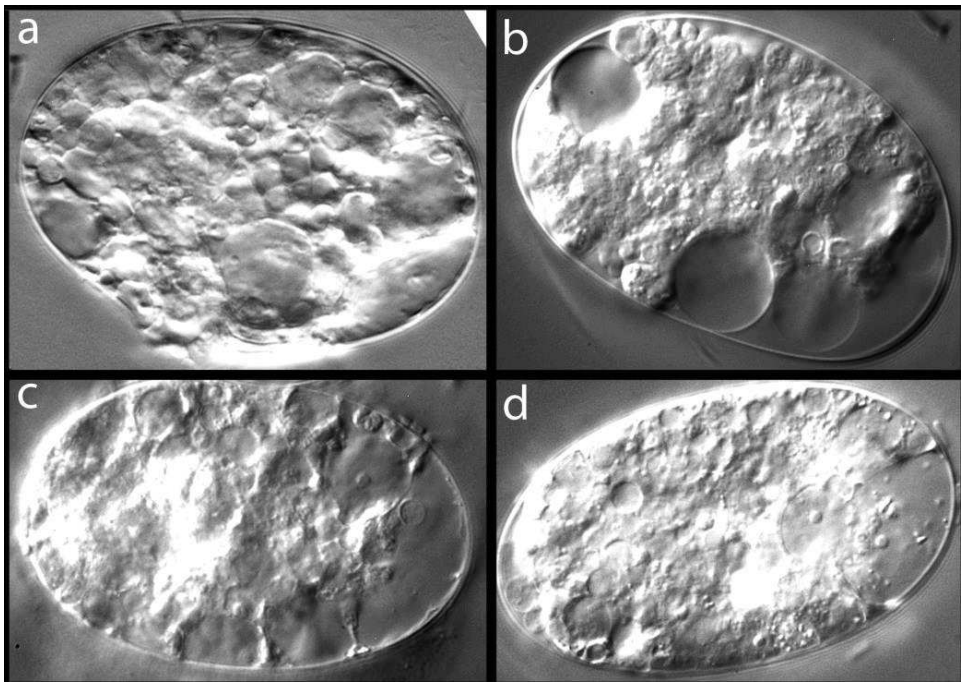

Figure 3-12: The RNAi phenotypes obtained among the progeny of *C. elegans* fed on *E. coli* clones expressing dsRNA for the embryonic lethal *C. elegans lmn-1 gene.* (a-c) Embryos at various developmental stages with abnormal cells sizes, including large vacuolar structures. (d) a defective late stage embryo probably midway through embryogenesis with no cuticle.

3.5.1 Inconclusive efficiency of RNAi by feeding in *Panagrolaimus sp.* (PS1159)

No abnormal RNAi phenotypes were scored among the progeny of *Panagrolaimus sp.* (PS1159) fed on bacterial clones expressing dsRNA for the embryonic lethal *C. elegans lmn-1* construct. Unlike in *C. elegans* where about 100 % arrest and lethality was seen, the hatched eggs developed normally in the *Panagrolaimus sp.* (PS1159). Therefore, I generated a species-specific *Panagrolaimus sp.* (PS1159) construct with the embryonic lethal *ama-1* gene. However, even this contruct did not produce knock-down phenotype since treated worms laid eggs continued normal embryogenesis and hatched into healthy worms.

Less than 5 % abnormal monster-like embryos were seen to arrest in development at different stages using a negative control GFP construct (see Figure 3-13). But such abnormal embryos were also found in wild type worms in similar proportions in untreated *Panagrolaimus sp.* (PS1159). Therefore, these abnormalities cannot be specifically attributed to the RNAi treatment.

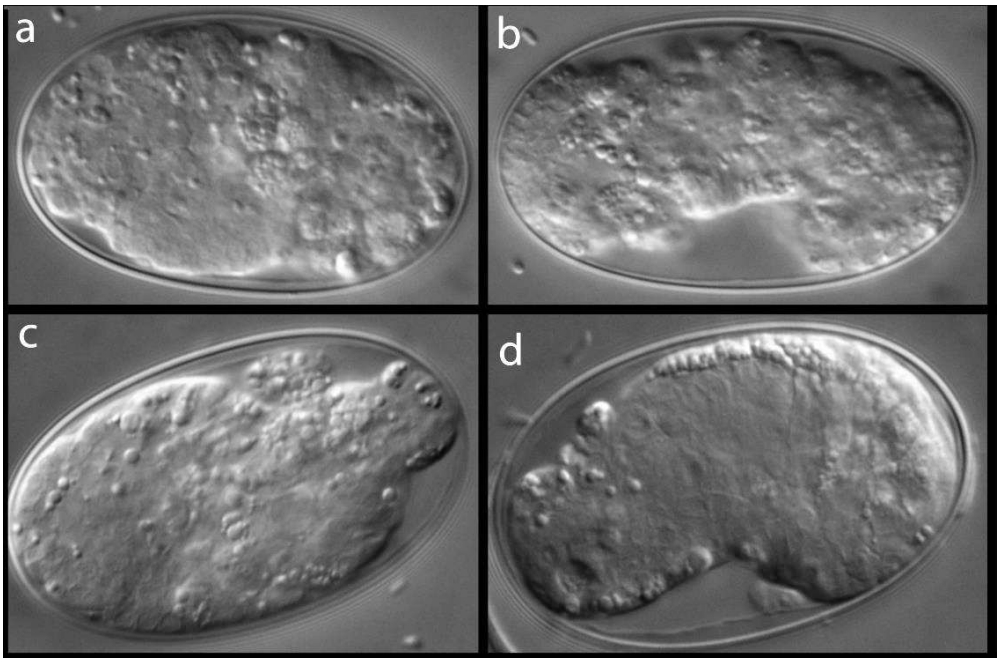

Figure 3-13: Embryonic lethal arrest phenotypes obtained after placing *Panagrolaimus sp.* (PS1159) eggs on a lawn of *E. coli* expressing the negative control GFP construct. About 5 % abnormal monster-like embryos were seen that arrested at different stages of development. Such abnormal embryos were also in less than 5 % of the wild type worms that were not subjected to RNAi treatment. They were fed with the normal *E. coli* OP50 bacteria strain.

In summary, no comprehensive embryonic RNAi effects for genes tested could be established in the parthenogenetic *Panagrolaimus sp.* (PS1159) nematode with several species-specific contructs. The reproducibility of the amenability of *Panagrolaimus sp.* (PS1159) to RNAi by feeding (Shannon et al., 2008) could not be confirmed in our hands. Also in other organisms, RNAi works on a limited number of genes and in some cases the effect is small and difficult to reproduce. The reason why the RNAi approach established in *C. elegans* has limited efficiency in *Panagrolaimus* might be due to differences in the uptake of dsRNA and or transport into cells and between cells.

3.6 Isolation of gene fragments from other nematodes

Unless otherwise stated, the other genes studied in this project were isolated in a similar approach as in section 3.2.

C. elegans gene homologs were searched for in available nematode genomes from various clades for homologous partners. Genome sequence data from the parthenogenetic *Panagrolaimus sp.* (PS1159) and the hermaphroditic

Propanagrolaimus sp. (JU765) were kindly provided by Phillipp Schiffer (Schierenberg lab, University of Cologne). The parthenogenetic *A. nanus* was chosen as the representative of the genus *Acrobeloides* since its genome was readily accessible thanks to Itai Yanai's lab (Technion Haifa, Israel), and *D. coronatus* from Yuji Kohara (NIG, Mishima, Japan). The *Caenorhabditis* genomic data and genomes from the other nematodes are largely accessible from the *C. elegans* Sequencing Consortium (1998) and at the National Center for Biotechnology Information (NCBI) respectively.

The *C. elegans skn-1* gene encodes a bZip transcription factor, SKN-1 that is maternally provided and is required for specification of the EMS blastomere, during early embryogenesis. The basic regions present in SKN-1, are highly conserved among diverse phyla (Bowerman et al., 1993; Blackwell et al., 1994; Choe et al., 2012). Multiple sequence alignment of *skn-1* gene homologs from different organisms obtained from GenBank enabled the design of degenerated primers for amplification of *skn-1* fragments in *A. nanus*, *Panagrolaimus sp.* (PS1159) and *Propanagrolaimus sp.* (JU765).

PCR with cDNA prepared from these animals yielded amplification products of the expected size. Full length SKN-1 sequences were obtained using RACE PCR with a SL1 anchor primer complementary to the splice leader 1 sequence from *C. elegans* (Krause and Hirsh 1987) and 3´ gene specific primers for the different *skn-1* we obtained the missing 5´region of both *Panagrolaimus* species and *A. nanus* including the 5´ UTR, a putative translation initiation ATG. The deduced amino acid sequences of the isolated fragments from all species show a high similarity in the important conserved motifs in the basic region and the bZIP domain of SKN-1 from *C. elegans*.

Protein alignments

Protein BLAST searches were performed using *C. elegans* proteins as the query sequences (McGinnis and Madden 2004). Searches were done for proteins or DNA translations in Augustus or the database of the National Center for Biotechnology Information (NCBI). The final set of proteins was aligned with AlignX, a component of the Vector NTI software, version 10.3.0 (Invitrogen). In this way, we were able to identify, and thereby isolate, the general region that corresponds to the known conserved domain for DNA binding in *C. elegans*. To further confirm the alignments, we then realigned this isolated region for all species with Geneious software.

3.7 Evaluation of interacting gene networks and gene analysis

The diversity in nematode biology is reflected in the diversity of their genomes, and with several nematode genomes sequenced and more in progress (Blaxter et al., 2012) a huge amount of genome sequence information is now readily available at http://www.ncbi.nlm.nih.gov. Functional studies of gene networks for a broad collection of organisms are available through programs such as N-Browse, the bioPIXIE system, Functional Coupling, MouseNet, STRING and GeneMANIA websites (Pena-Castillo et al., 2008; Mostafavi et al., 2008; Warde-Farley et al., 2010). We used GeneMANIA to search for candidate genes homologs in other nematodes with *C. elegans* as a reference.

3.7.1 In genomes of different nematode species, a SKN-1 homolog is absent

The *skn-1* gene occupies a central position in the *C. elegans* endomesoderm gene regulatory network and also functions as a transcription factor activating target genes (Bowerman et al., 1992; Maduro, 2006). Besides its role in early embryogenesis, during postembryonic stages the SKN-1 protein regulates a key Phase II detoxification gene in *C. elegans* (An and Blackwell, 2003; Choe et al., 2012). The *skn-1* gene therefore functions in connection with several other factors in mediating its biological function in several biological processes through protein interactions.

Figure 3-14 depicts the *C. elegans* SKN-1 network connectivity showing the significant protein interactions based on genetic interactions, co-localisation, protein domain similarity and co-expression.

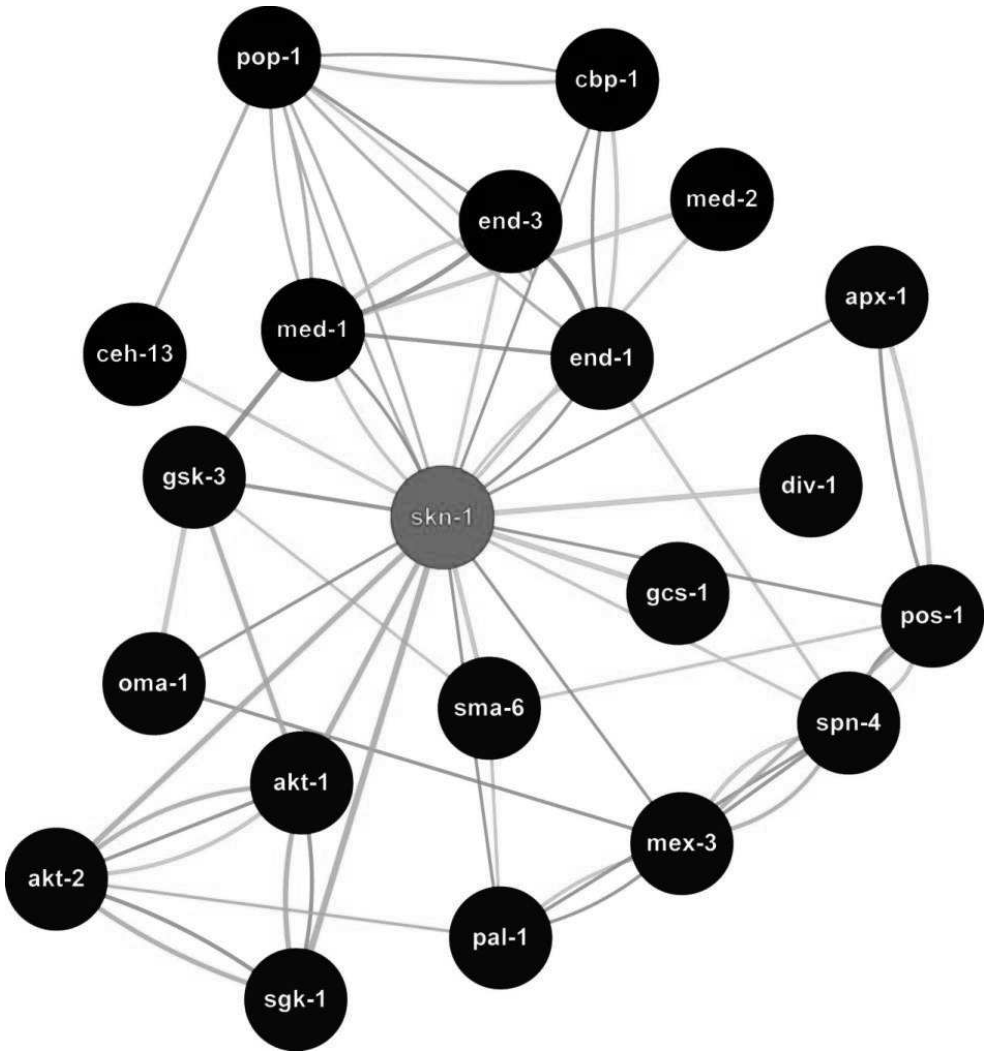

Figure 3-14: *In silico* analysis of the *C. elegans skn-1* gene network. Gene interaction map generated by GeneMANIA showing the 20 most related genes that react in various pathways with *skn-1* in *C. elegans*. SKN-1 is highlighted in red and the others marked in black circles, physical interactions (light pink lines) and genetic interactions (green lines) are shown. Predicted interactions based on co-expression data are shown in grey coloured lines.

Almost nothing is known about the gene interaction network and function of the *skn-1* gene in other nematodes. To determine if the same *C. elegans* SKN-1 interacting components are also present in other nematodes, we utilised GeneMANIA to localise SKN-1 within an *in silico* association network with *C. elegans skn-1* as the query. Genes involved in embryogenesis with significant

physical and genetic interactions were considered and investigated. BLAST searches (Altschul et al., 1990) in combination with analysis using the Augustus software that predicts genes in eukaryotic genomic sequences were performed. My analysis revealed that only a part of the *C. elegans* gene homologs are present in other nematodes (Figure 3-15, Table 13).

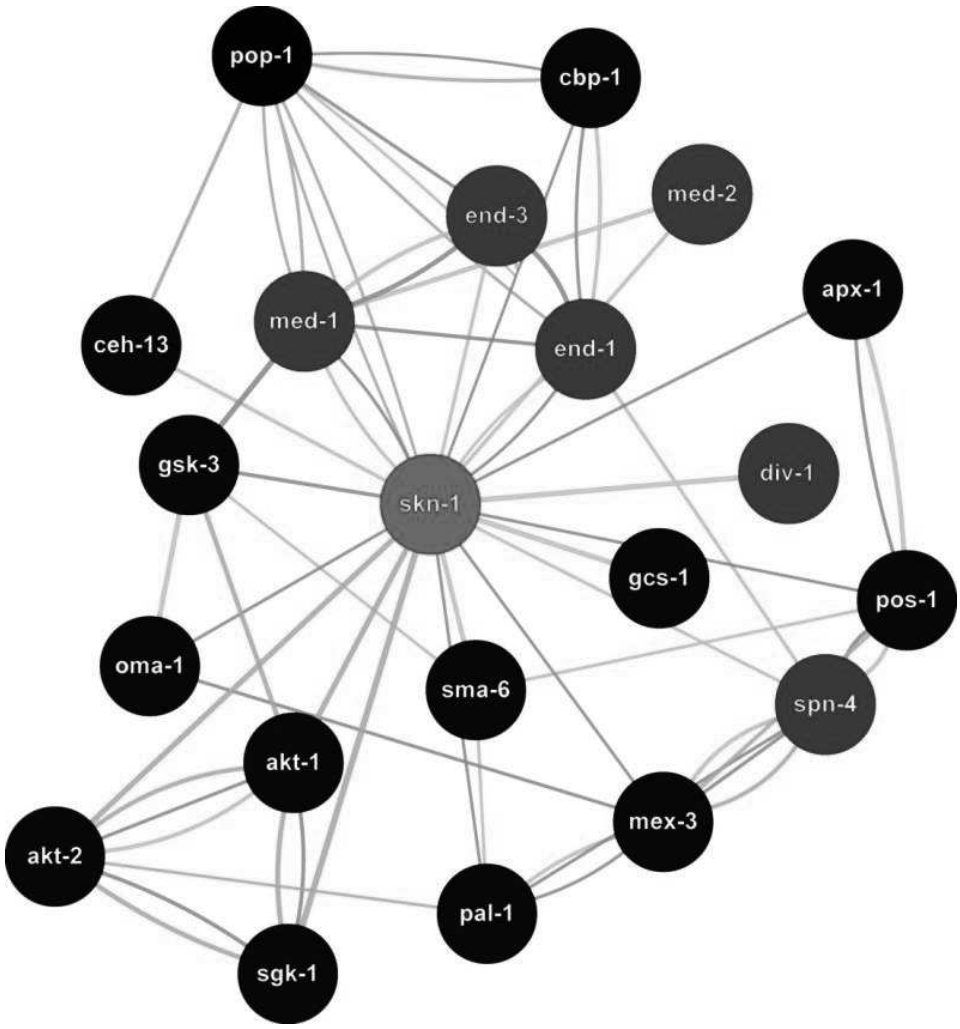

Figure 3-15: The *skn-1* gene network in other nematodes. GeneMANIA gene interaction map highlighting the gene orthologs (in blue circles) that were not found in the *Panagrolaimus* and *Acrobeloides* species whose *skn-1* mRNA localisation has been studied in this thesis. *C. elegans skn-1* was used as the query and the network was limited to the 20 most related genes to *C. elegans skn-1*, depicting physically (light pink lines) and genetically (light green lines) linked interactions. Predicted interactions based on co-expression data are shown in grey lines.

Our findings suggest that the *skn-1* gene network and possibly the function of the SKN-1 protein varies amongst the different clades, firstly since its mRNA expression

differs among nematodes (see section 3.8) and secondly, some major SKN-1 interacting and associated gene othologs necessary for normal embryogenesis in *C. elegans* appear to be absent in these species (Table 12). Based on this bioinformatics analysis, it is tempting to postulate that in other nematodes, the gene regulatory activity with SKN-1 occupying a central role in important pathways cannot be the same as in *C. elegans*.

Table 12: A list of the *skn-1* gene orthologs from multiple nematodes of different clades across the nematode phylum. +: present, -: absent. Species are Ts = *Trichinella spiralis*, Rc = *Romanomermis culicivorax*, Pa = *Plectus aquatilis*, Bm = *Brugia malayi*, As = *Ascaris suum*, Lo = *Loa loa*, Pp = *Pristionchus pacificus*, Dc = *Diploscapter coronatus*, Cr = *Caenorhabditis remanei*, Cb = *Caenorhabditis briggsae*, Ce = *Caenorhabditis elegans*, Ps = *Panagrolaimus sp.* (PS1159), Ju = *Panagrolaimus sp.* (JU765), An = *Acrobeloides nanus*, Mi = *Meloidogyne incognita*, Bx = *Bursaphelenchus xylophilus*.

Clades	**2**		**6**	**8**			**9**					**10**		**11**	**12**	
Species	**Ts**	**Rc**	**Pa**	**Bm**	**As**	**Lo**	**Pp**	**Dc**	**Cr**	**Cb**	**Ce**	**Ps**	**Ju**	**An**	**Mi**	**Bx**
Genes																
akt-1	+	+	+	+	+	+	+	+	+	+	+	+	+	+	+	+
akt-2	+	+	+	+	+	+	+	+	+	+	+	+	+	+	+	+
apx-1	+	+	+	+	+	+	+	+	+	+	+	+	+	+	+	+
cbp-1	+	+	+	+	+	+	+	+	+	+	+	+	+	+	+	+
ceh-13	+	+	+	+	+	+	+	+	+	+	+	+	+	+	+	+
div-1	+	+	-	+	+	+	+	+	+	+	+	-	-	-	-	-
end-1	+	+	+	+	-	+	+	+	+	+	+	+	+	+	-	+
end-3	-	-	+	+	-	+	+	+	+	+	+	+	+	+	-	-
gcs-1	+	+	+	+	+	+	-	+	+	+	+	+	+	+	+	+
gsk-3	+	+	+	+	+	+	+	+	+	+	+	+	+	+	+	+
med-1	-	-	-	-	-	-	-	-	+	+	+	-	-	-	-	-
med-2	-	-	-	-	-	-	-	-	+	+	+	-	-	-	-	-
mex-3	-	+	+	-	+	-	+	+	+	+	+	+	+	+	+	+
oma-1	+	-	+	+	+	+	+	+	+	+	+	+	+	+	+	+
pal-1	+	+	+	+	+	+	+	+	+	+	+	+	+	+	+	+
pop-1	+	+	+	+	+	+	+	+	+	+	+	+	+	+	+	+
pos-1	+	+	+	+	+	+	+	+	+	+	+	+	+	+	+	+
sgk-1	+	+	+	+	+	+	+	+	+	+	+	+	+	+	+	+
skn-1	-	+	+	-	+	-	+	+	+	+	+	+	+	+	+	+
sma-6	+	+	+	+	+	+	+	+	+	+	+	+	+	+	+	+
spn-4	+	-	-	-	-	-	+	+	+	+	+	-	-	+	+	+

3.7.2 Not all available genomes of nematode species contain a PIE-1 homolog

In *C. elegans*, PIE-1 is required for the proper regulation of embryonic transcription in germline blastomeres (Seydoux et al., 1996). The localisation of *pie-1* mRNA is considerably different in *Acrobeloides* species and *Panagrolaimus* species compared to *C. elegans*. In order to further explore and characterise the function of the *pie-1* gene outside of *C. elegans*, we used GeneMANIA to examine the *pie-1* gene network in various nematodes with *C. elegans pie-1* as a standard (Figure 3-16).

We acknowledged the absence of a *pie-1* homolog in members of the lower clades 1 to 8 and *Meloidogyne incognita* of clade 12 (Figure 1-2). Similarly, in all nematode species lacking a *pie-1* homolog, most of the important genes that are required for the asymmetric distribution of the PIE-1 protein in *C. elegans* such as those coding for the zinc finger proteins, MEX-5 and MEX-6 (Schubert et al., 2000) are missing (Figure 3-16) together with ZIF-1 that targets CCCH zinc fingers proteins such as PIE-1 for degradation (Reese et al., 2000; DeRenzo et al., 2003). Furthermore, the germline transcriptional regulators *nos-2, pes-2.1* and *pes-10* genes were found only among the *Caenorhabditis* species. The *div-1* gene which is also involved in the asymmetric distribution of PIE-1 is absent in nematodes of higher clades 10, 11 and 12 and present only in clades 1 to 9 (Table 13). These findings indicate that the *pie-1* gene network and hence *pie-1* activity is not conserved in all nematodes.

My results with *in situ* hybridisation revealed major striking differences in the *skn-1* and *pie-1* mRNA expression in time and space in *C. elegans*, *Panagrolaimus sp.* (PS1159) and *A. nanus* (see below) suggesting these key genes may execute different roles in nematode development. Therefore, we wondered if these genes might have undergone structural changes that mirror the differences observed in the staining patterns of their mRNA transcripts.

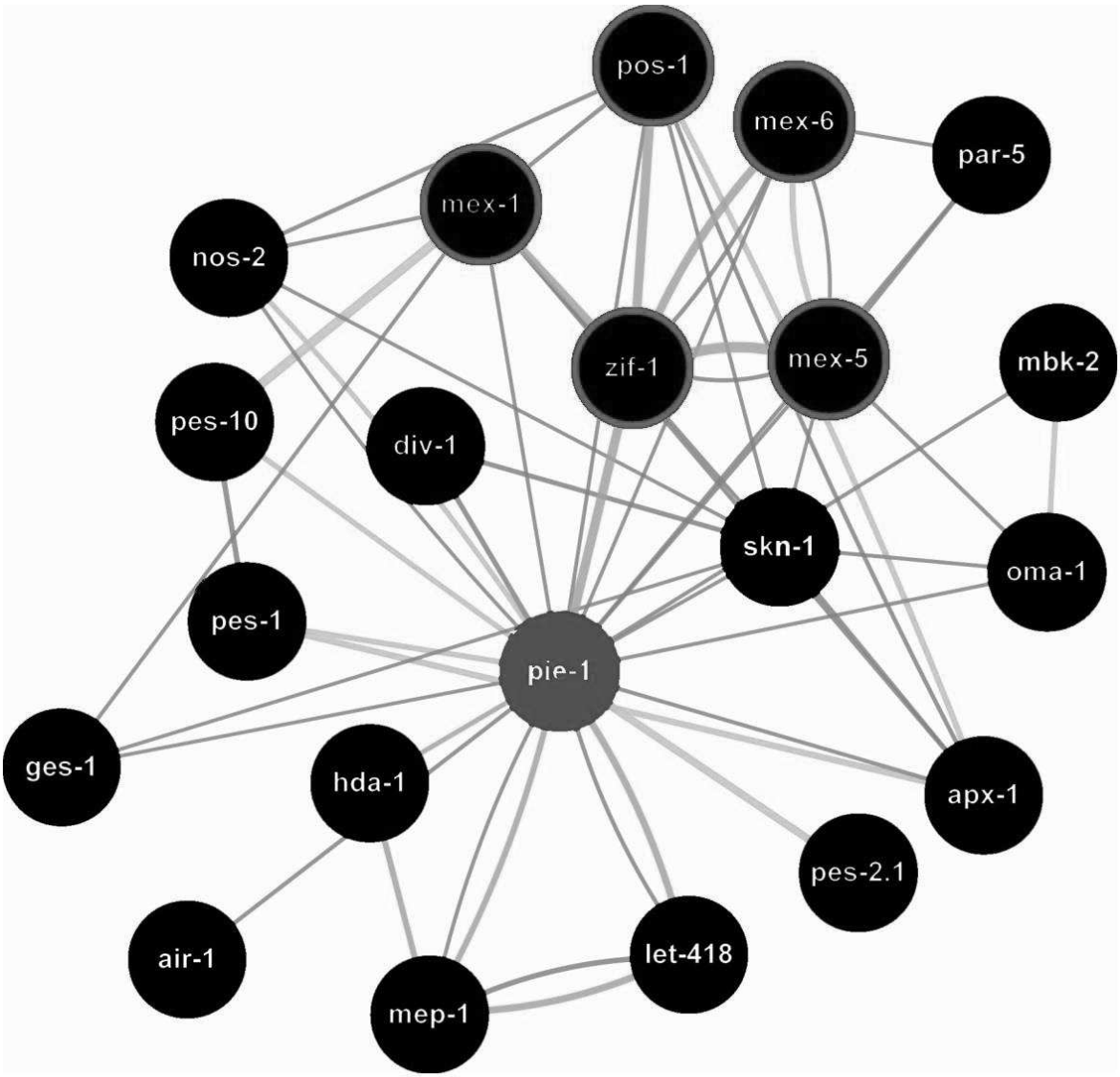

Figure 3-16: *In silico* analysis of the *C. elegans pie-1* gene network. Gene interaction map generated by GeneMANIA showing the 20 most related genes that reacted in various pathways with *pie-1* in *C. elegans*. The *pie-1* gene (green) and its interacting genes (black) are highlighted. Genes that encode for zinc finger proteins are circled in red. Physical interactions (light pink lines) and genetic interactions (light green lines) are shown. Predicted interactions based on co-expression data are shown in grey lines.

In silico predictions through genome analysis is a powerful approach to uncover and understand complex gene regulatory networks from one organism compared with those from other organisms on a genome-wide scale (Cho et al., 2003). The combined putative *pie-1* gene network in *Panagrolaimus sp.* (PS1159) and *A. nanus* is shown below.

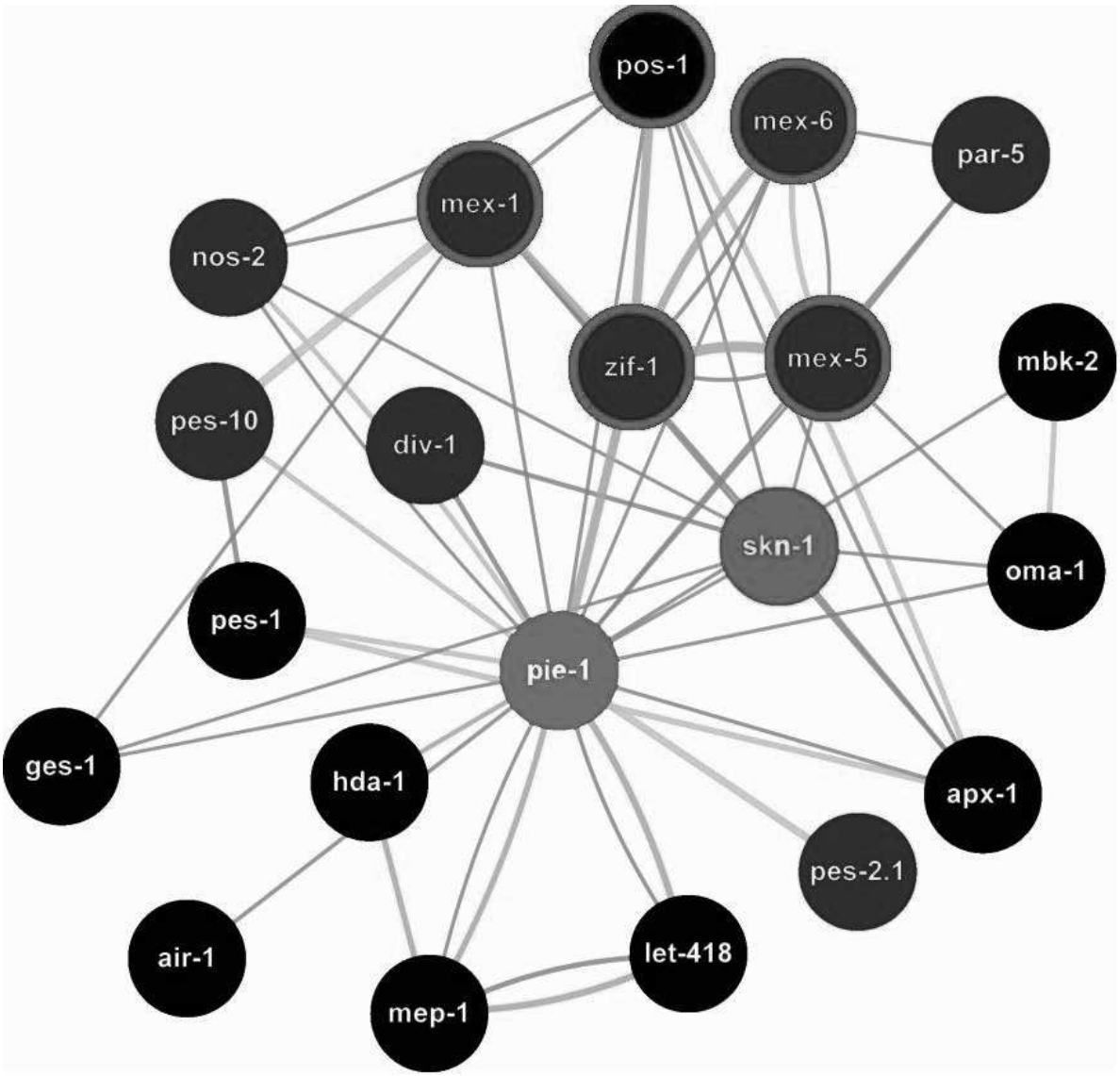

Figure 3-17: The *pie-1* gene network generated by GeneMANIA in *Panagrolaimius sp.* (PS1159) and *A. nanus*. Direct *pie-1* gene interactions were mapped to the 20 different associated genes involved in early embryogenesis. Genes that encode for zinc finger proteins are circled in red. Genes in blue-filled circles are orthologs that were not found in both nematodes studied. Physical interactions (light pink lines) and genetic interactions (light green lines) are shown. Predicted interactions based on co-expression data are shown in grey lines.

Table 13: *C. elegans pie-1* gene interactive gene homologs in various nematodes. + = present, - = absent. * For abbreviations see Table 12.

Clades	**2**		**6**	**8**			**9**					**10**		**11**	**12**	
Species	**Ts***	**Rc**	**Pa**	**Bm**	**As**	**Lo**	**Pp**	**Dc**	**Cr**	**Cb**	**Ce**	**Ps**	**Ju**	**An**	**Mi**	**Bx**
Genes																
air-1	+	+	+	+	+	+	+	+	+	+	+	+	+	+	+	+
apx-1	+	+	+	+	+	+	+	+	+	+	+	+	+	+	+	+
div-1	+	+	-	+	+	+	+	+	+	+	+	-	-	-	-	-
ges-1	+	+	+	+	+	+	+	+	+	+	+	+	+	+	+	+
hda-1	+	+	+	+	+	+	+	+	+	+	+	+	+	+	+	+
let-418	+	+	+	+	+	+	+	+	+	+	+	+	+	+	+	+
mbk-2	+	+	+	+	+	+	+	+	+	+	+	+	+	+	+	+
mep-1	+	+	+	+	+	+	+	+	+	+	+	+	+	+	+	+
mex-1	+	-	+	+	+	+	+	+	+	+	+	+	+	+	+	+
mex-5	-	-	-	-	-	-	-	+	+	+	+	-	-	-	-	-
mex-6	-	-	-	-	-	-	-	+	+	+	+	-	-	-	-	-
nos-2	-	-	-	-	-	-	-	-	+	+	+	-	-	-	-	-
oma-1	-	-	+	-	+	+	+	+	+	+	+	+	+	+	+	+
par-5	+	+	+	+	+	+	+	+	+	+	+	+	+	+	+	+
pes-1	+	+	+	+	+	+	+	+	+	+	+	+	+	+	+	+
pes-10	-	-	-	-	-	-	-	-	+	-	+	-	-	-	-	-
pes-2.1	-	-	-	-	-	-	-	-	+	+	+	-	-	-	-	-
pie-1	-	-	-	-	-	-	-	+	+	+	+	+	+	+	-	-
pos-1	-	-	+	+	+	+	+	+	+	+	+	+	+	+	+	+
skn-1	-	+	+	-	+	-	+	+	+	+	+	+	+	+	+	+
zif-1	-	-	-	-	-	-	-	-	+	+	+	-	-	-	-	-

3.7.3 Bioinformatic analysis of SKN-1 homologs from selected nematode species

The *C. elegans* SKN-1 protein is unique since it contains a basic region similar to those of the basic leucine zipper (bZIP) family of DNA binding transcriptional regulators (Blackwell et al., 1994; An and Blackwell, 2003). The structure and role of the SKN-1 protein in other nematodes is not fully understood. The deduced amino acid sequences of the isolated gene orthologs show a high similarity in the important conserved motifs of SKN-1 as known from *C. elegans* (Figure 3-19). The nucleotide sequences of the isolated *skn-1* cDNAs from the different nematodes noticeably differ in size (see below).

Table 14: SKN-1 protein structure in nematodes studied

	SKN-1 (aa)	% identity SKN-1 DNA-binding domain	% identity of SKN-1 entire protein sequence
Ce SKN-1*	623	100	100
Cb SKN-1	394	93.7	70.3
Cr SKN-1	611	91.3	61.6
Dc SKN-1	520	84.8	45.8
Ps SKN-1	570	63.3	34.9
Ju SKN-1	473	60.8	34.8
An SKN-1	745	52.1	31.1

* For abbreviations, see Table 12. The sequences of the *Caenorhabditis* species were obtained from the NCBI database at http://www.ncbi.nlm.nih.gov/.

To determine the degree of conservation of the SKN-1 basic regions in other nematode species, we performed protein BLAST searches and Vector NTI alignments using the *C. elegans* SKN-1 as the query protein sequence (McGinnis and Madden, 2004). We found out that SKN-1 homologs are not found in all 12 clades (Table 12). Most of the SKN-1 sequences in the lower clades were found to be either incomplete or absent. Therefore, we restricted our analysis to those nematodes where full length protein sequences are available.

The numerous leucines residues (L) that make up the leucine zippers of the typical bZIP protein sequence are found in all species (Figure 3-18). However, among all species studied, there is less conservation in the SKN-1 DIDLID region (Figure 3-18A) that is important for SKN-1 transcriptional activation in *C. elegans* (Blackwell et al., 1994; Rupert et a. 1998).

An alignment of the carboxyl-terminal basic regions of *C. elegans* SKN-1 protein (residues 539-623) that constitutes the 84 amino acids sufficient for binding to DNA (Blackwell et al., 1994; Rupert et a. 1998) is shown in Figure 3-18B. The core basic region which interacts with the major groove in the target DNA (Rupert et al., 1998) is found in all studied species (Figure 3-18B). Furthermore, all nematodes also share a unique upstream feature that corresponds to the second basic region where they

possess a conserved glycine that also contributes to DNA binding (Blackwell et al., 1994; Rupert et al., 1998; Kophengnavong et al., 1999).

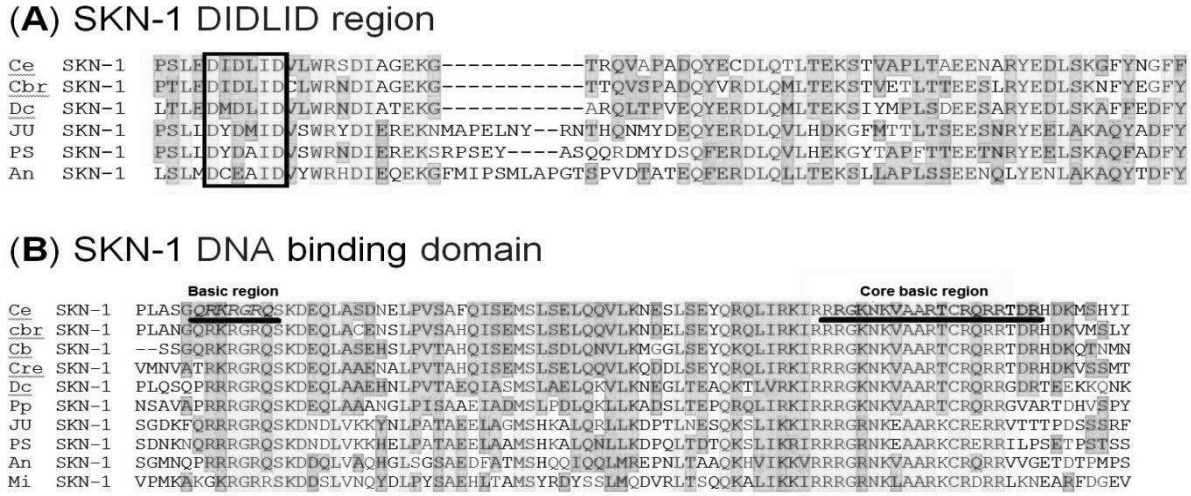

Figure 3-18: Alignment of *C. elegans* SKN-1 domain motifs with homologs from various nematodes A) Indicated is the conservation in the SKN-1 DIDLID region (boxed). B) alignment of the carboxyl-terminal basic regions of SKN-1 homologs that constitutes the 84 amino acids sufficient for binding to DNA in *C. elegans* (Blackwell et al., 1994; Rupert et al. 1998). Note the numerous leucines residues (L) that make up the leucine zippers of the typical bZIP protein sequence. Highlighted are the *C. elegans* SKN-1 basic region and the core basic region (underlined) (Blackwell et al., 1994, Bowermann et al., 1993). The amino acids are colour coded by degree of conservation; Yellow = identical, green = block of similar, blue = conservative, black = non-similar. Ce: *C. elegans*, Cbr: *C. briggsae*, C.b: *C. brenneri*, Pp = *Pristionchus pacificus*, JU = *Panagrolaimus sp.* (JU765), PS1159 = Panagrolaimus *sp.* (PS1159), An = *Acrobeloides nanus*, and Mi = *Meloidogyne incognita.*

The C-terminal basic regions of SKN-1 are not highly conserved outside of the genus *Caenorhabditis*

Genome analyses indicate that the minimal sequence of the SKN-1 amino-terminal required for SKN-1 DNA binding is present but not highly conserved amongst the studied nematodes. Although the most highly conserved basic residues seem to be conserved in all species, the sequences of the SKN-1 DNA binding domain of *A. nanus*, *Panagrolaimus sp.* (JU765) and *Panagrolaimus sp.* (PS1159) show some significant differences over the entire binding domain (Figure 3-18). This may indicate considerable differences in the structural conformations of these proteins that could result in different binding behavior or to different targets. These differences may account for the different spatial expression patterns in the nematodes of the various clades; further consolidating the assumption that the SKN-1 protein might play a different function among nematodes.

3.7.4 Bioinformatic analysis of PIE-1 homologs from selected nematode species

In *C. elegans*, the *pie-1* gene encodes a bi-functional PIE-1 protein with 2 zinc finger motifs (ZF1 and ZF2) that regulates both transcriptional repression and maternal RNA expression in germ-line blastomeres (Mello et al., 1996; Seydoux and Dunn, 1997; Tenenhaus and Seydoux, 2001). Both PIE-1 zinc finger domains (ZF1 and ZF2) are present in *Panagrolaimus sp.* (PS1159) and *A. nanus* (Figure 3-19). Amino acid sequence alignment of PIE-1 sequences from the parthenogenetic *Panagrolaimus sp.* (PS1159) and *A. nanus* revealed that about 76 % of the deduced amino acids of the two zinc finger domains are identical (Figure 3-19). The entire PIE-1 sequence in *Panagrolaimus sp.* (PS1159) is more similar to *C. elegans* PIE-1 than the *A. nanus* PIE-1 (data not shown). The ZF1 in *Panagrolaimus sp.* (PS1159) PIE-1 is 44 % similar to *A. nanus* ZF1, and the *Panagrolaimus sp.* (PS1159) ZF2 is 71 % identical to the ZF2 in *A. nanus*. This suggests that the ZF2 in *Panagrolaimus sp.* (PS1159) and *A. nanus* PIE-1 may fulfill similar roles as in *C. elegans*.

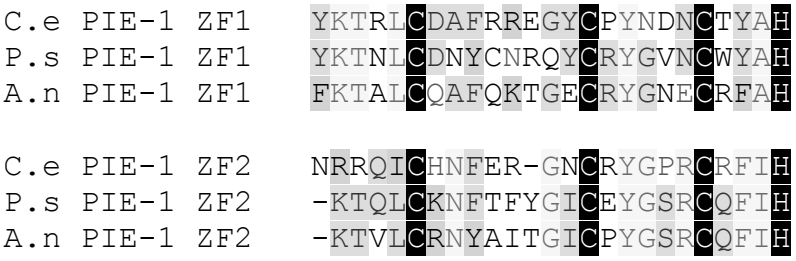

Figure 3-19: Alignment of the *C. elegans* PIE-1 CCCH-zinc finger motifs (ZF1 and ZF2) with sequences from *Panagrolaimus sp.* (PS1159) and *A. nanus*. C.e = *C. elegans*, P.s = *Panagrolaimus sp.* (PS1159) and A.n = *Acrobeloides nanus*. Highlighted in the black columns are the typical motifs of three cysteines and one histidine (CCCH) residues that function in regulating gene expression via directly binding to mRNA (Blackshear et al., 2005).

Table 15: Comparison of the *C. elegans* PIE-1 zinc finger (ZF) motifs with those in *Panagrolaimus sp.* (PS1159) and *A. nanus*.

	clade	ZF1 identity (%)	ZF2 identity (%)
C. elegans PIE-1	9	100	100
PS1159 PIE-1	10	56	42
A. nanus PIE-1	11	48	40

3.7.5 PAR-2 is present only in the genus *Caenorhabditis*

The *C. elegans par-2* gene encodes a RING-finger protein that has been shown to be asymmetrically localised to the posterior cortex of the 1- and 2-cell embryo via interdependent interactions with PAR-3, PAR-6, and PKC-3 (Nance and Priess, 2002; Gonczy, 2002; Pellettieri and Seydoux, 2002; Cuenca, et al., 2003; Munro et al., 2004). Except for the *par-2* gene, homologs of all the other *par* genes were found in all nematodes while the former was found only in the genus *Caenorhabditis* (Figure 3-20).

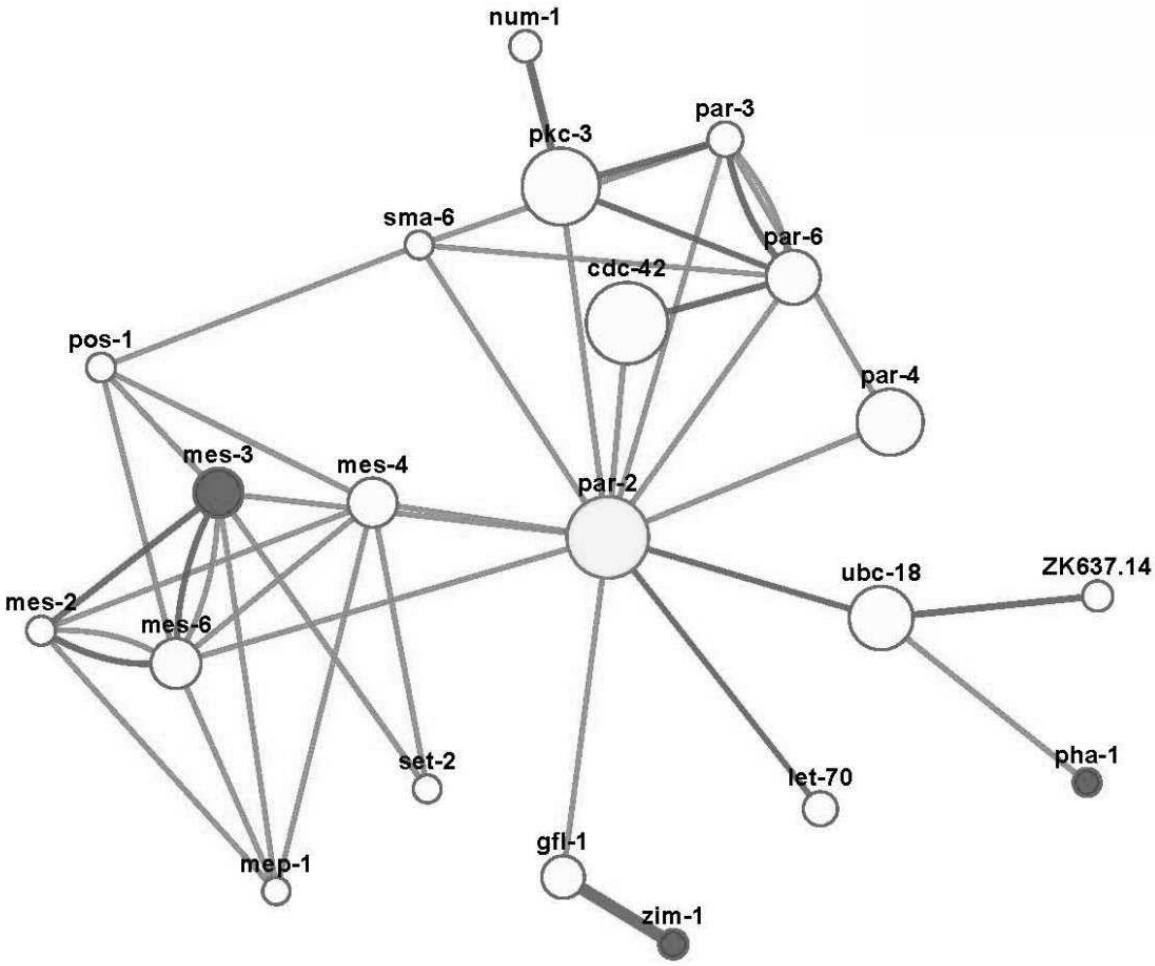

Figure 3-20: *In silico* analysis of the *par-2* gene network. Gene interaction map generated by GeneMANIA showing the 20 most related genes that reacted in various pathways with *par-2* in *C. elegans*. The *par-2* gene (yeloow) and its interacting gene are highlighted. Genes restricted to the genus *Caenorhabditis* are filled in red. Physical interactions (light blue lines) and genetic interactions (light green lines) are shown.

No clear orthologs of the *zim-1, mes-3 and pha-1* genes were found in any nematode group apart from members of the *Caenorhabditis* genus (Table 16).

Table 16: *par-2* interacting genes from various nematodes. + = present, - = absent. * For abbreviations see Table 12.

Clades	2		8			9					10	11	12
	Ts	Rc	Bm	As	Lo	Dc	Cn	Cr	Cb	Ce	Ps	An	Mi
cdc-42	-	+	+	+	+	+	+	+	+	+	+	+	+
gfl-1	+	+	+	+	+	+	+	+	+	+	+	+	+
let-70	+	+	+	+	+	+	+	+	+	+	+	+	+
mep-1	-	+	+	+	+	+	+	+	+	+	+	+	+
mes-2	-	-	+	+	+	+	+	+	+	+	+	+	+
mes-3	-	-	-	-	-	-	+	+	+	+	-	-	-
mes-4	-	-	+	+	+	+	+	+	+	+	+	+	+
mes-6	-	-	+	+	+	+	+	+	+	+	+	+	+
num-1	+	+	+	+	+	+	+	+	+	+	+	+	+
par-2	-	-	-	-	-	-	+	+	+	+	-	-	-
par-3	-	-	+	+	+	+	+	+	+	+	+	+	+
par-4	+	+	+	+	+	+	+	+	+	+	+	+	+
par-6	+	+	+	+	+	+	+	+	+	+	+	+	+
pha-1	+	+	-	-	-	-	+	+	+	+	-	-	-
pkc-3	+	+	+	+	+	+	+	+	+	+	+	+	+
pos-1	-	-	+	+	+	+	+	+	+	+	+	+	+
set-2	-	-	+	+	+	+	+	+	+	+	+	+	+
sma-6	+	+	+	+	+	+	+	+	+	+	+	+	+
ubc-18	+	+	+	+	+	+	+	+	+	+	+	+	+
ubc-21	-	-	+	+	+	+	+	+	+	+	+	+	+
zim-1	-	+	-	-	-	-	+	+	+	+	-	-	-

Most genes, proteins and other components execute their functions within a complex network of interactions and a single molecule can affect a wide range of other cell components. Searches of whole genome sequences and several databases have unveiled some gene homologs that are absent in distinct nematode clades. Previous studies have indicated that potential differences in the mode of cell specification exist in other nematodes compared to *C. elegans* (Schierenberg, 2005; Schulze and Schierenberg, 2007; Lahl et al., 2007). Taking these together and in order to better understand the role of the key maternal factors, the SKN-1 and PIE-1 proteins in cell specification, we analysed the spatial and temporal localisation of both *skn-1* and *pie-1* mRNAs by *in situ* hybridisation in several *Acrobeloides* and *Panagrolaimus* species.

3.8 Striking differences in the early embryonic expression pattern of *skn-1, mex-1,* and *pie-1* mRNAs among related nematodes

The translational regulation of specific mRNAs is important for controlling gene expression and early cell fate specification. To determine whether somatic and germ line expression of key maternal genes differ in other nematodes, we studied genes transcribed early in the embryo and determined their expression patterns by *in situ* hybridisation. Three vital genes in *C. elegans* transcribed before the onset of gastrulation (*pie-1, mex-1* and *skn-1*) were analysed in selected members of the genera *Panagrolaimus* and *Acrobeloides*. These belong to different clades with varied modes of reproduction (Figure 1-2). As in *C. elegans*, germline blastomeres divide asymmetrically in both *Panagrolaimus* and *Acrobeloides* species to give rise to one bigger somatic daughter and one smaller germline daughter (Figure 1-1).

Expression of *skn-1* mRNA in *C. elegans*

The distribution of *skn-1* mRNA in the early *C. elegans* embryo has been reported by Seydoux and Fire, (1994). Using our established *in situ* hybridisation method we confirmed mRNA distribution also in *C. elegans* early embryos showing that the applied alkaline bleach treatment has no deleterious effect. Initially, *skn-1* mRNA is equally distributed in the 1-cell stage, P0 (Figure 3-21A) and 2-cell stage blastomeres, AB and P1 (Figure 3-21B). During this second embryonic cell cycle, i.e. at the 4-cell stage, the *skn-1* mRNA appears to accumulate in much higher levels in P1 in both P1 daughters (P2 and EMS) than in the AB daughters (Aba and ABp). During the next cell cycle, *skn-1* mRNA disappears from most of the somatic cells and is only maintained in the germline cells P3 (Figure 3-21D) and P4 (Figure 3-21E). However, reappearance of *skn-1* mRNA has been reported in the gut primordium around the comma through pretzel stages, and in late proliferation stages, which is due to zygotic transcription (Seydoux and Fire, 1994).

The expression pattern of *skn-1* mRNA differs significantly between *C. elegans* and *A. nanus*

The genus *Acrobeloides* belongs to the family *Cephalobidae* of clade 11 (Figure 1-2). We compared *skn-1* staining patterns in *Acrobeloides* species to the model organism *C. elegans* (Rhabditidae) that belongs to clade 9. Within the genus

Acrobeloides, several species with different modes of reproduction are found, i.e. gonochoristic, hermaphroditic and parthenogenetic (Lewis et al., 2009).

Initially, we investigated the localisation pattern of the *skn-1* mRNA in the parthenogenetic *A. nanus* and compared this to the *skn-1* staining pattern known in the hermaphroditic *C. elegans* (Figure 3-21).

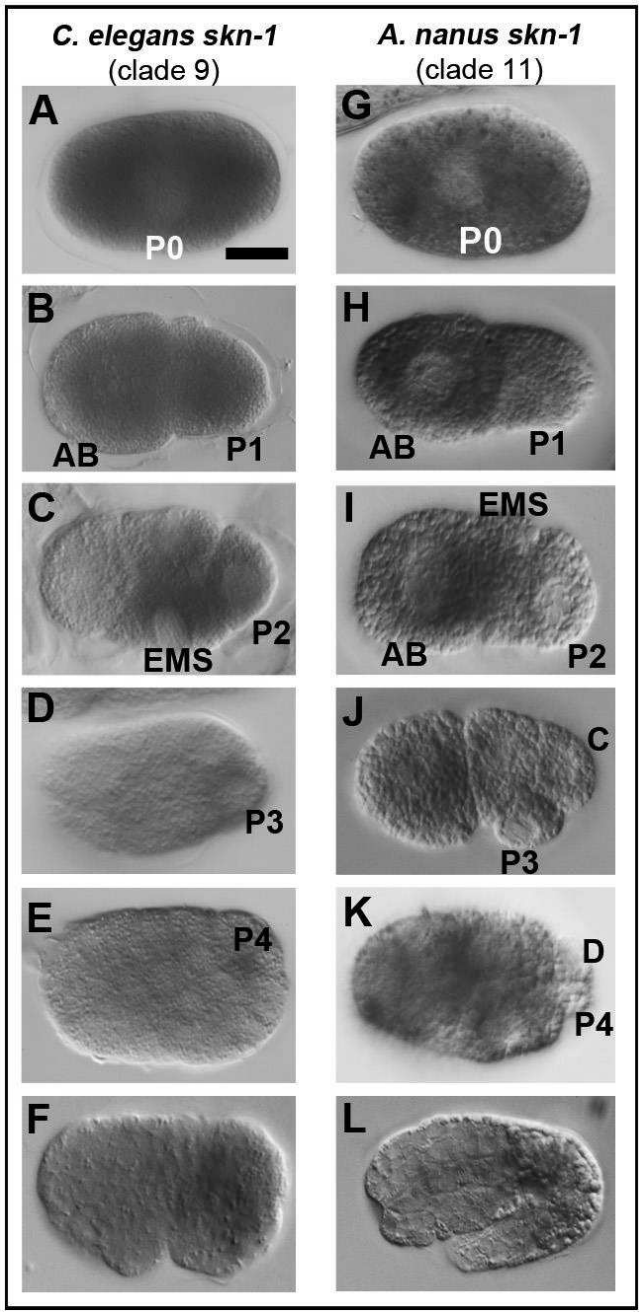

Figure 3-21: Localisation of the *skn-1* mRNA in *C. elegans* and *A. nanus*. The *skn-1* mRNA is initially uniformly distributed in the 1- cell stage embryo in all both species. In *C. elegans* (A-F), the transcript is maintained predominantly in the germline P2 cell and its sister cell EMS and successively lost from the somatic blastomeres. In *A. nanus* (G-L), staining of *skn-1* mRNA is observed exclusively in the somatic lineage from the 2- cell stage. Names of selected blastomeres are indicated. Orientation: Anterior is left, ventral is down, for all embryos. Scale bar: 10 µm.

In situ hybridisation with a *skn-1* mRNA probe specific for *A. nanus* revealed a uniform distribution of the mRNA in the 1-cell stage (Figure 3-21G), suggesting that *skn-1* mRNA in *A. nanus* is maternally provided. This early staining pattern in the 1-cell stage is similar to the localisation pattern observed in *C. elegans* (Figure 3-21A). However, from the 2-cell stage onward, the localisation of *skn-1* mRNA differs considerably in both species: In *A. nanus*, the *skn-1* transcript is detected exclusively in the somatic cells and is completely absent in the germline during embryogenesis (Figure 3-21G-K). In contrast, in *C. elegans, skn-1* mRNA is localised predominantly in the germline in early embryos (Figure 3-21A-E).

The unexpected differences in the *skn-1* mRNA expression between the hermaphroditic *C. elegans* and the parthenogenetic *A. nanus* could either be due to their different position in the phylogenetic tree (Figure 1-2) or it could be related to their different modes of reproduction. To obtain a better idea which of these options is more likely we examined three representatives of the genus *Acrobeloides* one of which is parthenogenetic (*A. maximus*) like *A. nanus* and two other species with sperm, the gonochoristic (strain SB374) and the hermaphroditic (strain PS1146) like *C. elegans*.

3.8.1 The distribution of *skn-1* mRNA is similar in all *Acrobeloides* species

Since the localisation of *skn-1* mRNA in the parthenogenetic *A. nanus* differs significantly from the hermaphroditic *C. elegans*, we wanted to know whether this remarkable finding in *skn-1* mRNA distribution is species-specific or appears to other *Acrobeloides* species as well. Therefore, we stained early embryos with the *skn-1* mRNA probe from *A. nanus* for heterologous hybridisation in three other *Acrobeloides* species with varied modes of reproduction; *Acrobeloides sp.* (SB374) (gonochoristic), *Acrobeloides sp.* (PS1146) (hermaphroditic) and *A. maximus* (parthenogenetic). Our experiments revealed that this probe visualises specific staining in somatic blastomeres in these *Acrobeloides* species as observed in *A. nanus*, indicating successful cross-hybridisation (Figure 3-22). In all *Acrobeloides* species tested, at the 2-cell stage, there was much less mRNA in the P1 cell compared to the AB cell (Figure 3-22B). The *skn-1* mRNA was successively lost from the germ line following each germ line division and there was absolutely no staining in the germ line by the time the primordial germ cell P4 was born (Figure 3-22Q).

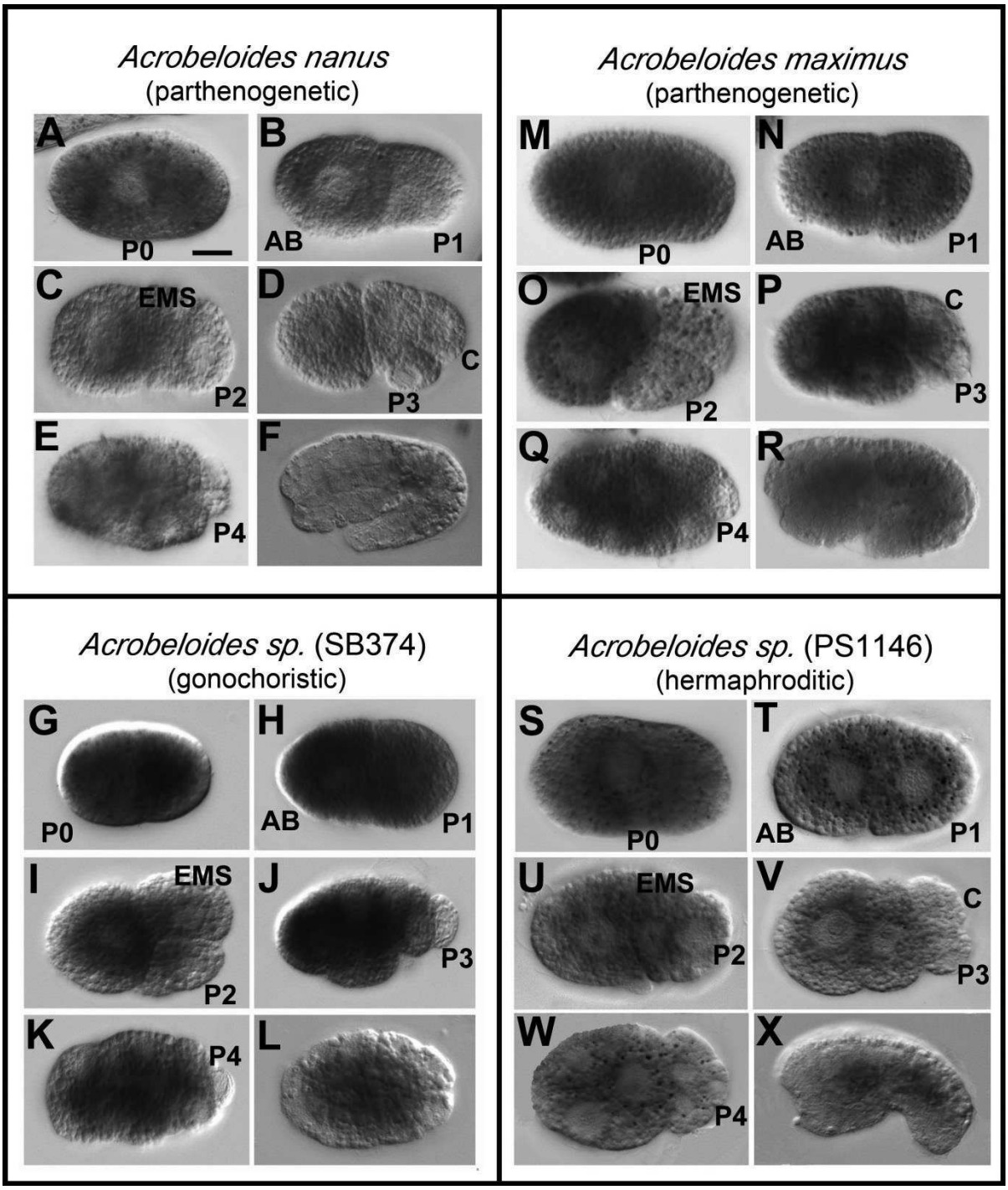

Figure 3-22: Distribution of *skn-1* mRNA in 4 Acrobeloides species by *in situ* hybridisation. Independent of the mode of reproduction, the *pie-1* mRNA is equally localised in early embryos up to the 2-cell stage. Afterwards, staining was absent in the germline blastomeres and maintained only in the somatic blastomeres in all *Acrobeloides* species. In late morphogenesis stages, the intestinal tract is also stained. Orientation: anterior is to left in all embryos. Scale bar = 10 µm.

In fact, all the 4 different *Acrobeloides* species investigated show the same staining pattern, demonstrating that the localisation of *skn-1* mRNA is not species-specific and that it is independent of the mode of reproduction. The major difference to the

expression patterns seen in *C. elegans* early embryos is that staining is concentrated in germline cells.

In morphgenesis stages of all *Acrobeloides* species, *skn-1* mRNA was detected in pharnygeal and gut primordia (Figure 3-22R). Interestingly, *C. elegans skn-1* mRNA has been reported in the gut primordium around the comma stage through pretzel stages (Seydoux and Fire, 1994). The staining in pharnygeal and gut primordia seen in the *Acrobeloides* species suggests a similar role for the *skn-1* gene in endomesoderm specification as is the case in *C. elegans* (Blackwell, 1992, Bowerman et al. 1993, Maduro, 2006).

3.8.2 *skn-1* mRNA localisation differs between *Panagrolaimus sp.* (PS1159) and the closely related *Propanagrolaimus sp.* (JU765)

The genus *Panagrolaimus* belongs to the family *Panagrolaimidae* and is positioned in clade 10 (Figure 1-2). Since *skn-1* mRNA distribution seems to be clade-specific with prominent differences in representatives of clades 9 and clade 11 (see above), we wondered whether the localisation of *skn-1* mRNA in nematodes of clade 10 is like that in *C. elegans* or like that in the *Acrobeloides* species. Two representatives were considered, the parthenogenetic *Panagrolaimus sp.* (PS1159) and the hermaphroditic *Propanagrolaimus sp.* (JU765).

In *Panagrolaimus sp.* (PS1159) the *skn-1* gene appears also to be maternally provided since the 1-cell stage embryo was uniformly stained (Figure 3-23A). 2-cell stage embryos show an asymmetrical *skn-1* mRNA distribution between the AB and P1 blastomeres, with higher staining in the posterior germline P1 blastomere than in the somatic AB cell (Figure 3-23B). At the 4-cell stage, *skn-1* mRNA staining was exclusively seen in the germline P2 daughter cell with no staining in its somatic sister cell EMS (Figure 3-23C). The *skn-1* mRNA was subsequently maintained only in the germline progeny P3, P4 and in the P4 daughter cells Z2 and Z3 throughout embryogenesis (Figure 3-23D-F).

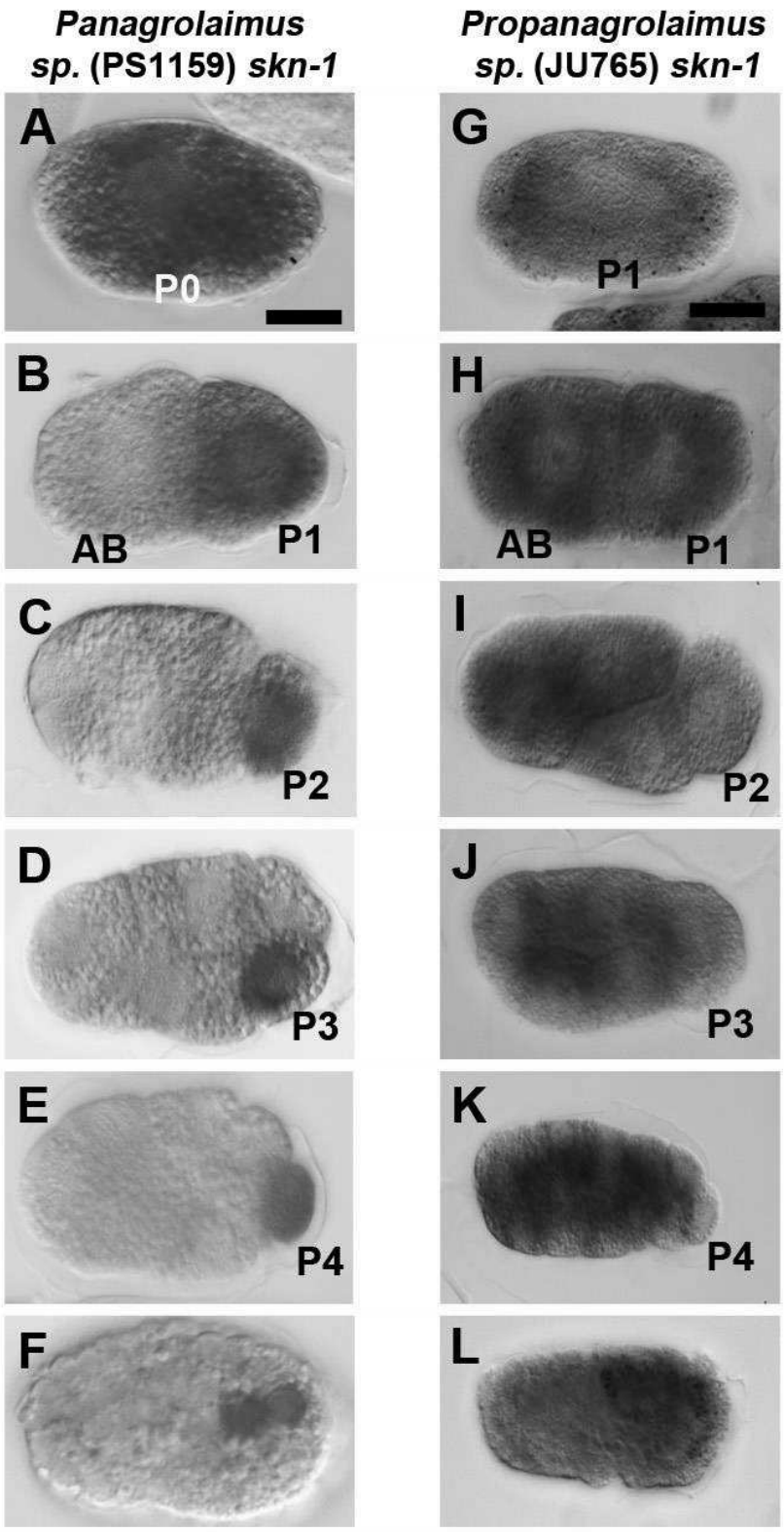

Figure 3-23: **Localisation of *skn-1* mRNA in the parthenogenetic *Panagrolaimus sp.* (PS1159) and the hermaphroditic *Panagrolaimus sp.* (JU765).** Unlike germline staining in *Panagrolaimus sp.* (PS1159), *skn-1* mRNA is restricted to the somatic cells in *Propanagrolaimus sp.* (JU765). Embryos are oriented with anterior to the left. Scale bar = 10µm

The localisation pattern observed in the *Panagrolaimus sp.* (PS1159) species is on the one hand like in *C. elegans* early embryos where staining is maintained mainly in the germline cells, and on the other hand, it is different to the *skn-1* mRNA distribution in *C. elegans*, where the *skn-1* transcript is not detected after the division of the primordial germ cell P4 (Seydoux and Fire, 1994). Unlike the exclusive localisation of *skn-1* mRNA in the germline in *Panagrolaimus sp.* (PS1159) throughout embryogenetic development, *skn-1* mRNA staining in *Propanagrolaimus sp.* (JU765) was restricted to the somatic cells and absent in the germline (Figure 3-23G-L). During late embryogenesis, *skn-1* mRNA is restricted to cells in the region of the pharynx and gut (Figure 3-23L) like in the *Acrobeloides* species (Figure 3-22) that belong to clade 11.

This surprising difference in *skn-1* mRNA expression among these closely related species that both belong to clade 10 indicate that *skn-1* mRNA spatial localisation could be related to the phylogenetic position and not related to the mode of reproduction, because the *Propanagrolaimus sp.* (JU765) is phylogenetically positioned closer to clade 11 than to clade 9 (personal communication P. Schiffer).

To decide whether the pattern as found in *C. elegans* and *Panagrolaimus sp.* (PS1159) is a synapomorphic character (derived state) and the pattern found in *A. nanus* and the *Propanagrolaimus* sp (JU765) is a plesiomorphic or ancestral state or vice versa, additional species from other clades need to be studied.

Similar germ line localisation of *mex-1* mRNA in *Panagrolaimus sp.* (PS1159) and *C. elegans*

Previous studies have shown that the maternal gene *mex-1* is essential for the development of germ cells during the first embryonic cleavages (Mello et al. 1992; Schnabel et al. 1996). In the hermaphroditic *C. elegans, mex-1* mRNA is found primarily in germline cells (Guedes and Priess, 1997). Because the zinc finger motif of MEX-1 has been shown to be involved in the regulation of SKN-1 at the level of *skn-1* mRNA translation and SKN-1 protein stability in *C. elegans* (Mello et al. 1996; Guedes and Priess, 1997), we asked whether the *mex-1* gene might have a similar distribution pattern in a representative of the genus *Panagrolaimus* that reproduces in the absence of sperm. Therefore, we cloned a *mex-1* homolog from the parthenogenetic *Panagrolaimus sp.* (PS1159) and analysed its expression by *in situ*

hybridisation. Like in *C. elegans,* (clade 9) *mex-1* mRNA was localised predominantly in the germline cells in *Panagrolaimus sp.* (PS1159) (Figure 3-24). However, unlike in *C. elegans* where *mex-1* mRNA is also found in the somatic sister cells of the germline blastomeres (Guedes and Priess, 1997), *Panagrolaimus sp.* (PS1159) *mex-1* mRNA is absent in all somatic blastomeres after the 2-cell stage (Figure 3-24I).

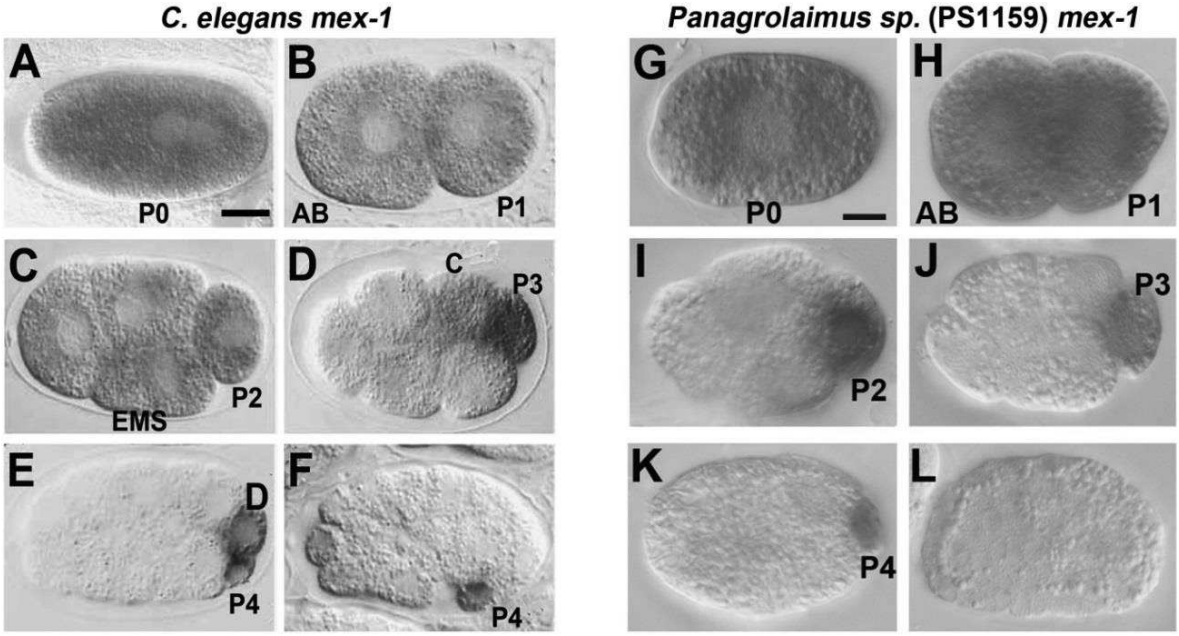

Figure 3-24: Localisation of *mex-1* mRNA in *C. elegans* (A-F) taken from Guedes and Priess, 1997, and *Panagrolaimus sp.* (PS1159) (G-L). In both nematodes, *mex-1* mRNA appears to be distributed uniformly in 1-cell (A, G) and early 2-cell (B, H) embryos. In the late 2-cell stage, in *Panagrolaimus sp.* (PS1159), *mex-1* mRNA appears to be at higher levels in the P1 blastomere than in AB (H). In the 4-cell stage embryo in *C. elegans* (C), *mex-1* mRNA appears more abundant in the germline blastomere P2 and its sister cell EM than in the somatic AB cells. In *Panagrolaimus sp.* (PS1159), *mex-1* mRNA is found exclusively in the P2 blastomere (I). In the *C. elegans* 8-cell embryo (D), *mex-1* mRNA is detected at high levels in the germline blastomere P3 and at lower levels in its somatic sister C, whereas staining in *Panagrolaimus sp.* (PS1159) is detected only in the P3 cell (J). Early *C. elegans* 28-cell embryo (E), *mex-1*mRNA is detected only in the germline blastomere P4 and its somatic sister D. In (K), only P4 is stained in *Panagrolaimus sp.* (PS1159). In the gastrulation stage embryo in *C. elegans* (F), *mex-1* mRNA is detected only in P4, but not in D. No staining of P4 in *Panagrolaimus sp.* (PS1159) late gastrulation stage (L). Embryos are oriented with anterior to the left. Scale bar = 10µm

Germline-restricted *pie-1* expression in *Panagrolaimus* differs only slightly from *C. elegans*

Like many maternal RNAs in *C. elegans*, the *pie-1* gene locus encodes a maternal RNA which is distributed uniformly in oocytes and early embryos. After the 4-cell stage, *pie-1* RNA is lost from somatic blastomeres and is maintained only in the germline (Figure 3-25A-D) (Seydoux and Fire 1994; Tenenhaus et al., 1998). Nothing is known about *pie-1* mRNA localisation in other nematodes besides *C. elegans* that belongs to clade 9. Therefore, we analysed the distribution of the *pie-1* message by *in situ* hybridisation in the parthenogenetic *Panagrolaimus sp.* (PS1159), a representative of the *Panagrolaimus* genus of clade 10 and compared this *C. elegans*.

Unlike in *C. elegans*, where *pie-1* mRNA is present in all cells up to the 4- cell stage (Figure 3-25A-D), in *Panagrolaimus sp.* (PS1159), *pie-1* mRNA was found to be uniformly distributed only in the 1-cell stage embryos (data not shown). In the 2-cell stage, *pie-1* mRNA localisation becomes asymmetrical with increased levels of *pie-1* mRNA segregated to the posterior blastomere P1, rather than in the anterior AB blastomere (Figure 3-25E). After the 4-cell stage, it is progressively lost from AB somatic descendants and retained in high levels mainly in germline blastomeres and only to a lesser degree in their somatic sister cells. This sequence of asymmetric localisation is repeated in each unequally dividing germline cell (Figure 3-25F-H). After division of P4, no *pie-1* mRNA transcripts were detected anymore in any cells (Figure 3-25I).

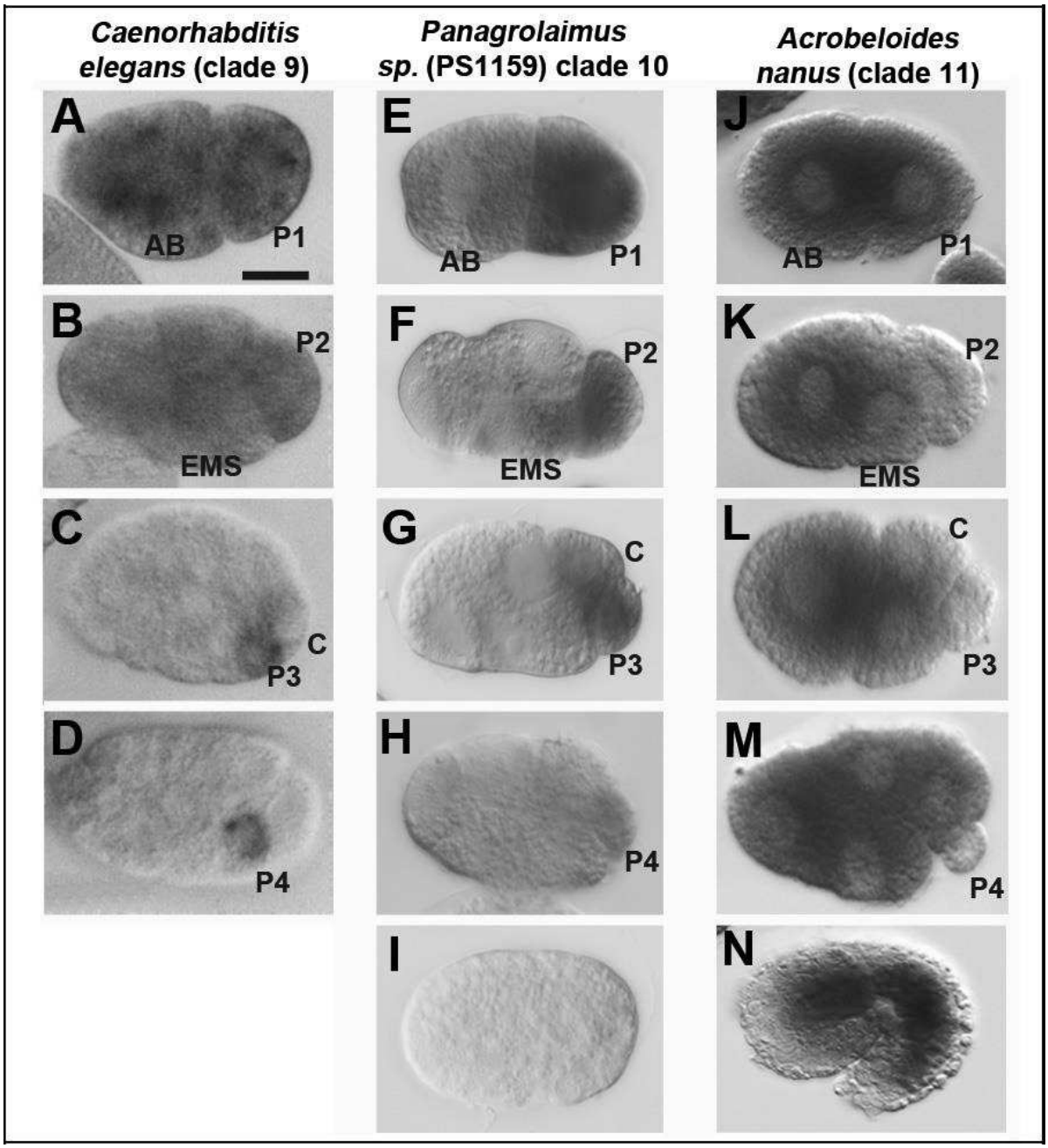

Figure 3-25: Localisation of *pie-1* mRNA in *C. elegans*, *Panagrolaimus sp.* (PS1159) and *A. nanus*. (A, B) Uniform distribution of the *pie-1* message in *C. elegans* 2-cell stage and 4-cell stage embryos. In *Panagrolaimus sp.* (PS1159), *pie-1* mRNA is present in higher amounts in the germline blastomeres P1 and P2 than in the anterior somatic AB or EMS cells (E, F). In embryos before the 24-cell stage (C and G), *pie-1* mRNA is mainly detected in the germline cell and to a lesser amount in the somatic sister cell. At about the 50-cell stage *pie-1* mRNA is found only in P4. (D). When P3 divides, the *pie-1* transcript becomes exclusively restricted to the germline precursor cell P4 (H). In *C. elegans* (data not shown) and *Panagrolaimus sp.* (PS1159), no *pie-1* mRNA was detected in the daughters of P4 (I). In *A. nanus pie-1* mRNA is excluded from the germline, except P1 (J) but found mainly in the somatic blastomeres (J-N). In some case, staining was seen in the pharyngeal and intestinal tissues in the morphogenesis stage (N). Figures A-D are taken from Tenenhaus et al. 1998. Embryos are orientated with anterior to left in all embryos. Scale bar = 10 µm.

Exclusive somatic *pie-1* mRNA localisation in *A. nanus*, opposed to germline localisation in *C. elegans*

The localisation of *pie-1* mRNA in the hermaphroditic *C. elegans* (clade 9) and the parthenogenetic *Panagrolaimus sp.* (PS1159) (clade 10) is predominantly in the germline blastomeres (Figure 3-25A-H). This could either be due to the phylogenetic position or the mode of reproduction. Therefore, it was imperative to test whether the spatial and temporal localisation pattern of *pie-1* mRNA was clade-specific or related to the mode of reproduction. In addition, we investigated the staining pattern of the *pie-1* gene in *A. nanus,* a parthenogenetic representative of clade 11. Our results suggest that the *pie-1* mRNA is also maternally provided in *A. nanus* as we observed uniform distribution of the mRNA in the 2-cell stage (Figure 3-25J). After the 2- cell stage, the *pie-1* mRNA was progressively excluded from the germline blastomeres and was found only in the somatic cells (Figure 3-25K-M) throughout embryogenesis. During late proliferation stages and morphogenesis, *A. nanus pie-1* mRNA was localised around the pharyngeal and gut primordial (Figure 3-25N).

These striking differences in the localisation pattern of the *pie-1* mRNA amongst different species from various clades may imply a different role for the *pie-1* gene in these species.

Unlike in *C. elegans*, Cephalobids reveal remarkable differences in *pie-1* mRNA localisation

The *Acrobeloides* group with several members having different modes of reproduction (Lewis et al., 2009) offers the opportunity to test whether these show the same staining pattern. Therefore, we tested *pie-1* mRNA staining in the parthenogenetic *A. maximus*, the gonochoristic *Acrobeloides sp.* (SB374) and the hermaphroditic *Acrobeloides sp.* (PS1146). We found that all 4 *Acrobeloides* species studied showed the same *pie-1* mRNA localisation pattern, with staining predominantly in the somatic blastomeres in early embryos and along the alimentary tract in late stages (Figure 3-26), indicating that this is independent on phylogenetic position or of the reproductive mode. From this it can be concluded that the *pie-1* gene activity seems to play the same role in all *Acrobeloides* species and its spatial expression pattern is not related to the reproductive mode.

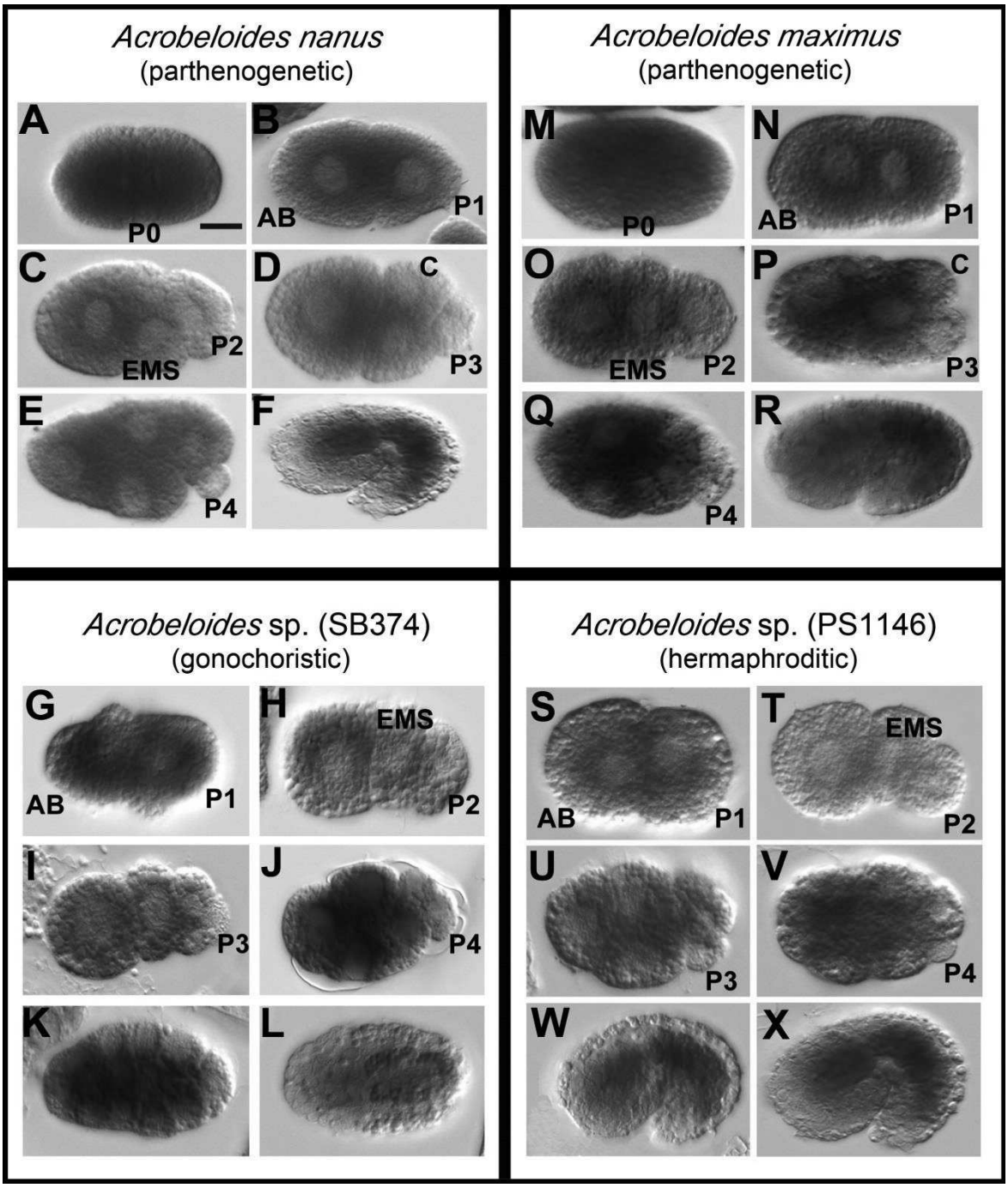

Figure 3-26: Distribution of *pie-1* mRNA in 4 *Acrobeloides* species by *in situ* hybridisation. Independent of the mode of reproduction, the *pie-1* mRNA is equally localised in early embryos up to the 2-cell stage. Afterwards, staining was absent in the germline blastomeres and maintained only in the somatic blastomeres in all *Acrobeloides* species. In morphogenesis stages, the intestinal tract is also stained. Anterior is to left in all embryos. Scale bar = 10 µm.

In summary, these findings revealed that the expression patterns of *skn-1* mRNA in nematodes from three different clades with different modes of reproduction differ significantly from each other. In the hermaphroditic *C. elegans skn-1* mRNA is maintained in the germ lineage up to the 28-cell stage (P4), during which it is

progressively lost from the somatic cells. No staining was detected in the P4 daughters Z2 and Z3, while staining from comma to pretzel stages has been reported around the gut region.

While the parthenogenetic *Panagrolaimus sp.* (PS 1159) shares the long-lasting and exclusive germline *skn-1* expression throughout embryogenesis, with no gut staining, its closely related species, the *Propanagrolaimus sp.* (JU765) shows more similarities to the *Acrobeloides* species independent of their mode of reproduction. However, *skn-1* mRNA was localised in pharyngeal and intestinal regions in *Acrobeloides* species as is known in *C. elegans*.

Table 17: Embryonic expression in *Panagrolaimus* and *Acrobeloides* species.

Panagrolaimus species (clade 10)			*Acrobeloides* species (clade 11)			
	PS1159	JU765	*A. nanus*	*A. maximus*	SB374	PS1146
	f	h	f	f	m,f	h
skn-1	+	-	-	-	-	-
pie-1	+	-	-	-	-	-
mex-1	+	Not analysed				

+ = similar; - = different expression patterns to *C. elegans.* f = female, m = male, h = hermaphrodite

The most significant finding of this study is that despite the similarity in structure of the hatched larva, *pie-1* and *skn-1* mRNAs in *C. elegans*, the *Acrobeloides* and *Panagrolaimus* species are localised in a very different fashion irrespective of clade number and mode of reproduction. This may suggest a different spatial role for these genes in various nematodes, although it needs to be shown to what extent the specific spatial localisation of these mRNAs correlates to the location of the respective functional proteins. Antibody staining in these species might shed more light to the possible differences in spatial action domains of these proteins among nematodes.

Considering the fact, that *skn-1* and *pie-1* mRNA expression show major differences in time and space in distinct nematodes suggests that the SKN-1 and PIE-1 proteins may execute discrete developmental functions. Therefore, we asked if development of a nematode can take place without participation of both proteins. Surprisingly by

searching nematode whole genome databases we identified several nematode species without well-defined SKN-1 and PIE-1 protein homologs.

3.9 MAP kinase activity and MSP genes in parthenogenetic nematodes

This part of my thesis is based on a co-operation with colleagues from our laboratory as a side project to investigate key elements of oocyte-to-embryo transition: MSP (major sperm protein) expression and MAP (mitogen-activated protein) kinase signalling, in parthenogenetic and non- parthenogenetic nematodes.

3.9.1 MAP kinase genes are conserved in parthenogenetic nematodes

MAP kinase activation is mediated by sperm and is known to play a central role during *C. elegans* embryonic development (Miller et al., 2001, Lee et al., 2007). Parthenogenetic nematodes lack sperm and thus might differ from hermaphrodites like *C. elegans* with respect to MAP kinase properties. To test this assumption, we cloned MAP kinase genes of the parthenogenetic nematode *A. nanus* and of its close relative with hermaphroditic reproduction, *Acrobeloides sp.* (PS1146), as well as the MAP kinase gene of a second parthenogenetic nematode, *D. coronatus*, a close relative of *C. elegans* (see Figure 3-27A; phylogeny after (Holterman et al., 2006).

We performed a phylogenetic analysis with a sequence set representing the five MAP kinase subfamilies and the resulting phylogenetic tree confirmed the placement of the newly isolated MAP kinase sequences to the Erk1/2 subfamily (Figure 3-27B). It further suggests that *C. elegans* MPK-2, whose function is not known so far, is a member of the Erk5 subfamily of MAP kinases. According to our phylogenetic tree, MPK-1 is the only Erk1/2 MAP kinase ortholog present in *C. elegans* suggesting that our cloned MAP kinase sequences, too, represent Erk1/2 orthologs with a possible role in oocyte maturation. Sequence comparison revealed that the MAP kinase sequences between phylogenetically related, but reproductively different pairs *A. nanus*/*Acrobeloides sp.* (PS1146) and *C. elegans*/*D. coronatus* are slightly more similar to each other than sequence pairs derived from nematodes with identical reproduction (95 % vs. 92 %, Figure 3-27A, B). The amino acid sequence of the entire activation loop is highly conserved in the MAP kinases of all nematode

species considered here (Figure 3-27C). In particular, T202 and Y204, which are phosphorylated during activation, are present in all MAP kinases and match the T-X-Y dual phosphorylation motif found in *C. elegans* MPK-1 and other Erk1/2 family members (Figure 3-27C). Thus, the considerable sequence conservation between hermaphroditic and parthenogenetic MAP kinases rejects the possibility of a specific alteration in parthenogenetic nematodes.

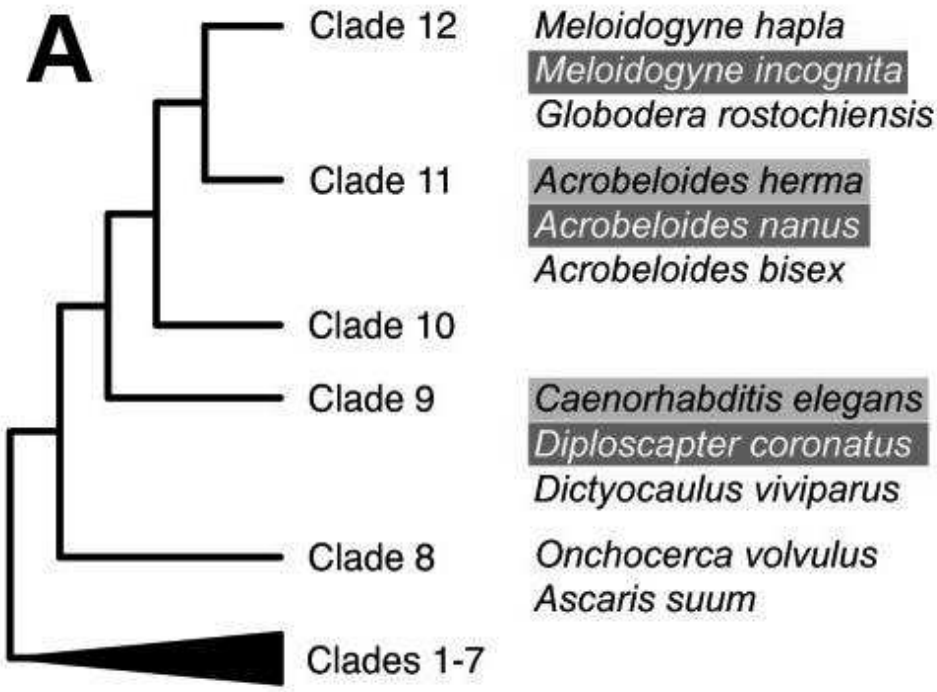

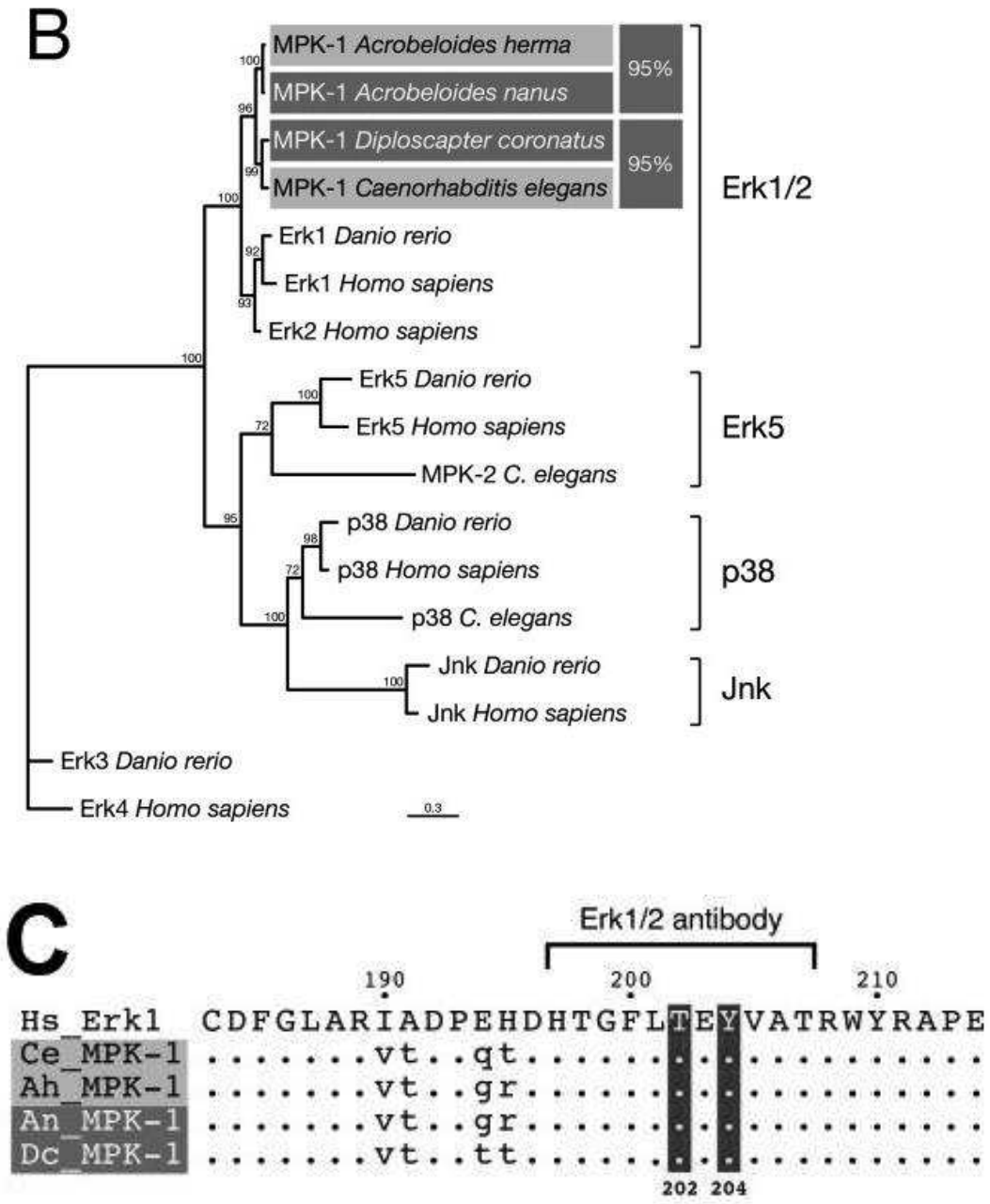

Figure 3-27: MAP kinase sequence is conserved in parthenogenetic nematodes. A: Simplified phylogenetic tree of the phylum nematoda. Species mentioned in this study are indicated and mapped to their respective clade. Clades 1-7 are collapsed into one branch. Colour assigns parthenogenetic (violet) or hermaphroditic reproduction (grey) through all figures. B: Phylogenetic analysis of MAP kinase genes from hermaphroditic (*C. elegans* and *Acrobeloides sp.* (SB374) (herma)) and parthenogenetic (*A. nanus* and *D. coronatus*) nematodes. All newly isolated nematode MAP kinase genes belong, like *C. elegans* MPK-1, to the Erk1/2 subfamily of MAP kinases. They group in line with the inferred phylogenetic position, not according to the underlying reproductive mode. *C. elegans* MPK-2, to which a function has not been ascribed so far, clusters to the Erk5 subfamily. C: Sequence alignment of the activation loop of human and nematode Erk1/2 MAP kinase proteins. Amino acids T202 and Y204 (numbering after human Erk1), which get phosphorylated during activation, are indicated (red). The epitope recognised by the antibody against active MAP kinase, including the dual phosphorylation motif, is highly specific for Erk1/2 family members and perfectly conserved in nematode MAP kinases irrespective of the reproductive mode. Hs = Homo sapiens, Ce = *C. elegans*, An = *A. nanus*, Ah = *Acrobeloides sp.* (PS1146), Dc = *D. coronatus*. (Taken from Heger et al., 2010).

MAP kinase activation is conserved in parthenogenetic nematodes

Since the MAP kinase activation loop including the dual phosphorylation motif is conserved in parthenogenetic nematodes (Figure 3-27C), we wanted to know whether MAP kinase activation is detectable in these nematodes despite the lack of sperm. Therefore, we stained gonad preparations of our nematode set with a monoclonal antibody highly specific for the activation loop of dephosphorylated Erk1/2 MAP kinase. Our experiments revealed that MAP kinase is active in late-stage oocytes of all species regardless of the reproductive mode (Figure 3-28). MAP kinase stainings of *C. elegans* gonads confirmed already published data (Miller et al., 2001, 2003; Lee et al., 2007) and gave a positive signal in proximal oocytes and the gonadal loop region (Figure 3-28A). This indicates that our experimental setup gives the anticipated results. As previously reported (Lee et al., 2007), we observed variable patterns of activated MAP kinase in the proximal oocytes of *C. elegans* (not shown), but also in the three *Acrobeloides* species. MAP kinase activation sometimes extended over three or four proximal oocytes (-1 to -4), occasionally interrupted by a non-activated cell, or could be restricted to the -2 or -3 oocyte without a signal in -1. We noticed such staining patterns in 4/11 (*A. nanus*) and 11/22 cases (*Acrobeloides sp.* (PS1146). As an example, an unusual staining of the second and fourth, but not the first, oocyte from the *Acrobeloides sp.* (SB374) gonad is shown (Figure 3-28E). It likely represents a snapshot shortly after activation of the -1 oocyte has been completed. In contrast to other nematodes, exclusively the most proximal oocyte was stained in *D. coronatus* (13/13 cases; Figure 3-28I). This difference may be attributed to the shorter gonadal arms of *D. coronatus* where just a single or at most two large, yolk containing oocytes are present (Figure 3-28I, J) compared to a row of 5-10 in the other species.

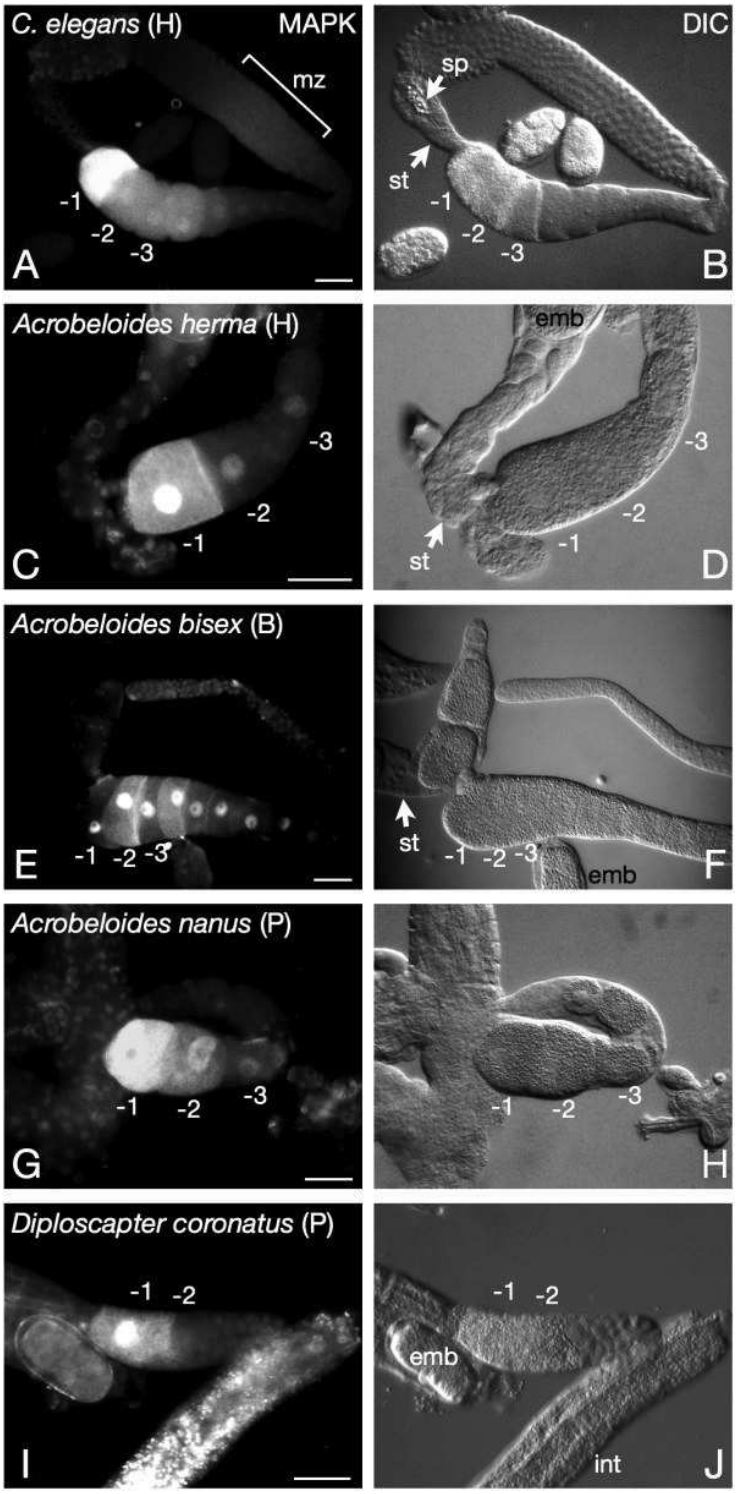

Figure 3-28: MAPK activation is conserved in parthenogenetic nematodes. Gonad preparations of parthenogenetic (P), hermaphroditic (H) and bisexual (B) nematode species stained for active MAP kinase (left panel; corresponding DIC picture: right panel). In all five nematode species with three different modes of reproduction, MAP kinase activation can be detected in proximal oocytes as described for the *C. elegans*system (Miller et al., 2001). It is therefore independent of the reproductive strategy. In*C. elegans*, MAP kinase activation is biphasic and can also be observed in the meiotic zone (mz) of the syncytial gonad (panel A, bracket; (Miller et al., 200; Page et al., 2001). The pronounced nuclear staining in *Acrobeloides* species might reflect early MAP kinase dependent gene expression. sp: sperm. st: spermatheca. int: intestine. emb: embryo. -1, -2, -3: proximal oocytes, -1 is most proximal. All gonads are oriented with proximal to the left. Bar: 20 µm. (Taken from Heger et al., 2010).

Furthermore, the percentage of stained oocytes was considerably lower in *D. coronatus* than in *C. elegans* or in the *Acrobeloides* species (roughly 10 % vs. 50 %). While *C. elegans* oocytes mature at a fast rate of one every 23 min (McCarter et al., 1999), this interval is several times longer in *D. coronatus* (data not shown) giving a likely explanation for the less frequent staining of oocytes in this species.

We sometimes observed in the *Acrobeloides* species a more pronounced MAP kinase signal in the nuclei of late stage oocytes than in *C. elegans* (Figure 3-28C, E). This might be a consequence of the need for early transcription in *Acrobeloides* embryos (McCarter et al., 1999) as compared to *C. elegans* (Edgar et al 1994). MAP kinase activation is also required at an earlier stage in developing *C. elegans* oocytes, for the exit from pachytene of the first meiotic prophase (Church et al., 1995), after which it is rapidly turned off. Therefore, a characteristic biphasic pattern of MAP kinase activation can be observed in the *C. elegans* germline (Figure 3-28A; (Miller et al., 2001). Like *C. elegans* and other non-parthenogenetic nematodes the parthenogenetic species *A. nanus* and *D. coronatus* undergo meiosis leading to the formation of polar bodies (Lahl et al., 2006). We wondered whether an analogous early activation of MAP kinase in conjunction with meiosis is detectable in the distal gonads of our parthenogenetic nematodes. Our preliminary data do not support the presence of a biphasic activation (not shown) suggesting that oocyte development as well as meiotic cell cycle regulation may be different in parthenogenetic vs. non-parthenogenetic nematodes.

In conclusion, activation of the Erk1/2 MAP kinase pathway is a hallmark of oocyte maturation in parthenogenetic nematodes as it is in many other animals. Therefore, MAP kinase activation in proximal oocytes does not mirror differences in the reproductive mode.

3.9.2 Major sperm protein is not detectable in parthenogenetic nematodes

In *C. elegans*, sperm trigger oocyte meiotic maturation and ovulation using the major sperm protein (MSP) as an extracellular signaling molecule (Miller et al., 2001). MAP kinase sequences and MAP kinase activation in the germline of parthenogenetic species appear similar to the model system *C. elegans*. Consequently, we asked whether MSP, the trigger of this activation in *C. elegans* (Miller et al., 2001), is also present in parthenogenetic nematodes. To test this possibility, we performed

immunofluorescence analysis of nematode gonads (Figure 3-29) with a monoclonal antibody against the highly conserved C-terminus of MSP (Kosinski et al., 2005). Staining of the hermaphroditic *C. elegans* gonad gives the expected signal of sperm-associated MSP coinciding with the DAPI signal of sperm nuclei (Figure 3-29A, B). The same could be observed after staining the gonads of hermaphroditic and bisexual *Acrobeloides* species (Figure 3-29E, F) indicating that the *C. elegans* antibody is able to recognise MSP from distant groups. In the cases where we detected sperm nuclei the corresponding MSP signal appeared slightly blurred (Figure 3-29B, D, F). This is consistent with the demonstration of cytoplasmatic and extracellular MSP in *C. elegans* (Kosinski et al., 2005) and suggests that the extracellular signaling function of MSP might be conserved in other nematode groups. In addition to the sperm-associated signal, the MSP antibody marked extracellular puncta at the surface of the -1 and occasionally the -2 oocyte (Figure 3-29A, inset). A similar localisation of secreted MSP in the *C. elegans* gonad has been reported in a previous paper (Kosinski et al., 2005) indicating an adequate sensitivity of our experimental setup. In contrast to the sexual species, we never observed such puncta or other MSP-related signals in gonad preparations of the parthenogenetic nematodes *A. nanus* and *D. coronatus* (Figure 3-29G, I). Likewise, we could not detect sperm nuclei in these species. As spermatocytes are the only known cells in nematodes where MSP is expressed (Klass et al., 1982; Jiang et al., 2008), the absence of MSP is expected in nematodes lacking sperm.

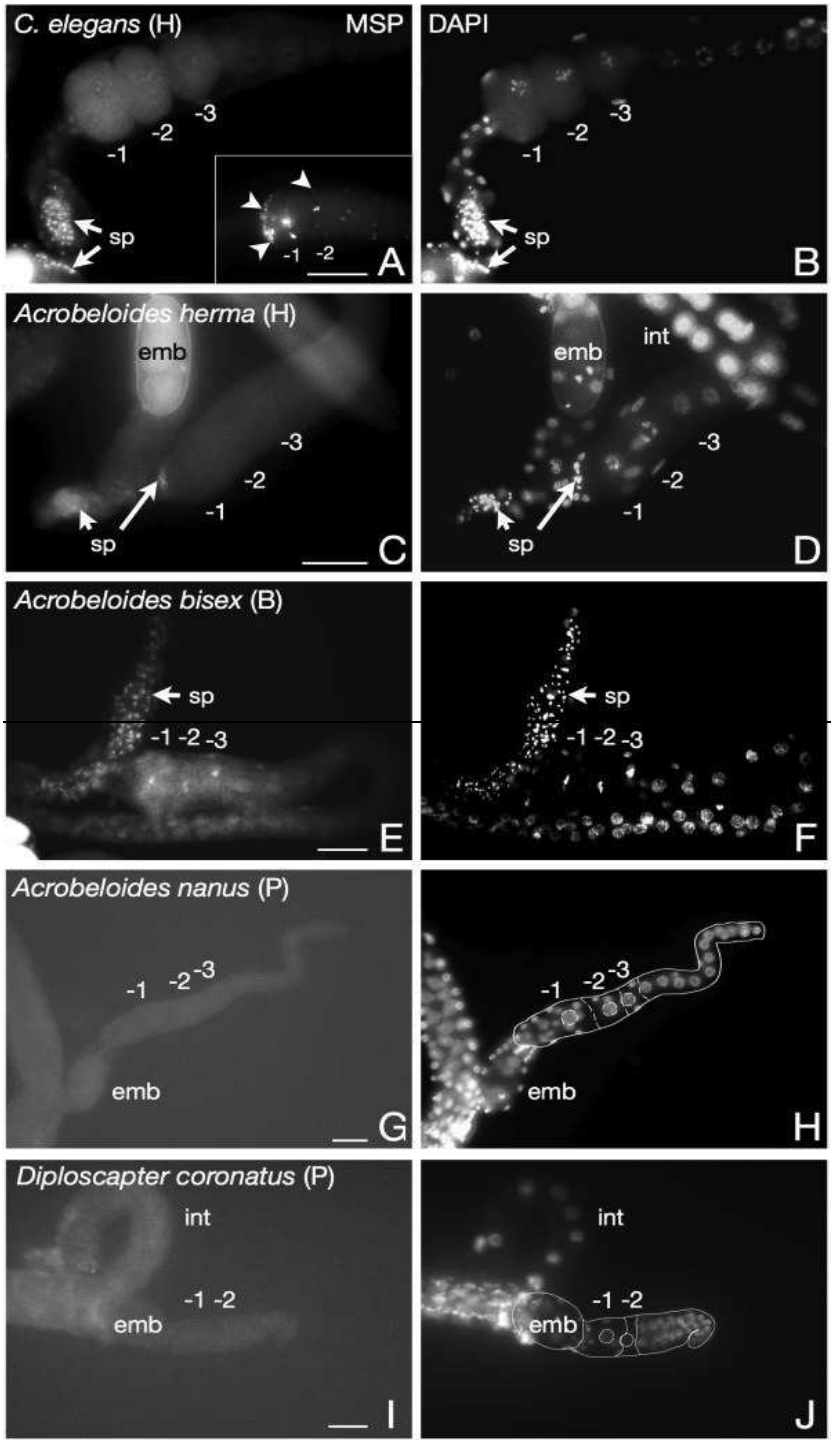

Figure 3-29: Immunofluorescence analysis of MSP in nematode gonads. Dissected gonad preparations of parthenogenetic (P), hermaphroditic (H) and bisexual (B) nematodes were doubly stained for MSP (left panel) and DNA (DAPI, right panel). While sperm associated MSP is revealed in the hermaphrodites *C. elegans* (panel A) and the distantly related species *Acrobeloides* (herma) and Acrobeloides (bisex) (panels C, E; arrows), a signal cannot be spotted in the parthenogenetic species *A. nanus* and *D. coronatus* (panels G, I). Arrowheads in panel A, inset, indicate puncta at the surface of the -1 oocyte resembling extracellular MSP as published previously (Kosinski et al., 2005). The inset of panel A and panels G-J are from the same experiment, panels A-F from another. The photographs of parthenogenetic animals were overexposed to demonstrate the lack of staining, and their gonadal shape is outlined for better orientation. sp: sperm. st: spermatheca. int: intestine. emb: embryo. -1, -2, -3: proximal oocytes, -1 is most proximal. All gonads are oriented with proximal to the left. Bar: 20 µm. (Taken from Heger et al., 2010).

To confirm the absence of MSP protein with an alternative method, we performed Western blot analysis of worm lysates using the C-terminal MSP antibody. In agreement with our immunostaining results, we could neither detect MSP signals in the two parthenogenetic species *A. nanus* and *D. coronatus* (Figure 3-30A) nor in two additional parthenogenetic species, *Acrobeloides maximus* and *Zeldia punctata* (Figure 3-30B). In contrast, a clear MSP signal at the size of the *C. elegans* control reveals the presence of MSP in the sperm-containing species *Acrobeloides sp.* (SB374) and *Acrobeloides sp.* (PS1146). This demonstrates cross-reactivity of the antibody to MSPs from other species as expected from the conservation of MSP C-termini in a wide range of nematodes.

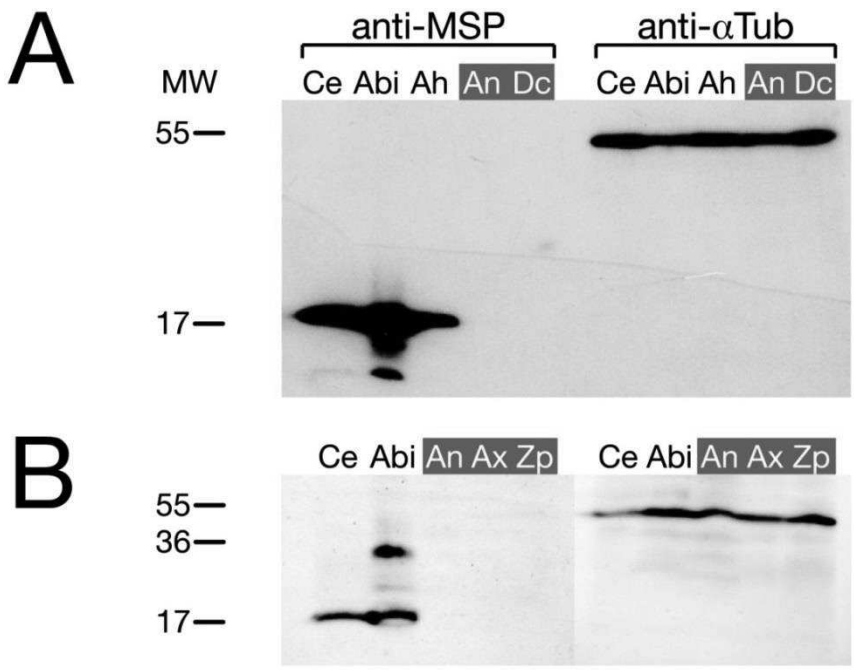

Figure 3-30: MSP analysis in whole nematode extracts. A): MSP is not detectable by Western blot in lysates of the parthenogenetic nematodes *A. nanus* and *D. coronatus*. Lysates of nematodes with various reproductive modes were, in roughly equal amounts, subjected to SDS-PAGE and Western blotting. One membrane of a duplicate set was incubated with monoclonal anti-MSP antibody, the other as a control with anti-α-tubulin antibody. While MSP is recognised in *C. elegans* and hermaphroditic or bisexual representatives of the distant *Acrobeloides* genus, none of the parthenogenetic species (violet) displays a signal. Ce: *C. elegans*; Abi: *Acrobeloides* (bisex); Ah: *Acrobeloides* (herma); An: *A. nanus*; Dc: *D. coronatus*. MW: molecular weight [kDa]. **B**): MSP is not detectable in additional parthenogenetic nematode species. As above, roughly equal amounts of nematode lysate were subjected to SDS-PAGE and Western blotting. While MSP is recognised in *C. elegans* and the sperm producing *Acrobeloides* (bisex), two further parthenogenetic species (violet) do not reveal a signal., Ce: *C. elegans*; Abi: *Acrobeloides* (bisex); An: *A. nanus*; Ax: *A. maximus*; Zp: *Z. punctata*. MW: molecular weight [kDa] (Taken from Heger et al., 2010).

Additional smaller bands in the *Acrobeloides sp.* (SB374) lane (Figure 3-30A) likely represent cleavage products of MSP which have also been reported for *C. elegans* (Kosinski et al., 2005). In some experiments, we observed an additional larger signal at 35 kDa. As MSP is known to form extremely stable dimers (Haaf et al., 1996), this signal likely indicates dimerised MSP (Figure 3-30B, *Acrobeloides sp.* (SB374) lane). In conclusion, our results show that MSP is not detectable and thus appears to be absent at the protein level in the parthenogenetic species we analysed.

3.9.3 Intact MSP genes are present in parthenogenetic nematodes

In the hermaphroditic nematode *C. elegans*, an MSP dependent pathway is utilised for MAP kinase activation and successive oocyte maturation with extracellular MSP released from sperm acting as activator (Miller et al., 2001, 2003). It was first described as a major component of *C. elegans* sperm representing 15 % of its total protein content (Klass and Hirsch, 1981). Parthenogenetic nematodes do not undergo spermatogenesis during which MSP is normally expressed. MSP seems to be absent at the protein level in the parthenogenetic species (Heger et al., 2010). We therefore expected that parthenogenetic nematodes do not require MSP, allowing the accumulation of mutations in MSP genes over time. A decay of genes specific to sex and recombination is predicted as an effect of the loss of sex on the eukaryotic genome (Normark et al., 2003). To investigate this hypothesis, we cloned MSP genes from the parthenogenetic nematode *A. nanus*, from its hermaphroditic sister species *Acrobeloides sp.* (PS1146) and from the parthenogenetic *D. coronatus*. We isolated and characterised several MSP genes from all three nematodes. Figure 3-31 shows an alignment of representative MSP coding sequences from the two parthenogenetic nematodes and closely related hermaphroditic species. It illustrates a strong conservation of the MSP coding sequence in parthenogenetic animals (> 90 % similarity to their hermaphroditic relatives). The MSP genes from parthenogenetic species were found to be intact and also strictly conserved in *D. coronatus* and *Acrobeloides sp.* (PS1146) (Figure 3-31), excluding the possibility that parthenogenetic species possess a modification within this epitope.

```
Ce_MSP-19 YDDKHTYHIKVINSSARRIGYGIKTTNMKRLGVDPPCGVLDPKEAVLLAVSCDA
Ce_MSP-45 YDDKHTYHIKVINSSARRIGYGIKTTNMKRLGVDPPCGVLDPKEAVLLAVSCDA
Dc_MSP-1  YDDKHTYHIKIINSSAPWIGWTIKATNMKRLGVDPLCGVLDPKESTLMAVSCDA
Dc_MSP-2  YDDKHTYHIKIINSSARRIGWAIKTTNMRRLGVDPPCGVLDPKESTLMAVSCDA

Ah_MSP-1  YDDKHTYHIKINNSSARRIGWAIKTTNATRLGVDPPCGVLDPKEAVLMAVSCDT
Ah_MSP-2  YDDKHTYHIKINNSSARRIGWAIKTTNATRLGVDPPCGVLDPKEAVLMAVSCDT
An_MSP-1  -DDKHTYHIKINNSSARLIGWAIKNTIAVRLGVDPPCGMLDPKEAVLMAVSCDA
An_MSP-2  YDDKHTYHIKINNSSTRRIVWAIKTNNAMRLGVDPPCGVLDPKETVLMAVSCNA

Ce_MSP-19 FAFGQEDTNNDRITVEWTNTPDGAAKQFRREWFQGDGMVRRKNLPIEYNP
Ce_MSP-45 FAFGQEDTNNDRITVEWTNTPDGAAKQFRREWFQGDGMVRRKNLPIEYNP
Dc_MSP-1  FAYGQEDTNNDRITVEWTNTPEGAAKQFRREWFQGDGMVRRKNLPIEYNP
Dc_MSP-2  FAYGQEDTNNDRITVEWTNAPEGAAKQFRREWFQGDGMVRRKNLPIEYNP

Ah_MSP-1  FDFAAEDTSNDRITVEWTNTPEGAAKQFRREWFQGDGMVRRKNLPIEYNP
Ah_MSP-2  FDFAAEDTSNDRITVEWTNTPEGAAKQFRREWFQGDGMVRRKNLPIEYNP
An_MSP-1  FDFASENFSKNCITGEWTNTLESAAKQFRCEWFQGDGMVRRKNLPIEYNP
An_MSP-2  FDFASEDTSNDHISIEWTNTPEGAAKQFRREWFQGDGMVRRKNLPIEYNP
```

Figure 3-31: Intact MSP genes in parthenogenetic nematodes. Sequence alignment of deduced MSP reading frames PCR-amplified from genomic DNA of parthenogenetic nematodes. Two closely related species pairs, *D. coronatus/C. elegans* and *A. nanus/Acrobeloides* (herma), with two representative sequences each are shown in separate alignment blocks. The C-terminal epitope recognised by the MSP antibody is bold, highlighted and underlined. Ce = *C. elegans*, An = *A. nanus*, Ah = *Acrobeloides sp.* (PS1146), Dc = *D. coronatus*.

Besides the intact MSP genes found in *D. coronatus* and *A. nanus*, we also looked for MSP coding regions in parthenogenetic species with a sequenced genome. Via BLAST searches, we identified among partial sequences and pseudogenes a set of complete MSP coding sequences in the genomes of the obligately parthenogenetic nematode *Meloidogyne incognita* and its facultatively parthenogenetic sister species *Meloidogyne hapla* (Triantaphyllou, 1981). We compared this MSP set to our above obtained sequences and to published MSP sequences from other, non-parthenogenetic nematodes. The deduced protein sequences of *M. incognita* and *M. hapla* are almost identical with each other (> 98 %; Figure 3-32). They have 73 % and 67 % identity to MSP sequences data from the parthenogenetic nematodes *A. nanus* and *D. coronatus* as well as with results from other species.

```
Ce_MSP-19    MAQSVPPGDIQTQPGTKIVFNAPYDDKHTYHIKVINSSARRIGYGIKTTNMKRLGVDPPCGVLDP
Mi_MSP-3     -MASVPPGDITTLPAVKVIFNAPFDDKHTYYMKIINSGGHRIGFAFKTTNPRRLNMDPPNGVLDP
Mi_MSP-1     -MASVPPGDITTLPAVKVIFNAPFDDKHTYYMKIINSGGHRIGFAFKTTNPRRLNMDPPNGVLDP
Mh_MSP-1     -MASVPPGDITTLPAVKVIFNAPFDDKHTYYMKIINSGGHRIGFAFKTTNPRRLNMDPPNGVLDP
Mh_MSP-3     -MATVPPGDITTLPAVKVIFNAPFDDKHTYYMKIINSGGHRVGFAFKTTNPRRLNMDPPNGVLDP

Ce_MSP-19    KEAVLLAVSCDAFAFGQEDTNNDRITVEWTNTPDGAAKQFRREWFQGDGMVRRKNLPIEYNP
Mi_MSP-3     KEAINIAISCDAFDPAAEATNNDRVTVEWTNTPEGAAKQFRREWFQGDGMVRRKNLPIEYNM
Mi_MSP-1     KEAINIAISCDAFDPAAEATNNDRVTVEWTNTPEGAAKQFRREWFQGDGMVRRKNLPIEYNM
Mh_MSP-1     KEAINIAISCDAFDPAAEATNNDRVTVEWTNTPEGAAKQFRREWFQGDGMVRRKNLPIEYNM
Mh_MSP-3     KEAINIAISCDAFDPAAEATNNDRVTVEWTNTPEGAAKQFRREWFQGDGMVRRKNLPIEYNM
```

Figure 3-32: Sequence alignment of two representative full length MSP coding regions identified in the genome sequences of the obligately parthenogenetic species *M. incognita* and the facultatively parthenogenetic species *M. hapla*. Ce_MSP-19 is included as a reference. With two exceptions (S4T, I42V), all deduced amino acid sequences in *M. incognita* and *M. hapla* are identical and highly similar to the *C. elegans* reference MSP-19. Amino acid numbering after Ce_MSP-19. Species: Ce = *C. elegans*, Mi = *M. incognita* and Mh = *M. hapla.*

In all *Meloidogyne* MSP loci analysed, we find purines (A) at the -3 position and the nucleotide G in position +4 (not shown). This indicates that the respective MSP start codons fulfil the requirements for a successful initiation of translation regardless of the reproductive mode. Thus, a remarkable conservation in genomic organisation and deduced protein sequence exists in MSPs from several parthenogenetic nematodes positioned in different clades.

4 Discussion

The aim of this thesis has been to investigate the variation in molecular and cellular events amongst closely related nematode species with different modes of reproduction. Previous studies have revealed an enormous diversity in early embryonic development of nematodes when compared to the model organism *C. elegans* (Schierenberg, 2001; Schulze and Schierenberg, 2008; Zhao et al., 2008; Yanai and Hunter, 2009; Levin et al., 2012). In this thesis, several new findings have been made regarding the differential expression and segregation of maternal gene products in nematodes.

Using the *C. elegans* P granules antibody, we observed cross-reactivity of this antibody, and considerable species-specific differences in the timing of perinuclear positioning of P granules in various nematode groups (see section 3.1).

Secondly, we found an astonishing amount of variation in the spatial and temporal expression and localisation of the maternal mRNAs *pie-1* and *skn-1* that are essential in early cell fate specification events in *C. elegans* (see section 3.8). Our analysis also revealed that the SKN-1 and PIE-1 protein interaction networks are not conserved among the studied nematodes. This indicates that there must be a significant plasticity in the molecular regulatory networks and signalling mechanisms active in nematodes. Such early variations seem enigmatic as they do not influence the resultant structure or performance of the emerging nematode larva (Schierenberg, 2001).

Our results thus support the proposal that the earliest periods of embryogenesis are the most divergent, in which early development evolves to accommodate changes in developmental time with significant ecological and evolutionary consequences (Kalinka and Tomancak, 2012).

4.1 Perinuclear localisation of P granules and regulation of early zygotic transcripts

A distinctive feature of germ cells is the possession of a specialized germ plasm, generically referred to as germ granules and specifically called polar granules in *Drosophila* and P granules in worms and nuages in other animal species (Strome,

1983; Wolf et al., 1983; Wylie, 1999). Post-transcriptional control in early primordial germ cells is a common theme to prevent them from differentiating in the same way as their somatic neighbours, although the regulators differ between species (Santos and Lehmann, 2004; Strome, and Lehmann, 2007; Hayashi et al., 2007). The perinuclear localisation of germ granules has been shown to be essential in post-transcriptional regulation across the animal kingdom.

Our data demonstrate that the *C. elegans* P granule antibody detects P granules from other nematode species, i.e. shows cross reactivity with antigens from other nematodes (see section 3.1). This implies that the antibody recognises conserved P granule components demonstrating the usefulness of this antibody to visualise germline granules in a variety of nematodes.

We found cross-species differences in the timing of perinuclear localisation of P granules within individual genera. For example, in *C. elegans* perinuclear localisation of P granules becomes prominent prior to the birth of the primordial germ cell, P4, whereas in its sister species, *C. briggsae* this occurs already in the P2 cell. In addition, our results show that representatives of the genus *Caenorhabditis* are the only species that show P granules randomly distributed in the cytoplasm in the early germline cells, P0 through P3 (see section 3.1.1). For all other species investigated, at least a few granules were already associated with the nuclear membrane even in the zygote, P0.

The association of P granules with the nuclear membrane in late germline cells of *C. elegans* and their segregation to each germline blastomere obviously serves two functions: Firstly, the segregation of P granules appear to sequester and enrich large amounts of maternal proteins and RNAs presumably preventing translation of mRNAs that are delivered to the nascent germ line (Pitt et al., 2000; Strome, 2005; Voronina, 2012). Secondly, the nucleus-associated P granules provide a perinuclear compartment where newly exported mRNAs are collected prior to their release to the cytoplasm. Thus, they regulate the trafficking of new transcripts as they exit the nucleus (Sheth et al., 2010; Voronina and Seydoux, 2010; Updike et al., 2010).

Our results demonstrate that in non-*C. elegans* nematodes, perinuclear positioning of P granules occurs earlier than in *C. elegans*. This points towards early transcription and an early necessity for post-transcriptional control in these species (Edgar et al., 1994; Garvin et al., 1998; Laugsch and Schierenberg, 2004). In fact,

experiments in *A. nanus* have demonstrated that early transcription is required from the onset of embryonic development because there appears to be very little maternal gene products in the beginning controlling early development (Wiegner and Schierenberg, 1998). The fact that early perinuclear positioning of tiny P granules is found in other species as well, suggests that early zygotic gene expression takes place in these species and is regulated by the germline granules that associate with the nuclear envelope.

The retarded perinuclear localisation of bigger P granules in *C. elegans* (Figure 3-1), is in accordance with the finding that in *C. elegans* early zygotic transcription is not required, due to a massive supply of maternal gene products that allow a rapid progression of early cleavages (Edgar et al., 1994; Wiegner and Schierenberg, 1998; Bowerman, 1998).

4.2 Differences in mRNA expression and protein sequence challenge a conserved role of SKN-1

In *C. elegans,* the maternal SKN-1 protein specifies the fate of a single cell, the EMS blastomere that gives rise to the gut (Bowerman et al., 1992). In *C. elegans* it fulfills additional functions during later development (Maduro, 2006; Choe et al., 2009). The *skn-1* mRNA is initially expressed in the germline up to the birth of the primordial germ cell, P4. Then it disappears but later a second expression domain is found in the gut primordium (Seydoux and Fire, 1994).

We found remarkable differences in *skn-1* mRNA expression during embryonic development in various nematodes when compared to *C. elegans*. In *Panagrolaimus sp.* (PS1159), *skn-1* mRNA is exclusively maintained in the germline throughout embryogenesis, whereas in *Acrobeloides* species, it is exclusively expressed in somatic cells and absent in the germline (see section 3.8).

This means that the translational control mechanism involved in *skn-1* mRNA and possibly in addition the role of the *skn-1* gene within gene networks regulating several programs might be different in these nematode species.

In the *Acrobeloides* species, a translational block seems to be present in the somatic cells. In addition, in *A. nanus*, it appears that the way how gut is generated differs considerably from *C. elegans* (Wiegner and Schierenberg, 1998). All blastomeres

(AB, EMS and P2) of the 3-cell stage in *A. nanus* carry the potential to generate gut cells without induction from P2, whereas in *C. elegans,* none of the early blastomeres is by itself able to establish a gut lineage (Wiegner and Schierenberg, 1999). Besides, in basal nematodes, endoderm is formed from the anterior blastomere of the 2-cell stage (Voronov et al., 1998; Schulze and Schierenberg, 2009), in contrast to derived taxa including *C. elegans*, where endoderm is formed from the posterior blastomere. This indicates that the specification of gut has been modified dramatically amongst the nematodes.

A straightforward explanation for the exclusive germline expression of the *skn-1* mRNA in *Panagrolaimus sp.* (PS1159) is the presence of a translational block in germ cells such that *skn-1* mRNA is not translated into protein in the germline. This would be unlike *C. elegans* where a transcriptional block in the germline inhibits its somatic differentiation (Seydoux et al., 1996; Batchelder et al., 1999). Therefore, it would be interesting to check other germline specific mRNAs in order to verify whether a general translational block is present in *Panagrolaimus sp.* (PS1159).

Despite these differences in *skn-1* mRNA expression, it remains to be determined whether this is also true at the level of the SKN-1 protein. Therefore, it could be worthwhile to test the rather speculative assumption that maternally provided SKN-1 protein is shunted into the EMS cell in *Panagrolaimus* and *Acrobeloides*, as found in *C. elegans* (Bowerman et al., 2003).

Until recently, the *Propanagrolaimus sp.* (JU765) has been considered to be a Panagrolaimus species. However, recent molecular phylogeny has defined a new genus *Propanagrolaimus*. Interestingy, the pattern of *skn-1* mRNA expression in *Propanagrolaimus sp.* (JU765) differs from *Panagrolaimus* and is more similar to the *Acrobloides* (see Figure 3-23). This gives additional support for a separate phylogenetic positioning of the *Propanagrolaimus* representative.

To decide which of the two alternative *skn-1* patterns is apomorphic and which one is plesiomorphic, additional species from outside of clades 10 and 11 should be studied.

An additional *skn-1* expression domain is found in the gut primordium during late embryonic development

The accumulation of *skn-1* mRNA in primordial pharyngeal and gut cells observed in *Acrobeloides* and the *Propanagrolaimus sp.* (JU765) species (see sections 3.8) is reminiscent of the previously reported *skn-1* mRNA staining in *C. elegans* pharyngeal and gut cells during late embryonic stages (Seydoux and Fire, 1994). In the later, the corresponding protein was found in the nuclei of these two tissues in response to oxidative stress (An and Blackwell, 2003). Therefore, the staining in pharnygeal and gut primordia seen in *Acrobeloides* and *Propanagrolaimus* may indicate a similar physiological role for this gene in these species (Bowerman et al., 1992; Blackwell, 1994, Maduro, 2006).

In contrast to the species described above, no expression of *skn-1* mRNA was detected in the gut primordium of the parthenogenetic *Panagrolaimus sp.* (PS1159) suggesting the absence of the corresponding protein. This may be tolerable due to the different ecological niche where oxidative stress does not pose a serious threat. Alternatively, SKN-1 function could be replaced by another gene while the remainder of the gene cascade has remained intact.

4.3 Variations in ZF1 and ZF2 motifs indicate differences in regulation of PIE-1 in nematodes

The main role of *PIE-1* in *C. elegans* is to protect germline fate by preventing the expression of somatic differentiation genes (Mello et al., 1992). PIE-1 is regulated at the protein level by two complementary mechanisms involving both of its zinc finger motifs (ZF1 and ZF2). In *C. elegans,* ZF1 targets PIE-1 for degradation in somatic blastomeres while the ZF2 motif is sufficient to direct PIE-1 binding to specific target RNAs on the P granules *(*Mello et al., 1996; Seydoux and Dunn, 1997; Reese et al., 2000; Tenenhaus and Seydoux, 2001). Sequence comparison between *Panagrolaimus sp.* (PS1159) and *A. nanus* shows that both species possess the ZF1 and ZF2 motifs (Table 15). In both species and also in *C. elegans*, there is a much higher similarity between the ZF2 motifs than between the ZF1 motifs.

With respect to the role of ZF2, and the asymmetric localisation of P granules to the germline in *Acrobeloides* and *Panagrolaimus* species (see sections 3.1.2 and 3.1.3),

we suggest that ZF2 may fulfill similar roles in the binding of PIE-1 to P granules in these species as found in *C. elegans*. Indeed, it has been shown that in the mammalian homolog of the PIE-1 protein, TTP (tristetraprolin), ZF2 can also associate with P granules when expressed in *C. elegans* embryos (Lai et al., 1999; Carballo et al., 1998).

On the other hand, the ZF1 motif is quite conserved between *C. elegans* and Panagrolaimus *sp.* (PS1159) but not in *A. nanus*. This may imply that in *A. nanus,* in contrast to the other two species, ZF1 is not be sufficient to target PIE-1 for degradation in somatic cells (Reese et al., 2000; Tenenhaus et al., 2001). This could explain the presence of *pie-1* mRNA in somatic blastomeres in *A. nanus* and the absence in the other species (see Figure 3-25).

Our data suggest that the ZF1-dependent degradation machinery specific to somatic blastomeres as found in *C. elegans* seems not be a commonly used strategy to exclude certain proteins from somatic lineages in all nematode species. Our results are compatible with the view that the role of ZF1 in somatic degradation of certain proteins might be a derived feature, found in clades 9 and 10. Studies of representatives from lower phylogenetic taxa may reveal whether the role of ZF1 in somatic degradation of certain proteins is in fact restricted to clades 9 and 10.

Indications for evolutionary modifications of SKN-1 structure and function

Although identification of an interspecific ortholog does not guarantee that the gene performs the same function, one straightforward question to ask when comparing underlying developmental mechanisms is whether the same components even exist in a related species. In addition to its embryonic function, in *C. elegans* the *skn-1* gene also functions in late embryonic development to maintain the differentiated state of intestinal cells (An and Blackwell, 2003). But in some other nematodes such as *Panagrolaimus sp.* (PS1159) the SKN-1 protein appears not to be active post-embryonically in alimentary tract cells (see above). It remains to be determined whether other gene products functionally redundant to SKN-1 take over its function.

In *C. elegans*, one example for such a redundant gene appears to be *srg-1* which also contains the DIDLID element. It has been previously suggested that *srg-1* can replace *skn-1* in alimentary tract cells during embryonic development (Bowerman et al., 1992; Farmer et al., 1997; Walker et al., 2000). Although we did not find a SRG-1

homolog outside of the *Caenorhabditis* genus, it may be worthwhile to look for the DIDLID binding element in other genes in search for other candidate replacement genes. Such partial functional redundancy has also been observed in several closely related proteins in *C. elegans*, such as APX-1 which can substitute for its homolog LAG-2 to direct cell interactions throughout *C. elegans* development (Lambie and Kimble, 1991; Gao and Kimble, 1995).

In contrast to our findings in Panagrolaimids and Cephalobids, in *A. suum* (clade 8), the SKN-1 homolog consists of only 130 amino acid residues (compared to 623 in *C. elegans*) and lacks the highly conserved 14-amino-acid transactivator element (DIDLID) that is important for SKN-1 driven transcription in *C. elegans* (Blackwell et al., 1994; Walker et al., 2000). The dramatic differences in SKN-1 activity could either be due to differences between parasitic and free-living lifestyles or depend on phylogenetic position. The latter appears more likely as in other nematodes of lower clades no SKN-1 homolog has been detected (see Table 12).

4.4 Evolutionary modification of PIE-1 function and somatic degradation

By analysis of whole genome sequence databases, we found prominent differences in the *pie-1* gene network components across the nematode phylum. Most strikingly, we acknowledged the absence of a *pie-1* homolog in most members of the basal clades 1 to 8 (see Table 13). Fascinatingly, in species lacking a *pie-1* homolog, in addition many maternally transcribed genes required for the early specification of blastomeres in *C. elegans* appear to be absent as well.. For example, we could neither find the zinc finger containing proteins PIE-1, POS-1 and MEX-1 (Mello et al., 1992; Guedes and Priess, 1997; Ogura et al., 2003; Tabara et al., 1999) nor a homolog of the ZIF-1 protein which binds to these zinc finger containing proteins and targets them for degradation in somatic lineages (DeRenzo et al., 2003; Strome 2005; Wang and Seydoux 2012). Furthermore, the PIE-1 regulators MEX-5, MEX-6, NOS-2 and PES-10 (Draper et al., 1996; Schubert et al., 2000) are found only in the *Caenorhabditis* genus.

The absence of a ZIF-1 homolog as well as it substrates MEX-5 and MEX-6 in in *Panagrolaimus sp.* (PS1159) implies that the degradation of PIE-1 in somatic cells must be initiated by a different, so far unknown mechanism.

The situation appears to be different in *Acrobeloides* species where the *pie-1* mRNA remains present in somatic cells (see Figure 3-25). Assuming that also in these species protein degradation in somatic blastomeres is essential for proper cell specification; one must postulate a mechanism to execute such a program even without a *C. elegans*-like degradation machinery. As stated above with respect to *skn-1* mRNA, a translational block may prevent the accumulation of the PIE-1 protein in the somatic cells. The observation that in *A. nanus* early blastomeres show a high regulative capacity supports the view that there the mechanism of cell specification must be different to the one found in *C. elegans* (Wiegner and Schierenberg, 1999).

4.5 Modification of gene regulatory networks

Our genomic analysis of various non-*Caenorhabditis* species revealed the absence of many genes indispensable for earliest periods of development in *C. elegans* (see section 3.7). It has been suggested that the absence of many *C. elegans* gene homologs in other nematode species may indicate that a large fraction of maternal genes are expressed non-functionally, providing only supplemental nutritional content to the developing embryo (Shen-Orr et al., 2010).

In addition to the differences in *skn-1* and *pie-1* gene networks (see above), genome comparison of *C. elegans* with other nematodes revealed the absence of further genes like *pgl-1, pgl-2* and *pgl-3,* and *med-1* and *med-2* outside of the *Caenorhabditis* genus (Maduro, 2006; Broitman-Maduro et al., 2006; Coroian et al., 2005; Kawasaki et al., 2004; Sheth et al., 2010).

This implies that gene regulatory networks must be considerably divergent amongst the studied nematodes i.e. there is significant plasticity in the gene networks active in the early embryo (Tautz and Schmid 1998; Storm and Angilletta, 2007). This indicates that there are many potential avenues leading to a healthy juvenile. A comprehensive comparison of 41 nematode species across 12 different clades found extensive divergence in several early developmental events, including cleavage and the specification of cell lineages, with no obvious effect on the phenotype of the hatched worm (Schulze and Schierenberg, 2011).

Changes in expression, temporal coordination, or modifications of components in early gene regulatory networks are common, and developmental mechanisms can change while conserving parts of the molecular pathways involved (Kalinka and Tomancak, 2012). Our findings corroborate previous studies that show that genetic control mechanisms may change while the general developmental function and the phenotypic outcome is preserved. This phenomenon has been termed 'developmental system drift' (True and Haag, 2001).

The question remains why during evolution, developmental modifications emerged and persisted essentially leading to the same goal. Variations during the early periods of development may be adaptive for instance by shortening developmental time and thus constitute improved fitness under specific ecological conditions (Schierenberg, 2001; Kalinka and Tomancak, 2012).

4.6 MAP kinase activity and MSP genes in parthenogenetic nematodes

In a collaborative side project, we investigated two key elements of oocyte-to-embryo transition, MSP (major sperm protein) expression and MAP (mitogen-activated protein) kinase signalling, in parthenogenetic and non-parthenogenetic nematodes (Heger et al., 2010). MAP kinase activation is an essential step during oocyte-to-embryo transition of animals (Abrieu et al., 2001). In the model organism *C. elegans*, the trigger for oocyte maturation and MAP kinase activation is MSP, secreted from sperm (Miller et al., 2001).

We found that while activated MAP kinase is present in all analysed nematodes irrespective of the reproductive mode (see section 3.9.1), MSP expression is absent in parthenogenetic species. However, genomic sequence analysis indicates that functional MSP genes are present in the studied parthenogenetic nematodes (see 3.9.3).

Our findings show that the genes involved in regulating oocyte-to embryo transition in parthenogenetic nematodes are conserved with respect to *C. elegans*. While the MAP kinase is functional in parthenogenetic nematodes, the question remains whether the intact MSP gene is transcribed in these species. We envision 3 possible

alternatives with respect to the unexpected discovery of intact MSP genes in parthenogenetic nematodes that lack sperm.

Firstly, the MSP protein might have lost its function as a trigger of MAP kinase activation and is not expressed in parthenogenetic nematodes. Activation of the MAP kinase pathway is achieved by another, unknown mechanism. Studies have suggested that there is an apparent strategy of mixing parthenogenesis with sexual reproduction instead of pursuing parthenogenesis alone. This can be evolutionarily beneficial (Hansen et al., 1973; Triantaphyllous and Fisher, 1976; Eisenback and Hirschmann, 1980).

Secondly, the unexpected discovery of intact MSP genes suggests either their strong maintenance by natural selection or a very recent origin of parthenogenesis based on the absence of an increased substitution rate or changed substitution pattern (Lunt, 2008). MSP genes might have remained intact during this short interval although they are useless.

Finally, we suggest that MSP expression has been shifted to non-sperm cells which could be achieved by mutations in regulatory sites. As *C. elegans* MSP is exported from sperm by a non-classical vesicle budding mechanism (Kosinski et al., 2005), one would further expect a similar mechanism in oocytes or sheath cells of parthenogenetic nematodes, but this is not known at the present time.

We cannot exclude the presence of MSP at levels too low for detection via Western blotting and immunofluorescence, where a low expression level could be sufficient for acting like a hormone to trigger MAP kinase activation and embryogenesis in parthenogenetic species. Unlike the first two scenarios, the last hypothesis provides a number of reasonable predictions and may serve as a starting point for further analysis.

5 Outlook

In conclusion, my studies reveal unexpected high differences in early embryonic gene expression and gene networks amongst nematodes that give further support to earlier findings, that development in this phylum is highly divergent. Taking into account the ancient origin of nematodes and the huge number of different species (see Introduction), it appears not surprising that during the long period of evolution, a large variety of developmental mechanisms have been established. What is really astonishing is the strong conservation of the body plan despite the divergent molecular underpinnings. The most straight forward explanation for this phenomenon is the construction principle making use of a single-chambered hydroskeleton which does not allow significant variations in the general phenotype.

Based on my findings, promising directions to go in the future could be the extension of comparative studies to a larger number of species from basal taxa. From clade 2, only two species have been sequenced so far, *Trichinella spiralis* and *Romanomermis culicivorax* and there are sparse data on other members of clades 1 and 2. Species of clades 3-7 are highly neglected partly due to the difficulty involved in culturing and studying them in the laboratory (Schiffer et al., 2013). Nevertheless, to try to bridge the gap between basal and more derived species, a sufficient number of individuals from lower taxa could be collected from the wild. With the aid of new sequencing technologies, DNA could be amplified and sequenced for a large-scale comparative transcriptomic analysis in nematodes. This would facilitate the identification of relevant genes to better understand genomic diversity and the intrinsic prerequisites involved in the implementation of embryonic novelty in the nematode phylum.

Furthermore, functional molecular analysis of species in most non-*Caenorhaditis* species is impeded by the lack of genetic tools such as mutant analysis or gene-knockdown via RNAi. But in absence of these powerful tools, it could be at least explored to what extent the specific spatial expression of maternal mRNAs (visualized via *in situ* hybridization) correlates with the location of the respective proteins (visualized via specific antibodies). Such an approach has been initiated in our laboratory.

6 Abstract

In this thesis, I studied aspects of early soma/germline separation, gene expression patterns, gene networks and oocyte-to-embryo transition in several nematodes with different modes of reproduction. Proper localisation of gene products is essential for accurate embryonic development. In the hermaphroditic *C. elegans*, the fertilizing sperm is the initial trigger for the generation of a molecular asymmetry which is reflected by the segregation of germline-specific P granules and differential expression of maternally inherited gene products.

In *C. elegans*, P granules are initially dispersed in the cytoplasm and only later accumulate around the nucleus prior to the birth of the primordial germ cell. In other related nemtodes, we found that P granules occupy an early perinuclear position irrespective of phylogeny and the mode of reproduction. We hypothesize that early perinuclear localisation of P granules may play a role in the regulation of early zygotic transcripts.

In *C. elegans*, the PIE-1 protein functions in the germline to maintain its pluripotency whereas the SKN-1 protein specifies EMS fate. The MEX-1 protein prevents the accumulation of PIE-1 and SKN-1 in the AB lineage. A great disparity in gene networks was found to exist in nematodes. Notably, no obvious PIE-1 and SKN-1 homolog were found in several basal clades. A significant number of vital *C. elegans* genes are absent in many nematode taxa, and restricted to the genus *Caenorhabditis*. This indicates that there is significant plasticity in the gene networks active in the early embryo and that there are many potential avenues leading to a healthy juvenile, independent of the reproductive strategy.

Striking differences in spatial and temporal expression of the *skn-1* and *pie-1* genes regardless of the mode of reproduction have been revealed in this work. We found exclusive localisation in somatic cells of *skn-1* and *pie-1* mRNAs in *Acrobeloides nanus* and other *Acrobeloides* species, in contrast to predominant germline expression in *Panagrolaimus* species. The localisation of *pie-1* and *mex-1* mRNAs is similar in both *Panagrolaimus sp.* (PS1159) and *C. elegans*. However, in the former, *skn-1* mRNA expression differs remarkably from the latter. A straightforward explanation for the exclusive germline expression of the *skn-1* mRNA in

Panagrolaimus sp. (PS1159) is the presence of a translational block in germ cells, and in the *Acrobeloides* species, a translational block in the somatic cells.

Mitogen-activated protein (MAP) kinase activation is essential in regulating oocyte-to-embryo transition in many organisms. Major sperm protein (MSP) genes trigger MAP kinase activation in the hermaphroditic *C. elegans*. While activated MAP kinase is present in all analysed nematodes regardless of the reproductive mode, MSP expression differs. In contrast to hermaphroditic or bisexual species, we do not find MSP expression at the protein level in parthenogenetic nematodes. However, genomic sequence analysis indicates that functional MSP genes are present in several parthenogenetic species. Thus, we suggest that MSP expression has been shifted to non-sperm cells at levels too low for detection via Western blotting and immunofluorescence. Thus, a low expression level could be sufficient for acting like a hormone to trigger MAP kinase activation and embryogenesis in parthenogenetic species.

In summary, our findings reveal unexpected high differences in early embryonic gene activity amongst nematodes that apparently does not translate into morphological differences, since the hatched larvae of different species look very similar. Nevertheless, differences in embryonic gene expression and cellular behavior might be important to allow the variability needed for adaptation to an ever-changing environment, which is reflected by the enormous number of nematode species occupying essentially all ecological niches.

7 Zusammenfassung

In dieser Arbeit, habe ich Aspekte von früher Soma/Keimbahn Trennung, von Gen-Expressionsmustern, von Gen-Netzwerken und des Oozyten-zu-Embryo Übergangs in Nematoden mit verschiedenem Reproduktionsmodus untersucht. Die spezifische Lokalisierung von Genprodukten ist wesentlich für die korrekte Embryonalentwicklung. Im hermaphroditischen *C. elegans* ist das Spermium die Initialzündung zur Erzeugung einer molekularen Asymmetrie, die durch die asymmetrische Verteilung von Keimbahn-spezifischen P-Granula und die differenzielle Expression von maternalen Genprodukten widergespiegelt wird. Während die P Granula in *C. elegans* anfänglich frei im Cytoplasma verteilt sind und sich erst später, bevor die Urkeimzelle entsteht, um den Nukleus sammeln, fanden wir, dass sie sich in mehreren anderen Nematoden früh perinukleär positionieren. Dieses Muster scheint nicht mit der phylogenetischen Stellung oder dem Reproduktionsmodus zu korrelieren. Wir nehmen an, dass die frühe perinukleäre Positionierung der P Granula eine Rolle für die Regulation früher zygotischer Transkripte spielt.

In *C. elegans* hat das PIE-1 Protein innerhalb der Keimbahn die Aufgabe Pluripotenz zu erhalten, während das SKN-1 Protein das Schicksal der Endomesoderm Vorläuferzelle EMS spezifiziert. Das MEX-1 Protein verhindert die Akkumulation von PIE-1 und SKN-1 in der AB Zelllinie.

Wir haben eine große Divergenz in den genregulatorischen Netzwerken innerhalb der Nematoden festgestellt. Bemerkenswerterweise konnten keine offensichtlichen PIE-1 und SKN-1 Homologe in mehreren Kladen gefunden werden. Eine signifikante Anzahl essentieller *C. elegans* Gene scheint auf die Gattung *Caenorhabditis* begrenzt und somit in vielen Gruppen nicht vorhanden zu sein. Dies deutet darauf hin, dass es eine erhebliche Plastizität in den genregulatorischen Netzwerken innerhalb früher Embryonen verschiedener Arten und damit, unabhängig von der Reproduktionsstrategie, viele potentielle Wege zur Bildung einer gesunden Larve gibt.

Ein Vergleich von *Acrobeloides nanus* und anderen *Acrobeloides* Arten mit *Panagrolaimus* Arten zeigte eine spezifische Lokalisation der *skn-1* und *pie-1*

mRNAs in somatischen Zellen in ersteren, und im Gegensatz dazu eine Expression hauptsächlich in der Keimbahn in letzteren. Die Lokalisation von *pie-1* und *mex-1* mRNAs ist in *Panagrolaimus* sp. (PS1159) und *C. elegans* vergleichbar. Allerdings unterscheidet sich die *skn-1* mRNA Expression drastisch zwischen beiden Nematoden. Eine mögliche Erklärung für die spezifische Keimbahnexpression der *skn-1* mRNA in *Panagrolaimus* sp. (PS1159) ist ein Translationsblock innerhalb der Keimzellen. Bei den *Acrobeloides* Arten könnte dagegen ein solcher Translationsblock innerhalb der somatischen Zellen vorhanden sein.

Eine Aktivierung durch das Mitogen-aktivierte Protein (MAP) Kinase ist unabdingbar für die Regulation des Oozyten-zu-Embryo-Übergangs in vielen Organismen. Major Sperm Protein (MSP)-Gene initiieren hierbei die MAP Kinase Aktivierung im hermaphroditischen *C. elegans*. Während die aktivierte MAP Kinase in allen analysierten Nematoden unabhängig vom Reproduktionsmodus exprimiert wird, unterscheidet sich die MSP Expression dramatisch. Im Gegensatz zu hermaphroditischen oder bisexuellen Arten, finden wir keine MSP Proteine in parthenogenetischen Nematoden. Genomsequenzanalysen zeigen jedoch, dass funktionelle MSP Gene in mehreren parthenogenetischen Arten vorhanden sind. Wir schlagen deshalb vor, dass die MSP Expression in Nicht-Spermazellen transferiert wurde und unterhalb der Nachweisgrenze von Western Blots und Immunofluoreszenz liegt. Eine geringe MSP Expression mit der Wirkung als Hormon könnte ausreichen, um die MAP Kinase Aktivierung und somit die Embryogenese in parthenogenetischen Spezies zu ermöglichen.

Zusammenfassend zeigen unsere Ergebnisse unerwartet große Unterschiede in der frühen embryonalen Genaktivität innerhalb der Nematoden, die scheinbar nicht in morphologische Unterschiede übersetzt werden, da die ausschlüpfenden Larven verschiedener Arten sehr ähnlich sind. Die gefundenen Unterschiede in embryonaler Genexpression und zellulärem Verhalten könnten wichtig sein, um eine Variabilität zu erlauben, die für die Adaption an sich fortwährend ändernde Umwelteinflüsse wichtig ist. Diese Anpassungsfähigkeit wird durch die enorme Anzahl an Nematoden Arten, die sämtliche ökologische Nischen besetzen, widergespiegelt.

8 References

Abrieu, A., Doree, M., Fisher, D. (2001). The interplay between cyclin-B-Cdc2 kinase (MPF) and MAP kinase during maturation of oocytes**.** *J. Cell Sci.*, **114**, 257-67.

Aguinaldo, A.M., Turbeville, J.M., Linford, L.S., Rivera, M.C., Garey, J.R., Raff, R.A. and Lake, J.A. (1997). Evidence for a clade of nematodes, arthropods and other moulting animals. *Nature* **387**, 489-493.

Altschul, S.F., Gish, W., Miller, W., Myers, E.W. and Lipman, D.J. (1990). Basic local alignment search tool. *J. Mol. Biol.* **215**, 403-410.

An, J.H., and Blackwell, T.K. (2003). SKN-1 links *C. elegans* mesendodermal specification to a conserved oxidative stress response. *Genes Dev.* **17**, 1882-93.

Ayala, F.J. and Rzhetsky, A. (1998). Origin of the metazoan phyla: molecular clocks confirm paleontological estimates. *Proc. Natl. Acad. Sci. USA* **95**, 606-61.

Baldwin, J.G. and Hirschmann, H. (1976). Comparative fine structure of the stomatal region of males of *Meloidogyne incognita* and *Heterodera glycines*. *J. Nematol.*, **8**, 1-17.

Bashirullah, A., Halsell, S., Cooperstock, R., Kloc, M., Karaiskakis, A., Fisher, W., Fu W., Hamilton, J., Etkin, L., Lipshitz, H. (1999). Joint action of two RNA degradation pathways controls the timing of maternal transcript elimination at the midblastula transition in *Drosophila melanogaster. EMBO J.* **18**, 2610–2620.

Batchelder, C., Dunn, M. A., Choy, B., Cassie, C., Shim, E. Y., et al., (1999). Transcriptional repression by the *Caenorhabditis elegans* germ-line protein PIE-1. *Genes Dev.* **13**, 202–212.

Bird, D.M. and Riddle, D.L. (1989). Molecular cloning and sequencing of *ama-1*, the gene encoding the largest subunit of *Caenorhabditis elegans* RNA polymerase II. *Mol. Cell. Biol.* **9**, 4119–4130.

Blackshear, P.J., Phillips, R.S. and Lai, W.S. (2005): Tandem CCCH zinc finger proteins in mRNA binding. In Zinc Finger Proteins: from Atomic Contact to Cellular Function. Edited by Iuchi S, Kuldell N. Kluwer Academic/Plenum Publisher, London; 80-90.

Blackwell, T.K., Bowerman, B., Priess, J., Weintraub, H. (1994). Formation of a monomeric DNA binding domain by *skn-1* bZIP and homeodomain elements. *Science* **266**, 621-628.

Blaxter, M.L., De Ley, P., Garey, J.R., Liu, L.X., Scheldeman, P., Vierstraete a, Vanfleteren, J.R., Mackey, L.Y., Dorris, M., Frisse, L.M., et al., (1998). A molecular evolutionary framework for the phylum Nematoda. *Nature* **392**, 71–75.

Blaxter, M. and Liu, L. (1996). Nematode spliced leaders - ubiquity, evolution and utility. *Int. J. for parasitology* **26**, 1025–1033.

Bowerman, B. (1998). Maternal control of pattern formation in early *Caenorhabditis elegans* embryos. *Curr. Top. Dev. Biol.* **39**, 73–117.

Bowerman, B.A. Eaton, J.R. (1992). Priess *skn-1*, a maternally expressed gene required to specify the fate of ventral blastomeres in the early *C. elegans* embryo *Cell* **68**, 1061–1075.

Bowerman, B., Draper, B.W., Mello, C.C., Priess, J.R. (1993). The maternal gene *skn-1* encodes a protein that is distributed unequally in early *C. elegans* embryos. *Cell* **74**, 443–452.

Brauchle, M., Kiontke, K., MacMenamin, P., Fitch, D., Piano, F. (2009). Evolution of early embryogenesis in rhabditid nematodes. *Dev. Biol*. **335**, 253-262.

Brenner, S. (1974). The genetics of *Caenorhabditis elegans. Genetics* **77**, 71-94

Broitman-Maduro, G., Lin, K.T-H., Hung, W., Maduro, M. (2006). Specification of the *C. elegans* MS blastomere by the T-box factor TBX-35. *Development* **133**, 3097-3106.

Carballo, E., Lai W.S., Blackshear, P.J. (2000). Evidence that tristetraprolin is a physiological regulator of granulocyte-macrophage colony stimulating factor messenger RNA deadenylation and stability. *Blood* **95,** 1891–1899.

Chalfie, M., Tu Y., Euskirchen G., Ward W.W., Prasher D.C. (1994). Fluorescent protein as a marker for gene expression. *Science* **263**, 802-805.

Chitwood, B.G. and M.B. Chitwood. (1950). An introduction to nematology. Baltimore Monumental Publishing Co. *Sec. 1, Anatomy. Rev. ed*. *213*.

Cho, J.-C. Park, K.-J. Ihm, H.-S. Park, J.-E. Kim, S.-Y. Kang, I. Lee, K.-H. Jahng, D. Lee, D.-H. Kim S.-J. (2004). A novel continuous toxicity test system using a luminously modified freshwater bacterium. *Biosens Bioelectron,* **20**, 338–344.

Choe, K.P., Leung, C.K., Miyamoto, M.M. (2012). Unique structure and regulation of the nematode detoxification gene regulator, SKN-1: implications to understanding and controlling drug resistance. *Drug Metab. Rev.* **44**, 209-223.

Cobb, N.A. (1914). Nematodes and their relationships. *U.D.o.A. Yearbook*, ed.

Coroian, C., Broitman-Maduro, G., Maduro, M.F. (2005). Med-type GATA factors and the evolution of mesendoderm specification in nematodes. *Dev. Biol.* **289**, 444–455.

Cottee, P.A., Nisbet, A.J., Boag, P.R., Larsen, M., Gasser, R.B. (2004). Characterization of major sperm protein genes and their expression in Oesophagostomum dentatum (Nematoda: Strongylida)**.** *Parasitology* **129**, 479-490.

Cowan, C.R. and Hyman, A.A. (2004). Centrosomes direct cell polarity independently of microtubule assembly in *C. elegans* embryos. *Nature* **431**, 92-96.

Cuenca, A.A., Schetter, A., Aceto, D., Kemphues, K., Seydoux, G. (2003). Polarization of the *C. elegans* zygote proceeds via distinct establishment and maintenance phases. *Development* **130**, 1255-1265.

De Ley, P., and Blaxter, M.L. (2002). Systematic Position and Phylogeny. *In The Biology of Nematodes.* Edited by Lee DL. London: *Taylor and Francis*, 1-30.

DeRenzo, C., Reese, K.J., Seydoux, G. (2003). Exclusion of germ plasm proteins from somatic lineages by cullin-dependent degradation. *Nature* **424**, 685-689.

Dolinski, C., Baldwin, J.G., Thomas, W.K. (2001). Comparative survey of early embryogenesis of Secernentea (Nematoda) with phylogenetic implications. *Can. J. Zool.* ***79***, 82–94.

Douzery, E.J., Snell, E.A., Bapteste, E., Delsuc, F. and Philippe, H. (2004). The timing of eukaryotic evolution: does a relaxed molecular clock reconcile proteins and fossils? *Proceedings of the National Academy of Sciences of the USA* **101**, 15386–15391.

Draper, B.W., Mello, C.C., Bowerman, B., Hardin, J., Priess, J.R. (1996). MEX-3 is a KH domain protein that regulates blastomere identity in early *C. elegans* embryos*. Cell* **87**, 205–216.

Eddy, E.M. (1975). Germ plasm and the differentiation of the germ cell line. *Int. Rev. Cytol.* **43**: 229–280.

Edgar, L.G., Goldstein, B. (2012). Culture and manipulation of embryonic cells. *Methods Cell Biol.* **107**, 151–175.

Edgar, L.G., Wolf, N., Wood, W.B. (1994). Early transcription in *Caenorhabditis elegans* embryos. *Development* **120**, 443–451.

Eisenback, J.D. and Hirschmann, H. (1980). Morphological comparison of *meloidogyne* males by scanning electron microscopy**.** *J. Nematol*. **12**, 23-32.

Encalada, S.E., Martin, P.R., Phillips, J.B., Lyczak, R., Hamill, D.R., Swan, K.A., Bowerman, B. (2000). DNA replication defects delay cell division and disrupt cell polarity in early *Caenorhabditis elegans* embryos. *Dev. Biol.* **228**, 225–238.

Farmer, S.C., Sun, C.W., Winnier, G.E., Hogan, B.L., Townes, T.M. (1997). The bZIP transcription factor LCR-F1 is essential for mesoderm formation in mouse *Development Genes and Dev.* **11**, 786-798.

Fire, A., Xu, S., Montgomery, M.K., Kostas, S.A., Driver, S.E., Mello, C.C. (1998). Potent and specific genetic interference by double-stranded RNA in *Caenorhabditis elegans. Nature* **391**, 806–811.

Fitch, D.H. and Thomas, W.K. (1997). Evolution. In Riddle D.L., Blumenthal T., Meyer B.J., Priess J.R. (eds.). *C elegans* II, pp 815-850. *New York: Cold Spring Harbor Laboratory Press*.

Gao, D., and Kimble, J. (1995). APX-1 can substitute for its homolog LAG-2 to direct cell interactions throughout *Caenorhabditis elegans Development Proc. Natl. Acad. Sci. USA* **92**, 9839-9842.

Garvin C., Holdeman R., Strome S. (1998). The phenotype of *mes-2*, *mes-3*, *mes-4* and *mes-6*, Maternal-effect genes required for survival of the germline in *Caenorhabditis elegans*, is sensitive to chromosome dosage. *Genetics* **148**, 167-185.

Gaudet, J. and Mango, S.E. (2002). Regulation of organogenesis by the *Caenorhabditis elegans* FoxA protein PHA-4. *Science* **295**, 821-825.

Gehring, W.J. and Ikeo, K. (1999). Pax 6: Mastering eye morphogenesis and eye evolution. *Trends Genet.* **15**, 371-377.

Geley, S., and Müller, C. (2004). RNAi: ancient mechanism with a promising future. *Experimental gerontology*, **39**, 985–998.

Gönczy, P. and Rose, L.S. (2005). Asymmetric cell division and axis formation in the embryo. *WormBook*, ed. The *C. elegans* Research Community, WormBook, doi/10.1895/wormbook.1.30.1, http://www.wormbook.org

Goldstein, B. (1992). Induction of gut in *Caenorhabditis elegans* embryos. *Nature* **357**, 255–257.

Goldstein, B. (2001). On the evolution of early *Development* in the Nematoda. *Philos. Trans. R. Soc. Lond.* ***356***, 1521–1531.

Goldstein B., Frisse, L.M., Thomas, W.K. (1998). Embryonic axis specification in nematodes: evolution of the first step in Development. *Curr. Biol.* **8**, 157–160.

Goldstein, B. and Hird, S.N. (1996). Specification of the anteroposterior axis in *Caenorhabditis elegans*. *Development* **122**, 1467–1474.

Golding, G.B. and Dean, A.M. (1998). The structural basis of molecular adaptation. *Mol. Biol. Evol.* **15**, 355-369.

Goszczynski, B. and McGhee, J.D. (2005). Reevaluation of the role of the *med-1* and *med-2* genes in specifying the *Caenorhabditis elegans* endoderm. *Genetics* **171**, 545–555.

Grenier, J.K. and Carroll, S.B. (2000). Functional evolution of the Ultrabithorax protein *Proc. Natl. Acad. Sci. USA,* **97**, 704–709.

Gruenbaum, Y., Goldman, R.D., Meyuhas, R., Mills, E., Margalit, A., Fridkin, A., Dayani, Y., Prokocimer, M., Enosh, A. (2003).The nuclear lamina and its functions in the nucleus. *Int. Rev. Cytol.* **226**, 1–62.

Guedes, S. and Priess, J.R. (1997). The *C. elegans* MEX-1 protein is present in germline blastomeres and is a P granule component. *Development* **124**, 731-739.

Guven-Ozkan, T., Robertson, S.M., Nishi, Y., Lin, R. (2010). *zif-1* translational repression defines a second, mutually exclusive OMA function in germline transcriptional repression *Development* **137**, 3373-3382

Hajnal, A. and Berset, T. (2002). The *C. elegans* MAPK phosphatase LIP-1 is required for the G(2)/M meiotic arrest of Developing oocytes. *EMBO J.* **21**, 4317-4326.

Hamilton, W.D., Axelrod, R., Tanese, R. (1990). Sexual reproduction as an adaptation to resist parasites. *Proc. Natl. Acad. Sci. USA* 87, 3566-3573.

Hansen, E., Buecher, E., Yarwood, E. (1973). Alteration of sex of *Aphelenchus avenae* in culture**.** *Nematologica*, **19**,113-116.

Hayashi, K., de Sousa Lopes, S.M., Surani, M.A. (2007). Germ cell specification in mice Science, 316, 394-396.

Heger, P., Kroiher, M., Ndifon, A.N., Schierenberg E. (2010). Conservation of MAP kinase activity and MSP genes in parthenogenetic nematodes. *BMC Developmental Biology*, 10:51 doi:10.1186/1471-213X-10-51.

Hill, R.C., de Carvalho, C.E., Salogiannis, J., Schlager, B., Pilgrim, D., Haag, E.S. (2006). Genetic flexibility in the convergent evolution of hermaphroditism in *Caenorhabditis* nematodes. *Dev. Cell* **10**, 531-538.

Holterman, M., Van der Wurff, A., Van den Elsen, S., Van Megen, H., Bongers, T., Holovachov, O., Bakker, J., Helder, J., Wurff A. Van Der, Elsen, S. Van Den et al., (2006). Phylum-wide analysis of SSU rDNA reveals deep phylogenetic relationships among nematodes and accelerated evolution toward crown Clades. *Mol. Biol. Evol.* **23**, 1792–800.

Houthoofd, W., Jacobsen, K., Mertens, C., Vangestel, S., Coomans, A., Borgonie, G. (2003). Embryonic cell lineage of the marine nematode *Pellioditis marina*. *Dev. Biol.* **258**, 57–69.

Hugot, J.P., Baujard, P., and Morand, S. (2001). Biodiversity in helminths and nematodes as a field of study: an overview. *Nematology* **3**, 199–208.

Inoue, H., Nojima, H., Okayama, H. (1990). High efficiency transformation of *Escherichia coli* with plasmids. *Gene* **96**, 23–28.

Jiang, D., Li, B.W., Fischer, P.U., Weil, G.J. (2008). Localisation of gender regulated gene expression in the filarial nematode Brugia malayi**.** *Int. J. Parasitol.* **38**, 503-512.

Kalinka, A. and Tomancak, P. (2012). The evolution of early animal embryos: conservation or divergence? *Trends in Ecology and Evolution,* **27**, 385-393.

Kallenbach, R.J. (1985). Ultrastructural analysis of the initiation and Development of cytasters in sea urchin eggs**.** *J. Cell Sci.* **73**, 261–278.

Kamath, R.S. and Ahringer, J. (2003). Genome-wide RNAi screening in *Caenorhabditis elegans Methods*, **30**, 313–321

Kawasaki, I., Amiri, A., Fan, Y., Meyer, N., Dunkelbarger, S., Motohashi, T., Karashima, T., Bossinger, O., Strome, S. (2004). The PGL family proteins associate with germ granules and function redundantly in *C. elegans* germline development. *Genetics*. **167**, 645–661.

Kimble, J. and White, J. G. (1981). On the control of germ cell development in *Caenorhabditis elegans*. *Dev. Biol.* **81**, 208-219.

Kimble, J. and Hirsh, D. (1979). The postembryonic cell lineages of the hermaphrodite and male gonads in *Caenorhabditis elegans*. *Dev. Biol.* **70**, 396-417.

Kiontke, K., and Fitch, D.H. (2005). The phylogenetic relationships of *Caenorhabditis* and other rhabditids. WormBook. 1–11.

Kiontke, K., Gavin, N.P., Raynes, Y., Roehrig, C., Piano, F., Fitch, D.H. (2004). *Caenorhabditis* phylogeny predicts convergence of hermaphroditism and extensive intron loss. *Proc. Natl. Acad. Sci. USA,* **101**, 9003–9008.

Klass, M., Dow, B., Herndon, M. (1982). Cell-specific transcriptional regulation of the major sperm protein in *Caenorhabditis elegans***.** *Dev. Biol.* **93**, 152-164.

Klass, M.R. and Hirsh, D. (1981). Sperm Isolation and Biochemical Analysis of the Major Sperm Protein from *Caenorhabditis elegans***.** *Dev. Biol.* **84**, 299-312.

Kondrashov, A.S. (1993). Classification of hypothesis on the advantages of amphimixis. *J. Hered* **84**, 372–387.

Kophengnavong, T., Carroll, A.S., Blackwell, T.K. (1999). The SKN-1 amino terminal arm is a DNA specificity segment. *Mol. Cell Biol.* **19**, 3039-3050.

Kosinski, M., McDonald, K., Schwartz, J., Yamamoto, I., Greenstein, D. (2005). *C. elegans* sperm bud vesicles to deliver a meiotic maturation signal to distant oocytes**.** *Development* 2005, **132**, 3357-69.

Krieg, C., Cole, T., Deppe, U., Schierenberg, E., Schmitt, D., Yoder, B., Ehrenstein, G Con. (1978). The cellular anatomy of embryos of the nematode *Caenorhabditis elegans*. Analysis and reconstruction of serial section electron micrographs. *Dev. Biol.* **65**:193–215.

Kuntzinger, T., Bornens M. (2000). The centrosome and parthenogenesis. *Curr. Top. Dev. Biol.* **49**, 1–19.

Lackner, M.R., Kornfeld, K., Miller, L.M., Horvitz, H.R., Kim, S.K. (1994). A MAP kinase homolog, mpk-1, is involved in ras-mediated induction of vulval cell fates in Caenorhabditis elegans**.** *Genes Dev.* **8,** 160-73.

Lahl, V., Halama, C., Schierenberg, E. (2003). Comparative and experimental embryogenesis of Plectidae (Nematoda). *Dev. Genes Evol.* **213**, 18–27.

Lahl, V., Sadler, B., Schierenberg, E. (2006). Egg Development in parthenogenetic nematodes: variations in meiosis and axis formation. *Int. J. Dev. Biol.* **50**, 393-398.

Lahl V., Schulze J., Schierenberg, E. (2009). Differences in embryonic pattern formation between *Caenorhabditis elegans* and its close parthenogenetic relative *Diploscapter coronatus*. *Int. J. Dev. Biol.* **53**, 507-515.

Lai, W.S., Carballo, E., Strum, J.R., Kennington, E.A., Phillips, R.S., Blackshear, P.J. (1999). Evidence that tristetraprolin binds to AU-rich elements and promotes the deadenylation and destabilization of tumor necrosis factor alpha mRNA. *Mol. Cell Biol.* **19**, 4311-4323.

Lambshead (1993). Recent Developments in marine benthic biodiversity research. *Oceanis* **19**, 5-24.

Lambie, E. J. and Kimble, J. (1991). Two homologous regulatory genes, *lin-12* and *glp-1*, have overlapping functions. *Development* **112**, 231-240.

Laugsch, M. and Schierenberg, E. (2004). Differences in maternal supply and early Development of closely related nematode species. *Dev. Biol.* **662**, 655-662.

Levin, M., Hashimshony, T., Wagner, F., Yanai, I. (2012). Developmental milestones punctuate gene expression in the *Caenorhabditis Embryo. Developmental Cell* **22**, 1101–1108.

Lunt, D.H. (2008). Genetic tests of ancient asexuality in root knot nematodes reveal recent hybrid origins. *BMC Evol Biol*, **8**, 194. doi:10.1186/1471-2148-8-194.

Maduro, M.F. (2006). Endomesoderm specification in *Caenorhabditis elegans* and other nematodes. *Bioessays* **28**, 1010–1022.

Maduro, M.F. (2009). Structure and evolution of the *C. elegans* embryonic endomesoderm network. *Biochim Biophys Acta* **1789**, 250–260.

Maduro, M.F., Broitman-Maduro, G., Mengarelli, I., Rothman, J.H., (2007). Maternal deployment of the embryonic SKN-1 → MED-1,2 cell specification pathway in *C. elegans*. *Dev. Biol.* **301**, 590–601.

Maduro, M., Hill, R.J., Heid, P.J., Newman-Smith, E.D., Zhu, J., Priess, J., Rothman, J. (2005a). Genetic redundancy in endoderm specification within the genus *Caenorhabditis*. *Dev. Biol*. **284**, 509–522.

Maduro, M.F., Kasmir, J.J., Zhu, J., Rothman, J.H. (2005b). The Wnt effector POP-1 and the PAL-1/Caudal homeoprotein collaborate with SKN-1 to activate *C. elegans* endoderm *Dev*elopment. *Dev. Biol.* **285**, 510–523.

Maduro, M.F., Meneghini, M.D., Bowerman, B., Broitman-Maduro, G., Rothman, J.H. (2001). Restriction of mesendoderm to a single blastomere by the combined action of SKN-1 and a GSK-3beta homolog is mediated by MED-1 and -2 in *C. elegans. Mol. Cell.* **7**, 475–485.

Maduro, M.F. and Rothman, J.H. (2002). Making worm guts: the gene regulatory network of the *Caenorhabditis elegans* endoderm. *Dev. Biol.* **246**, 68–85.

Malakhov, V.V. (1994). Nematodes, Structure, *Development* Classification and Phylogeny. (Washington, DC: Smithsonian Institution Press).

Maupas, E. (1900). Modes et formes de reproduction des nematodes**.** *Archives de Zoologie Experimentale et Generale*, **8**, 463-624.

Maynard-Smith J. (1978). *The Evolution of Sex*. Cambridge: Cambridge University Press.

McGinnis, S. and Madden, T.L. (2004). BLAST: at the core of a powerful and diverse set of sequence analysis tools. *Nucleic Acids Res.* **32**, W20–W25.

Mello, C.C., Draper, B.W., Krause, M., Weintraub, H., Priess, J.R. (1992). The *pie-1* and *mex-1* genes and maternal control of blastomere identity in early *C. elegans* embryos. *Cell* **70**, 163–176.

Mello, C.C., Schubert, C., Draper, B.W., Zhang, B., Lobel, W., Priess, R.J.R. (1996). The PIE-1 protein and germline specification in *C. elegans* embryos *Nature* **382**, 710–712.

Miller, M. A., Nguyen, V.Q., Lee, M.H., Kosinski, M., Schedl, T., Caprioli, R.M., Greenstein, D. (2001). A sperm cytoskeletal protein that signals oocyte meiotic maturation and ovulation**.** *Science* **291**, 2144-2147.

Montgomery, M.K., Xu, S., and Fire, A. (1998). RNA as a target of double-stranded RNA-mediated genetic interference in *Caenorhabditis elegans*. *Proceedings of the National Academy of Sciences of the United States of America*, *95* (26), 15502–15507.

Mullis, K., Faloona, F., Scharf, S., Saiki, R., Horn, G., Erlich, H. (1986) Specific enzymatic amplification of DNA *in vitro*: *the polymerase chain reaction*. *Cold Spring Harb. Sym.* **51**, 263–273.

Munro, E.M. (2006). PAR proteins and the cytoskeleton: a marriage of equals. *Curr. Opin. Cell Biol.* **18**, 86-94.

Nance, J. and Priess, J. R. (2002). Cell polarity and gastrulation in *C. elegans*. *Development* **129**, 387-397.

Nayak, S., Goree, J., Schedl, T. (2005). *fog-2* and the evolution of self-fertile hermaphroditism in *Caenorhabditis*. *PLoS Biol*. **3**, 57-71.

Nebreda, A.R. and Ferby, I. (2000). Regulation of the meiotic cell cycle in oocytes**.** *Curr. Opin. Cell Biol.* **12,** (6), 666-675.

Nioi, P., T. Nguyen, et al., (2005). The carboxy-terminal Neh3 domain of Nrf2 is required for transcriptional activation. *Mol. Cell Biol.* 25 **24**, 10895-10906.

Ogura, K., Kishimoto, N. Mitani, S. Gengyo-Ando, K., Kohara, Y. (2003). Translational control of maternal *glp-1* mRNA by POS-1 and its interacting protein SPN-4 in *Caenorhabditis elegans*. *Development* **130**, 2495-2503.

Patel, N.H. and Goodman, C.S. (1992). Preparation of digoxygenin-labeled single stranded DNA probes. In ‘‘Non-Radioactive Labeling and Detection of Biomolecules’’ (C. Kessler, Ed.), Springer–Verlag, Berlin 377–381.

Pellettieri, J. and Seydoux, G. (2002). Anterior-posterior polarity in *C. elegans* and *Drosophila.* PARallels and differences. *Science* **298**, 1946-1950.

Pitt, J.N., Schisa, J.A., Priess, J.R. (2000). P granules in the germ cells of *Caenorhabditis elegans* adults are associated with clusters of nuclear pores and contain RNA. *Dev. Biol.* **219**, 315–333.

Poinar, G.O. (2011). The evolutionary history of nematodes: as revealed in stone, amber and mummies. Leiden: Brill.

Priess, J.R., Schnabel, H., Schnabel, R. (1987). The *glp-1* locus and cellular interactions in early *C. elegans* embryos. *Cell* **51**, 601–611.

Ramirez-Perez, S.S. Sarma et al., (2004). Effects of mercury on the life table demography of the rotifer *Brachionus calyciflorus* Pallas (Rotifera). *Ecotoxicology* **13**, 535–544.

Reese, K.J., Dunn, M.A., Waddle, J.A., Seydoux, G. (2000). Asymmetric segregation of PIE-1 in *C. elegans* is mediated by two complementary mechanisms that act through separate PIE-1 protein domains. *Mol. Cell* **6**, 445-455.

Riparbelli, M.G. and Callaini G. (2003). *Drosophila* parthenogenesis: a model for de novo centrosome assembly *Dev. Biol.* **260**, 298–313.

Rocheleau, C.E., Downs, W.D., Lin, R., Wittmann, C., Bei, Y., Cha, Y.H., Ali, M., Priess, J.R., Mello, C.C. (1997). Wnt signaling and an APC-related gene specify endoderm in early *C. elegans* embryos. *Cell* **90**, 707–716.

Rodriguez-Trelles, F., Tarrio, R., Ayala, F.J. (2002). A methodological bias toward overestimation of molecular evolutionary time scales*. Proc. Natl. Acad. Sci. USA* **99**, 8112–8115.

Rossomando, A.J., Payne, D.M., Weber, M.J., Sturgill, T.W. (1989). Evidence that pp42, a major tyrosine kinase target protein, is a mitogen-activated serine/threonine protein kinase**.** *Proc. Natl. Acad. Sci. USA* **86,** 6940-3.

Rudel, D. and Sommer, R.J. (2003). The evolution of developmental mechanisms *Dev. Biol.,* **264**, 15–37.

Rupert, P.B., Daughdrill, G.W., Bowerman, B., Matthews, B.W. (1998). The binding domain of *skn-1* in complex with DNA: a new DNA-binding motif. *Nat. Struct. Biol.* **5**, 484–491.

Santos, A.C. and Lehmann R. (2004). Isoprenoids control germ cell migration downstream of HMGCoA reductase *Dev. Cell* **6**, 283–293.

Schedl, T. and Kimble, J. (1988). *fog-2*, a germ-line-specific sex determination gene required for hermaphrodite spermatogenesis in *Caenorhabditis elegans*. *Genetics* **139**, 579-606.

Schierenberg, E. (1997). Nematodes: the roundworms. In: *Embryology. Constructing the Organism*, S.F. Gilbert, and A.M. Raunio, eds. (Sunderland, MA: Sinauer Associates), 131-147.

Schierenberg, E. (2001). Three sons of fortune: early embryogenesis, evolution and ecology of nematodes. *Bioessays* **23,** 841–847.

Schierenberg E. (2005b). Unusual cleavage and gastrulation in a freshwater nematode: Developmental and phylogenetic implications. *Dev. Genes Evol.* **215**, 103–108.

Schierenberg, E. (2006). Embryological variation during nematode development. In Wormbook; doi:10,1895/wormbook.1.55.1. http://www.wormbook.org.

Schierenberg, E., and Wood, W.B. (1985). Control of cell-cycle timing in early embryos of *C. elegans*. *Dev. Biol.* **107**, 337–354.

Schiffer, P.H., Kroiher, M., Kraus, C., Koutsovoulos, G.D., Kumar, S., Camps, J.I.R., Ndifon, A.N., Stappert, D., Frommolt, P., Morris, K., Nuernberg, P., Thomas, K.W., Blaxter L.M., Schierenberg E. (2013). Major changes in the core *Dev*elopmental pathways of nematodes: *Romanomermis culicivorax* reveals the derived status of the *Caenorhabditis elegans* model. Submitted, 2013.

Schisa, J. A., Pitt, J. N., Priess, J. R. (2001). Analysis of RNA associated with P granules in germ cells of *C. elegans* adults. *Development* **128**, 1287-1298.

Schubert, U., Antón, L.C., Gibbs, J., Norbury, C.C., Yewdell, J.W., Bennink, J.R. (2000). Rapid degradation of a large fraction of newly synthesized proteins by proteasomes. *Nature* **404**, 770-774.

Schulze, J., Houthoofd, W., Uenk, J., Vangestel, S. Schierenberg, E. (2012). *Plectus* - a stepping stone in embryonic cell lineage evolution of nematodes. *EvoDevo* **3**, 13.

Schulze, J., and Schierenberg, E. (2008). Cellular pattern formation, establishment of polarity and segregation of colored cytoplasm in embryos of the nematode *Romanomermis culicivorax. Dev. Biol.* **315**, 426–436.

Schulze J. and Schierenberg E. (2009). Embryogenesis of *Romanomermis culicivorax*: an alternative way to construct a nematode. *Dev. Biol.* **334**, 10-21.

Schulze J. and Schierenberg E. (2011). Evolution of embryonic Development in nematodes. *EvoDevo* **2**, 18.

Scott, A.L., Dinman, J., Sussman, D.J., Ward, S. (1989). Major sperm protein and actin genes in free-living and parasitic nematodes**.** *Parasitology* **98,** 471-478.

Seydoux G. and Braun R.E. (2006). Pathway to totipotency: lessons from germ cells. *Cell* **127**, 891–904.

Seydoux, G. and Dunn, M.A. (1997). Transcriptionally repressed germ cells lack a subpopulation of phosphorylated RNA polymerase II in early embryos of *Caenorhabditis elegans* and *Drosophila melanogaster. Development* **124**, 2191-2201.

Seydoux, G. and Fire A. (1994). Soma-germline asymmetry in the distributions of embryonic RNAs in *Caenorhabditis elegans. Development* **120**, 2823–2834.

Seydoux, G., Mello, C.C., Pettitt, J., Wood, W.B., Priess, J.R., et al., (1996). Repression of gene expression in the embryonic germ lineage of *C. elegans*. *Nature* **382**, 713–716.

Seydoux, G. and Schedl, T. (2001). The germline in *C. elegans*: origins, proliferation, and silencing. *Int. Rev. Cytol.* **203**, 139–185.

Seydoux, G. and Strome, S. (1999). Launching the germline in *Caenorhabditis elegans*: regulation of gene expression in early germ cells *Development* **126**, 3275–3283.

Shannon, A.J., Tyson, T., Dix, I., Boyd, J., Burnell, A.M. (2008). Systemic RNAi mediated gene silencing in the anhydrobiotic nematode *Panagrolaimus superbus*. *BMC molecular Biology*, **9**, 58.

Shen-Orr, S.S., Pilpel, Y., Hunter, C.P. (2010). Composition and regulation of maternal and zygotic transcriptomes reflects species-specific reproductive mode. *Genome Biol.* **11**, R58.

Sheth, U., Pitt, J., Dennis, S., Priess, J.R. (2010). Perinuclear P granules are the principal sites of mRNA export in adult *C. elegans* germ cells. *Development* **137**, 1305-1314.

Skiba, F., and Schierenberg, E. (1992). Cell lineages, *Dev*elopmental timing, and spatial pattern formation in embryos of free-living soil nematodes. *Dev. Biol.* **151**, 597–610.

Smith, H. (2006). Sperm motility and MSP**.** *WormBook*:1-8.

Stathopoulos, A. and Levine, M. (2005). Genomic regulatory networks and animal development. *Dev. Cell,* **9**, 449–462.

Sternberg, P.W. and Horvitz H.R. (1981). Gonadal cell lineages of the nematode Panagrellus redivivus and implications for evolution by the modification of cell lineage*. Dev. Biol.* **88**, 147–166.

Storm, M.A. and Angilletta, M.J. (2007). Rapid assimilation of yolk enhances growth and *Dev*elopment of lizard embryos from a cold environment. *J. Exp. Biol.* **210**, 3415-3421.

Strome, S. (2005). Specification of the germ line. The *C. elegans* Research Community, Worm Book, doi/10.1895/wormbook.1.9.1, http://wormbook.org.

Strome, S., Garvin, C., Paulsen, J., Capowski, E., Martin, P., Beanan, M. (1994). Specification and Development of the germline in *Caenorhabditis elegans*. *Ciba Found. Symp.* **182**, 31–45.

Strome, S. and Lehmann, R. (2007). Germ versus soma decisions: lessons from flies and worms. *Science* **316**, 392-393.

Strome, S. and Wood, W.B. (1982). Immunofluorescence visualization of germ-line-specific cytoplasmic granules in embryos, larvae, and adults of *Caenorhabditis elegans*. *Proc. Natl. Acad. Sci. USA* **79**, 1558-1562.

Strome, S. and Wood, W.B. (1983). Generation of asymmetry and segregation of germ-line granules in early *C. elegans* embryos. *Cell* **35**, 15-25.

Sulston, J.E. and Horvitz, H.R. (1977). Post-embryonic Cell Lineages of the Nematode, *Caenorhabditis elegans*. *Dev. Biol.* **156**, 110–156.

Sulston, J.E., Schierenberg, E., White, J.G., Thomson, J.N. (1983). The embryonic cell lineage of the nematode *C. elegans*. *Dev. Biol.* **100**, 64–119.

Tabara, H., Hill R.J., Mello, C.C., Priess, J.R., Kohara Y. (1999). *pos-1* encodes a cytoplasmic zinc-finger protein essential for germline specification in *C. elegans Development* **126**, 1–11.

Tautz, D. (2000). Evolution of transcriptional regulation. *Curr. Opin. Genet. Dev.* **10**, 575–579.

Tautz, D. and Schmid, K.J. (1998). From genes to individuals: *Dev*elopmental genes and the generation of the phenotype. *Philos. Trans. R. Soc. Lond. B. Biol. Sci.* **353**, 231–240.

Tenenhaus,C., C. Schubert, G. Seydoux. (1998). Genetic requirements for PIE-1 localisation and inhibition of gene expression in the embryonic germ lineage of *Caenorhabditis elegans. Dev. Biol.* **200**, 212–224.

Tenenhaus, C., Subramaniam, K., Dunn, M.A., Seydoux. G. (2001). PIE-1 is a bifunctional protein that regulates maternal and zygotic gene expression in the embryonic germ line of *Caenorhabditis elegans. Genes Dev.* **15**, 1031–1040.

Timmons, L. and Fire, A. (1998). Specific interference by ingested dsRNA. *Nature* **395**: 854. doi:10.1038/27579.

Triantaphyllou, A. (1981). Oogenesis and the chromosomes of the parthenogenetic root-knot nematode *Meloidogyne incognita*. *J. Nematol.* **13**: 95-104.

Triantaphyllou, A.P. and Fisher, J.M. (1976). Gametogenesis in Amphimictic and Parthenogenetic Populations of *Aphelenchus avenae***.** *J. Nematol*. **8**, 168-77.

Traunspurger W. (2002). Nematoda In *Freshwater Meiofauna: Biology and Ecology* (Eds S.D. Rundle, A.L. Robertson and J.M. Schmid-Araya), 63–104. Backhuys Publishers, Leiden.

True, J.R. and Haag, E.S. (2001) Developmental system drift and flexibility in evolutionary trajectories. *Evol. Dev*. **3**, 109–119.

The *C. elegans* Sequencing Consortium (1998). Genome Sequence of the Nematode *C. elegans*: A platform for investigating Biology. *Science* **282**, 2012-2018.

Updike, D. L. and Strome, S. (2010). P granule assembly and function in *Caenorhabditis elegans* germ cells. *J. Androl.* **31**, 53-60.

Updike, D. L., Hachey, S. J., Kreher, J., Strome, S. (2011). P granules extend the nuclear pore complex pore complex environment in the *C. elegans* germ line. *J. Cell Biol.* **192,** 939-948.

von Baer, K. E. (1828). Ueber Entwicklungsgeschichte der Tiere. Borneträger, Königsberg.

Voronina, E. (2012). The diverse functions of germline P granules in *C. elegans*. *Mol. Reprod. Dev.* DOI: 10.1002/mrd.22136.

Voronina, E., and Seydoux, G. (2010). The *C. elegans* homolog of nucleoporin Nup98 is required for the integrity and function of germline P granules. *Development* **137**, 1441-1450.

Voronina, E., Seydoux, G., Sassone-Corsi, P., Nagamori, I. (2011). RNA granules in germ cells. Cold Spring Harb. Perspect. *Biol*. **3**, pii: a002774.

Voronov, D.A. (1999). The embryonic development of *Pontonema vulgare* (Enoplida: Oncholaimidae) with a discussion of nematode phylogeny. *Russ. J. Nematol.* **7**, 105–114.

Voronov, D.A., Panchin, Y.V. (1998). Cell lineage in marine nematode *Enoplus brevis. Development* **125**, 143–150.

Walker, A.K., See, R., Batchelder, C., Kophengnavong, T., Gronniger, J.T., Shi, Y., Blackwell, T.K. (2000). A conserved transcription motif suggesting functional parallels between *C. elegans* SKN-1 and Cap 'n' Collar-related bZIP proteins. *J. Biol. Chem.* **275**, 22166-22171.

Waskiewicz, A.J., Cooper, J.A. (1995). Mitogen and stress response pathways: MAP kinase cascades and phosphatase regulation in mammals and yeast. *Curr. Opin. Cell. Biol.* **7,** 798-805.

Ward, S. and Klass, M. (1982). The location of the major protein in *Caenorhabditis elegans* sperm and spermatocytes. *Dev. Biol.* **92**, 203-208.

Warde-Farley, D., Donaldson, S., Comes, O., Zuberi, K., Badrawi, R., Chao P., Franz, M., Grouios, C., Kazi, F., Lopes, C. (2010). The GeneMANIA prediction server: biological network integration for gene prioritization and predicting gene function. *Nucleic Acids Res.* **38**, W214–220.

White, J.G., Southgate, E., Thomson, J.N., Brenner, S. (1986). The structure of the nervous system of *Caenorhabditis elegans. Philosophical Transactions of the Royal Society of London B.* **314**, 1-340.

Widmann, C., Gibson, S., Jarpe, M.B., Johnson, G.L. (1999). Mitogen-activated protein kinase: conservation of a three-kinase module from yeast to human**.** *Physiol. Rev.* **79**, 143-180.

Wiegner, O. and Schierenberg, E. (1998). Specification of gut cell fate differs significantly between the nematodes *Acrobeloides nanus* and *Caenorhabditis elegans*. *Dev. Biol.* **204**, 3-14.

Wiegner O. and Schierenberg, E. (1999). Regulative Development in a nematode embryo: a hierarchy of cell fate transformations. *Dev. Biol.* **215**, 1–12.

Woolley, S.C., Sakata, J.T., Crews. D. (2004). Tracing the evolution of brain and behavior using two related species of whiptail lizards: *Cnemidophorus uniparens* and *Cnemidophorus inornatus*. *ILAR Journal* **45**, 46–53.

Wolf, N., Priess, J., Hirsh, D. (1983). Segregation of germline granules in early embryos of *Caenorhabditis elegans*: an electron microscopicanalysis. *J. Embryol. Exp. Morphol.* **73**, 297–306.

Wu, Y. and Han. M. (1994). Suppression of activated Let-60 ras protein defines a role of Caenorhabditis elegans Sur-1 MAP kinase in vulval differentiation**.** *Genes Dev.* **8,**147-59.

Wylie, C. (1999). Germ cells. *Cell* **96**, 165–174.

Yanai, I. and Hunter, C.P. (2009). Comparison of diverse developmental transcripto mes reveals that coexpression of gene neighbors is not evolutionarily conserved. *Genome Res.* **19**, 2214-2220.

Zhao, Z., Boyle, T., Bao, Z., Murray, J.I., Mericle, B., Waterston, R.H. (2008). Comparative analysis of embryonic cell lineage between*Caenorhabditis briggsae* and *Caenorhabditis elegans*. *Dev. Biol.* **314**, 93–99.

Zhang, Y., Yan, L., Zhou, Z., Yang, P. Tian, E., Zhang, K., Zhao, Y., et al., (2009). SEPA-1 mediates the specific recognition and degradation of P granule compone nts by autophagy in *C. elegans*. *Cell* **136**, 308-321.

9 Declaration

Ich versichere, dass ich die von mir vorgelegte Dissertation selbständig angefertigt, die benutzten Quellen und Hilfsmittel vollständig angegeben und die Stellen der Arbeit - einschließlich Tabellen, Karten und Abbildungen −, die anderen Werken im Wortlaut oder dem Sinn nach entnommen sind, in jedem Einzelfall als Entlehnung kenntlich gemacht habe; dass diese Dissertation noch keiner anderen Fakultät oder Universität zur Prüfung vorgelegen hat; dass sie − abgesehen von unten angegebenen Teilpublikationen − noch nicht veröffentlicht worden ist sowie, dass ich eine solche Veröffentlichung vor Abschluss des Promotionsverfahrens nicht vornehmen werde.
Die Bestimmungen der Promotionsordnung sind mir bekannt. Die von mir vorgelegte Dissertation ist von Herrn Prof. Dr. Einhard Schierenberg betreut worden.

Teilpublikationen:

1. Heger, P., Kroiher, M., **Ndifon, A.N**., Schierenberg E. (2010)

   Conservation of MAP kinase activity and MSP genes in parthenogenetic nematodes. *BMC Developmental Biology*, 10:51 doi:10.1186/1471-213X-10-51.

2. Schiffer, P.H., Kroiher, M., Kraus, C., Koutsovoulos, G.D., Kumar, S., Camps, J.I.R., **Ndifon, A.N**., Stappert, D., Frommolt, P., Morris, K., Nuernberg, P., Thomas, K.W., Blaxter L.M., Schierenberg E. (2013)

   Major changes in the core Developmental pathways of nematodes: *Romanomermis culicivorax* reveals the derived status of the *Caenorhabditis elegans* model. *BMC Genomics,* 14: 923.

3. Schiffer, P. H., **Ndifon, A. N.**, Grotehusmann H., Kroiher, M., Loer, C., Schierenberg, E. (2014)

   Developmental variations among Panagrolaimid nematodes indicate developmental system drift within a small taxonomic unit. *Development Genes and Evolution* (in press), doi: 10.1007/s00427-014-0471-2.

10 Acknowledgements

First and foremost, I would like to thank my supervisor, Prof. Dr. Einhard Schierenberg, for wholeheartedly welcoming me into his lab and for his continuous involvement and guidance throughout my project. You have given me the opportunity to explore an exciting field in amazing company. I feel extremely lucky for this chance and to have a supervisor who cared so much about my work and who always responded to my questions promptly.

I would like to express my gratitude to PD. Dr. Michael Kroiher for constructive criticisms that helped shape my thesis. You have been key in the development of this project. This thesis would not have been possible without his support, guidance and encouragement.

I am equally grateful to Prof. Dr. Plickert and Prof. Dr. Roth for accepting to be part of my thesis evaluation committee.

Last but certainly not least, I must express my gratitude to my family for all their infinite love, support and encouragement.

A special thanks goes to the past and present members of the Schierenberg lab. I am particularly indebted to Dr. Julia Camps, Phillipp Schiffer, Christopher Kraus for constructive feedback and invaluable support. I am also thankful to Dr. Peter Heger for sharing his expertise and help. I would also like to acknowledge technical assistance from Hayati, Elizabeth and Gülay. Without you all, my project would not have been possible and enjoyable.